National Library of Canada
Bibliothèque nationale du Canada

Canadian Theses Service
Service des thèses canadiennes

Ottawa, Canada
K1A 0N4

NOTICE

The quality of this microform is heavily dependent upon the quality of the original thesis submitted for microfilming. Every effort has been made to ensure the highest quality of reproduction possible.

If pages are missing, contact the university which granted the degree.

Some pages may have indistinct print especially if the original pages were typed with a poor typewriter ribbon or if the university sent us an inferior photocopy.

Previously copyrighted materials (journal articles, published tests, etc.) are not filmed.

Reproduction in full or in part of this microform is governed by the Canadian Copyright Act, R.S.C. 1970, c. C-30.

AVIS

La qualité de cette microforme dépend grandement de la qualité de la thèse soumise au microfilmage. Nous avons tout fait pour assurer une qualité supérieure de reproduction.

S'il manque des pages, veuillez communiquer avec l'université qui a conféré le grade.

La qualité d'impression de certaines pages peut laisser à désirer, surtout si les pages originales ont été dactylographiées à l'aide d'un ruban usé ou si l'université nous a fait parvenir une photocopie de qualité inférieure.

Les documents qui font déjà l'objet d'un droit d'auteur (articles de revue, tests publiés, etc.) ne sont pas microfilmés.

La reproduction, même partielle, de cette microforme est soumise à la Loi canadienne sur le droit d'auteur, SRC 1970, c. C-30.

NL-339 (r. 88/04)

Canada

THE UNIVERSITY OF ALBERTA

CALCULATION OF ICE JAM PROFILES

BY

© GREGORY M. FLATO

A THESIS

SUBMITTED TO THE FACULTY OF GRADUATE STUDIES AND RESEARCH

IN PARTIAL FULFILMENT OF THE REQUIREMENTS FOR THE DEGREE

OF MASTER OF SCIENCE

DEPARTMENT OF CIVIL ENGINEERING

EDMONTON, ALBERTA

SPRING 1988

Permission has been granted to the National Library of Canada to microfilm this thesis and to lend or sell copies of the film.

The author (copyright owner) has reserved other publication rights, and neither the thesis nor extensive extracts from it may be printed or otherwise reproduced without his/her written permission.

L'autorisation a été accordée à la Bibliothèque nationale du Canada de microfilmer cette thèse et de prêter ou de vendre des exemplaires du film.

L'auteur (titulaire du droit d'auteur) se réserve les autres droits de publication; ni la thèse ni de longs extraits de celle-ci ne doivent être imprimés ou autrement reproduits sans son autorisation écrite.

ISBN 0-315-42747-7

THE UNIVERSITY OF ALBERTA

RELEASE FORM

NAME OF AUTHOR: GREGORY M. FLATO

TITLE OF THESIS: CALCULATION OF ICE JAM PROFILES

DEGREE: MASTER OF SCIENCE

YEAR THIS DEGREE GRANTED: SPRING 1988

Permission is hereby granted to the UNIVERSITY OF ALBERTA LIBRARY to reproduce single copies of this thesis and to lend or sell such copies for private, scholarly or scientific research purposes only.

The author reserves other publication rights, and neither the thesis nor extensive extracts from it may be printed or otherwise reproduced without the author's written permission.

.....
(Student's signature)

..R.R.#.1...LEDUC....AB..
(Student's permanent address)

...T9E 2X1.....

Date: ....27/JAN./88..

THE UNIVERSITY OF ALBERTA

FACULTY OF GRADUATE STUDIES AND RESEARCH

The undersigned certify that they have read, and recommend to the Faculty of Graduate Studies and Research, for acceptance, a thesis entitled **CALCULATION OF ICE JAM PROFILES** submitted by GREGORY M. FLATO in partial fulfilment of the requirements for the degree of MASTER OF SCIENCE.

.....
(Supervisor)

.....

.....

Date 21 Dec 87

This thesis is dedicated to my Family.
To my Mother and Father for their inspiration and boundless generosity and to my Grandmother and Grandfather for their continued encouragement.

ABSTRACT

One of the most dramatic and unpredictable features of river ice behaviour is the phenomenon of ice jamming. Ice jams, particularly those that form during spring break up, can cause water levels much higher than even rare open water events. One of the challenges in Hydrotechnical Engineering is prediction of the water surface profile in a jammed river reach.

In this thesis, the relavent literature is reviewed and the existing theory concerning ice jam profile calculation is presented. The results of an experimental verification of some of the assumptions made in the developement of this theory are then discussed. The experiments indicate that the passive pressure coefficient provides a valid relationship between the streamwise and vertical stresses near the centerline of a jam. The results also point out that this relationship is only approximate over the remainder of the jam cross-section and that the common assumption that streamwise stress is a constant across the channel is invalid.

Current ice jam theory is then incorporated into a computer program which calculates the thickness and water surface profiles over the entire length of a jam in a non-prismatic, non-rectangular channel. The model assumes that the jam has a floating toe and that the ice mass can be assumed cohesionless.

The computer model is applied to several hypothetical prismatic channels so that the length required for a fully-developed jam can be ascertained. This length is found to vary over the order of 10 - 100 stream widths. However, the calculated lengths of the transition regions do not compare very well with those calculated in two previous studies; the reasons for this are unknown.

The present computer model is also compared to the HEC-2 water surface profile model for real channel data. The ice jam thickness in the latter case is calculated assuming equilibrium theory is valid at every cross-section. The resulting profiles agree quite well in the approximately equilibrium reach of the jam but the comparison is not extended to the transition regions.

ACKNOWLEDGEMENTS

The author is deeply indebted to his supervisor, Dr. R. Gerard, for the support, advice and encouragement he was afforded. The freedom the author was given and the opportunity to conduct this work off-campus made the experience even more rewarding. The author is also grateful to the National Water Research Institute, Canada Centre for Inland Waters, for their hospitality. In particular, Dr. S. Beltaos, Mr. W. Moody, Mr. G. Voros, Mr. J. Heidt, Mr. T. Nudds, Mr. D. Fekyt, and Mr. B. Trapp provided valuable assistance and advice in the design and construction of the experimental apparatus. The author is grateful to Dr. R. Gerard, Dr. S. Beltaos and Mr. J. Wong for the valuable discussions and review comments on various portions of this manuscript.

TABLE OF CONTENTS

	page
CHAPTER 1: REVIEW OF ICE JAM PROCESSES	1
Introduction	1
Ice Jam Features	3
Analytical Requirements	8
Current Profile Models	10
CHAPTER 2: LITERATURE REVIEW	12
Introduction	12
Early Research	13
Recent Developments	20
Discussion	26
CHAPTER 3: EXPERIMENTAL VERIFICATION OF PASSIVE PRESSURE CONCEPT	28
Introduction	28
The Passive Pressure Concept	29
Experimental Program	31
Experimental Procedure	38
Experimental Results	38
CHAPTER 4: ICE JAM THEORY	50
Introduction	50
Theory	51
Boundary Conditions	59
CHAPTER 5: ICE JAM PROFILE MODEL	65
Introduction	65

Computer Model Development 67
Discussion 72
CHAPTER 6: MODEL DEVELOPMENT AND EVALUATION 74
Introduction 74
Preliminary Tests 75
Influence of Parameters 81
CHAPTER 7: APPLICATION OF MODEL TO CASE STUDIES 96
Introduction 96
Application to Rectangular, Prismatic Channels 97
Comparison Between Present Model and Equilibrium Assumption 105
CHAPTER 8: CONCLUSIONS 109
Future Directions 111
LIST OF REFERENCES 114
APPENDIX A: MEASUREMENT OF MATERIAL PARAMETERS FOR POLYETHYLENE BEADS 119
Measurement of Ø for Polyethylene Beads 119
Measurement of Specific Gravity and Porosity 130
APPENDIX B: DETAILS OF ICE JAM PROFILE MODEL 134
Introduction 134
Subroutine THICK 134
Subroutine GVF 137

Program ICEJAM ver. 1.5 141

Definition of Variables 141

Program Listing 144

Sample Data File 169

LIST OF TABLES

		page
Table 3.1	Results of passive pressure experiments	44
Table 6.1	Quantities used to examint the effect of changes in node spacing	76
Table 6.2	Quantities used in preliminary test runs	82
Table 6.3	Comparison of calculated ice volumes	95
Table 7.1	Results of tests on rectangular channel data	99
Table A1	Shear box test results	131

LIST OF FIGURES

		page
Figure 1.1	Hypothetical ice jam profile.	4
Figure 2.1	Plan view of a rectangular 'Janssen' element.	14
Figure 2.2	Plan view of a parabolic 'Caquot' element.	17
Figure 2.3	Nezhikovskiy's relationship between jam roughness and thickness in terms of roughness height, k.	19
Figure 3.1 a	Sketch of experimental apparatus (side view).	33
Figure 3.1 b	Sketch of experimental apparatus (plan view).	34
Figure 3.1 c	Photo of apparatus (side view).	35
Figure 3.1 d	Photo of apparatus (oblique view).	35
Figure 3.1 e	Close-up view of transducer.	36
Figure 3.1 f	Close-up view of transducer array.	36
Figure 3.2	Assumed triangular stress distribution.	41
Figure 3.3	Plot of force vs. time record for transducer no.4 (ie. centreline), experiment no.401.	43
Figure 3.4	Forces measured at T=0 for each experiment.	45

Figure 3.4	Continued.	46
Figure 3.5	Mohr's circle for experiment no.401.	48
Figure 3.6	Deformation pattern at the end of a test shown by curved lines of confetti.	48
Figure 4.1	Oblique view of ice jam element used in force balance.	52
Figure 4.2	Hypothesized developement of jam toe	61
Figure 5.1	Flowchart of ICEJAM program.	69
Figure 6.1 a	Comparison of calculated profiles with step sizes of 500m and 1000m.	77
Figure 6.1 b	Comparison of calculated profiles with step sizes of 500m and 2000m.	78
Figure 6.1 c	Comparison of calculated profiles using variable step sizes.	79
Figure 6.2 a	Calculated profile for run no. 01.	83
Figure 6.2 b	Calculated profile for run no. 20.	84
Figure 6.2 c	Calculated profile for run no. 30.	85
Figure 6.3	Dimensionless calculated thickness profiles for differing values of Q and K_{xy}.	87
Figure 6.4	Dimensionless calculated thickness profiles for differing values of k_1 and μ.	88
Figure 6.5	Magnitude of terms in differential thickness equation over length of jam.	91
Figure 6.6	Dimensionless calculated overall depth profiles for various values of μ.	93
Figure 7.1	Comparison of observed and calculated	

	water surface profiles for Athabasca River case study.	103
Figure 7.2	Comparison of present model with HEC-2 for Athabasca River case study.	107
Figure A1	Sketch of shear box apparatus.	120
Figure A2	Load displacement curves for shear box tests on polyethylene beads.	122
Figure A2	Continued.	123
Figure A2	Continued.	124
Figure A2	Continued.	125
Figure A2	Continued.	126
Figure A2	Continued.	127
Figure A2	Continued.	128
Figure A2	Continued.	129
Figure A3	Failure envelope for shear box tests on polyethylene beads.	132
Figure B1	Definition sketch for forward difference algorithm used in thickness calculations.	136
Figure B2	Definition sketch for 'standard step' algorithm used in depth calculations.	139

CHAPTER 1: REVIEW OF ICE JAM PROCESSES

INTRODUCTION

It is only in the last twenty years that ice related phenomena have received much attention in Canada. This, in spite of the fact that problems related to river ice have been identified for at least a century (eg. Henshaw, 1887, Barnes, 1928). One aspect of river ice behaviour that has caused severe damage in the past is the phenomenon of ice jamming.

River ice jams are a fact of life in the cold regions of the world. They can range in size from an innocuous lodgement to a massive barrage; they can cause severe flooding when they are in place and the liberation of surges and high velocity flow when they release.

Increased use of flood plains and the alteration of the natural flow regime in rivers for hydro power, transportation, land reclamation and other projects, has emphasized the need for greater understanding of ice jam problems. Some of the questions that arise are:

a) What are the conditions necessary to form an ice jam?

b) What are the mechanics of ice jam formation?

c) What action can be taken to prevent the formation of a jam?

d) How can a jam be released once it is in place?

e) What is the maximum water level that can be caused by a jam?

f) What is the probability associated with ice jam events?

The answers to these questions are the subject of much of the research that has been done. The main objective is to integrate ice jam theory into flood hazard zone delineation to aid in flood plain management and planning. At present, ice jam effects are often ignored in flood risk assessments although it is well established that ice jam-induced flood levels can be much higher at some locations than evem rare open water levels.

There are at least two approaches to ice jam related flood frequency analysis. The most direct is to simply analyze all existing historical data and separate ice-induced from open water events. In many situations, however, historical data may be unavailable or inappropriate, such as when evaluating the effect of proposed changes to a natural river. A deterministic approach, in which ice jam theory is used to establish water levels, must then be employed.

Another problem is the calculation of the water surface profile produced by an ice jam. While this a relatively simple matter under open water conditions, the ice jam case is not so straightforward. It is toward the end of improving analyses of this type that the present work is directed.

ICE JAM FEATURES

An ice jam can be simply described as an accumulation of ice floes or fragments in a river. Such an accumulation will cause a local rise in water level. The rise in water level is caused partly by the presence of the rough jam underside and partly by the draft of the submerged ice. In Figure 1.1 a hypothetical profile along an ice jam is sketched showing the various components of a jam.

A jam can form any time ice is present in a river. In the fall, as part of the freeze-up process, it will be composed of frazil slush or pans or perhaps the fragmented remains of a solid ice cover which formed upstream. Later in the season, a jam may form as part of the break-up process. It will then usually be composed of solid ice fragments. The size of particles comprising a jam can therefore vary over several orders of magnitude: from a dimension of several millimetres for frazil ice to several metres for solid ice floes in a break-up jam.

Ice floes of any size are transported downstream by the river until they meet some obstruction. In the case of a break up jam, this obstruction is often the undisturbed solid ice sheet. Other possiblities include 'arching' of the floes at a narrow section of the channel or obstacles like islands, shoals, bridge piers and ice booms. An ice jam develops as the floes accumulate upstream of this obstruction.

A jam experiences three forces in the streamwise

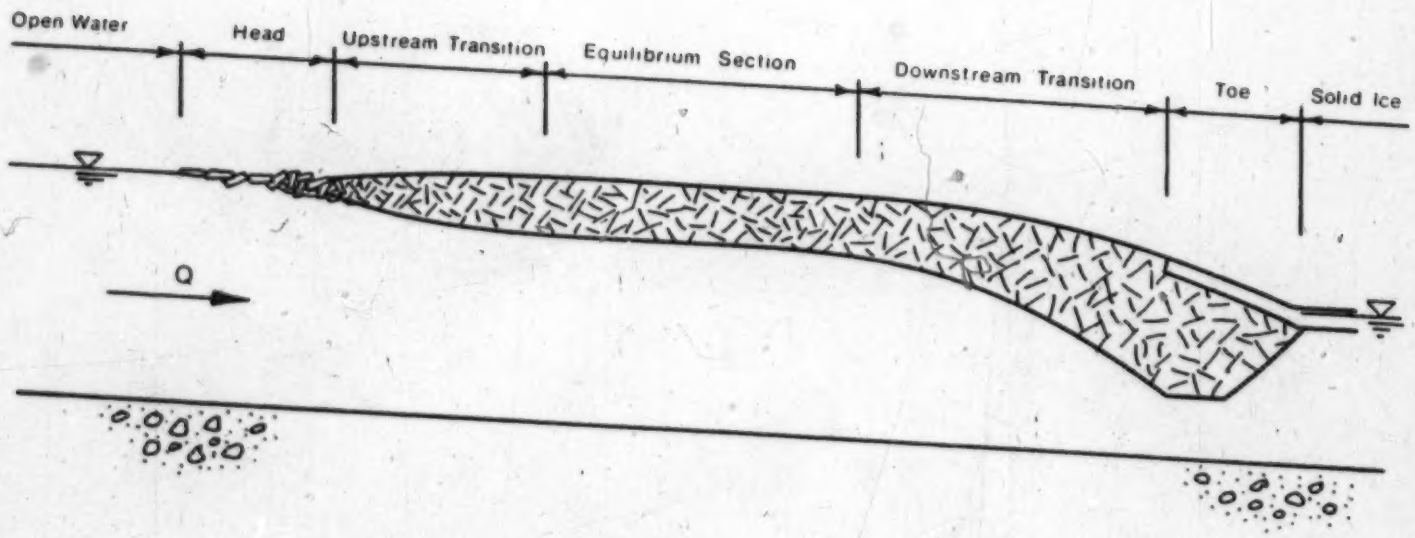

Figure 1.1 Hypothetical ice jam profile.

direction. The first is the downslope component of the weight of the jam (this includes the water in the pores as well as the weight of the ice). The second is a result of the shear stress imposed on the jam underside by the flowing water. The third force is applied at the upstream end or 'head' of the jam and may be a result of either the momentum change in the flow as it accelerates under this 'blunt' leading edge or momentum of the incoming floes (or a combination of the two). These streamwise forces are resisted by friction between the jam and the channel banks and by the obstruction at the downstream end or 'toe'.

An ice jam must have some internal strength to withstand the forces applied to it. There are two possible mechanisms for this internal strength and these determine whether the jam is of the 'cold weather' or 'warm weather' type. As the names imply, cold weather jams are those that form at sub-zero temperatures (usually associated with ice floe accumulation in the fall), and warm weather jams are those that occur when signifigant refreezing cannot take place.

A warm weather jam can only rely on interparticle friction for its internal strength, much like a granular soil. To mobilize the internal strength of a granular material some confining stress must be present. In the case of a floating ice jam this confining stress is due to the opposing actions of the buoyancy of the submerged ice particles and the weight of the unsubmerged ones. Clearly this confining stress increases with increasing jam thickness.

As ice floes accumulate at the head of a jam, the streamwise force on an element a short distance downstream of the head increases. At some point, this force will become too large and the jam in the vicinity of this element will collapse or 'shove' to attain a new, larger thickness which will provide sufficient resistance to the applied forces. The thickness profile in the upstream transition is a result of the increasing force experienced by an element as the jam lengthens upstream. This trend does not continue indefinitely because the accumulated resistance offered by the banks also increases with thickness and with distance along the pack. In other words, the jam transfers some of the applied force to the bank - a process which has been termed 'load shedding'. At some point, the upstream transition will be long enough that the total streamwise force will just be balanced by the resistance at the banks and so any additional increase in accumulation length will not increase the force on an element downstream of this transition. The thickness so attained is called the 'equilibrium thickness'. It should be noted that an equilibrium section will only form if the channel is more or less prismatic and if the jam is long enough that the upstream and downstream transition regions do not overlap, in which case the jam is said to be 'fully-developed'.

In some cases the thickness at the head of the jam will be sufficient that no further increase is required as the jam lengthens upstream (ie. the thickness at the head is equal to

or greater than the equilibrium thickness). In this case the thickness is determined completely by the mechanism governing the accumulation of floes at the head. This may be simple juxtaposition of the floes to form a single layer or it may be underturning and deposition of the floes depending primarily on the upstream velocity. Such a jam is called a 'narrow channel jam' while the more usual case described previously is a 'wide channel jam', both terms following from the fact that the equilibrium thickness depends on the channel width.

The behaviour of the toe of an ice jam is the most poorly understood aspect of the phenomenon. One possible toe configuration - which may be termed a 'floating toe' - is that shown in Figure 1.1 in which the jam is restrained by the solid ice cover. The resistance is mostly provided by friction between the submerged ice fragments and the solid ice underside. The accumulation is supported only by buoyancy (hence the term 'floating toe') and the flow is through the open waterway beneath.

In the usual mild channel the change in roughness from the relatively smooth solid ice sheet to the rougher jam underside gives rise to a gradually varied flow profile of the M2 type. This flow profile extends through the 'downstream transition' section of the jam. If the jam is long enough, the gradually varied flow profile will reach uniform flow conditions in the equilibrium section.

A result of the M2 water surface profile is an increase in thickness for two reasons. One is due to the increase in

the downslope component of jam weight and the other is the increase in shear on the jam underside.

A cold weather jam is one in which the internal strength is due to freezing together of the ice particles. Michel (1978 b) has discussed this concept and points out that just a thin layer of solid ice frozen into an accumulation of floes provides far more resistance than internal friction. This can be an important mechanism in a freeze-up jam when air temperatures are low. It should be pointed out that the upstream transition shown in Figure 1.1 would not exist in a jam of this type. In a cold weather jam the thickness is governed by conditions at the head of the jam only since sections further downstream have adequate strength (via the refreezing process) to withstand the applied forces and so no further modification is required.

The remainder of this thesis will concentrate only on the warm weather type of jam since it is the worst case and the most common cause of flooding. Furthermore only the wide channel case will be discussed since it is by far the most common circumstance.

ANALYTICAL REQUIREMENTS

A common problem in Hydrotechnical Engineering is prediction of flood levels at a particular site. For open water conditions there is a vast body of literature and well

developed theory which allows reliable predictions to be made. Unfortunately the same is not true for ice covered conditions even though, in cold regions such as Canada, flood levels caused by an ice jam are often well in excess of those caused by a severe open water flood.

Perhaps the main reason for this is the uncertainty regarding the formation of a jam. Jam formation is very dependent on local channel and ice characteristics as well as meteorological conditions. At present it is almost impossible to predict when, where, or even if, a jam will form near a particular site in a given year. However the fact remains that in many cases ice jam induced floods produce the highest water levels and so some cognizance of them must be taken in any flood study of a reach in which they are known to occur.

Perhaps the simplest means of incorporating ice effects into a flood frequency analysis is that proposed by Gerard and Karpuk (1979) in which the peak break-up water levels for the period of record are analyzed using their concept of 'perception stage'. This method allows not only gauging station records but also newspaper and other historical accounts to be used. Another, more deterministic, method uses discharge records and ice jam theory to develop a flood frequency relationship (Gerard and Calkins, 1984).

Usually both of these method yield a design water level at one location: the problem is then to compute the water surface profile throughout the reach of interest. Whereas this is a relatively simple problem under open water

conditions for which there are readily available computer programs (for example HEC-2), under ice-covered conditions only crude methods are presently available.

CURRENT PROFILE MODELS

As described above, an ice jam in a prismatic channel will, if it is long enough, have a reach - the equilibrium section - characterized by constant thickness and uniform flow. It can be argued that the equilibrium stage is the highest that can be attained by a jam and calculation of the water level and thickness in an equilibrium reach is straightforward. Such equilibrium calculations seem to form the basis of many of the existing ice jam profile models.

Since prismatic channels are relatively rare, some assumptions are required to justify such applications of the equilibrium theory to the usual non-uniform reach. The assumption usually made is that the equilibrium thickness is applicable at any cross-section and can be calculated from local channel geometry and flow conditions. The thickness is often calculated using the stability criteria of Pariset et. al. (1966) which will be discussed later (see for example, Clement and Petryk, 1980, Petryk et. al. 1980, and US Army Corps of Engineers, 1982). Keenhan et. al. (1980) briefly discuss three computer models which are based on this assumption.

Such an assumption obviously has some serious limitations. One of these being that in many cases an equilibrium section cannot exist because the jam is too short or the channel too non-prismatic. It has not yet been established what length a jam must have to be fully-developed, even in a prismatic channel. Another unresolved question is the effect of the interaction between the water surface and thickness profiles in a non-uniform reach. Clearly the two are intimately related and it remains to be shown that the application of equilibrium theory at each section in a non-uniform reach is a valid simplification. Furthermore, some of the assumptions underlying the development of equilibrium ice jam theory remain to be independently tested.

Some of these problems were addressed in this investigation by developing a computer model which is capable of calculating the thickness and water surface profiles of an ice jam over its entire length in a non-uniform channel. This model is based on the usual gradually varied flow equation as well as the differential thickness equation which has been developed by others. This model will allowed calculation of the length of an ice jam required for it to be fully-developed and an assessment of the validity of the equilibrium thickness assumption which is used in present models. It can also be used to investigate the influence of various parameters on jam profile shape.

CHAPTER 2: LITERATURE REVIEW

INTRODUCTION

A considerable body of literature dealing with ice jam behaviour has evolved over the past two or three decades. Of particular interest here is the literature concerned with the wide-channel type of jam. Although many gaps still exist in the present state of knowledge, it is possible to develop a rational model of ice jam behaviour based on this pioneering work.

Most of the early river ice research was inspired by difficulties encountered in winter operation of hydro-electric plants in both Canada and the USSR. This early research was primarily qualitative in nature and used observations to establish guidelines for reliable operation. These observations soon led to a theoretical framework which could be used to anticipate changes in ice regime brought about by changes in channel geometry or discharge. Later, observations were extended to natural rivers and laboratory models so that the problem of ice-related flooding could be addressed.

EARLY RESEARCH

One of the earliest attempts to incorporate observations of ice jam behaviour into a theoretical framework was that of Pariset and Hausser (1961) and Pariset, Hausser, and Gagnon (1966). The analysis drew heavily on the experience and observations of the Quebec Hydroelectric Commission regarding the operation of several hydro-electric facilities. This early work was important in that it identified the basic concepts and provided simple methods of analysis, most of which survive today. In particular, Pariset et al. differentiated between 'wide' and 'narrow' channel jams and developed expressions to predict their thickness. The analysis of the wide channel case, as pointed out by Gerard (1979), was the same as that performed by Kennedy (1958) in a study of the forces involved in pulpwood holding grounds.

The wide channel jam analysis was based on the apparent analogy between ice blocks (or pulpwood logs) confined between the banks of a river and a granular material confined between silo walls. This silo analogy allowed use of the pioneering theory of Janssen (1895) whose formulation results from a force balance on a planar element of small thickness oriented perpendicular to the long axis of the silo. Such a 'Janssen

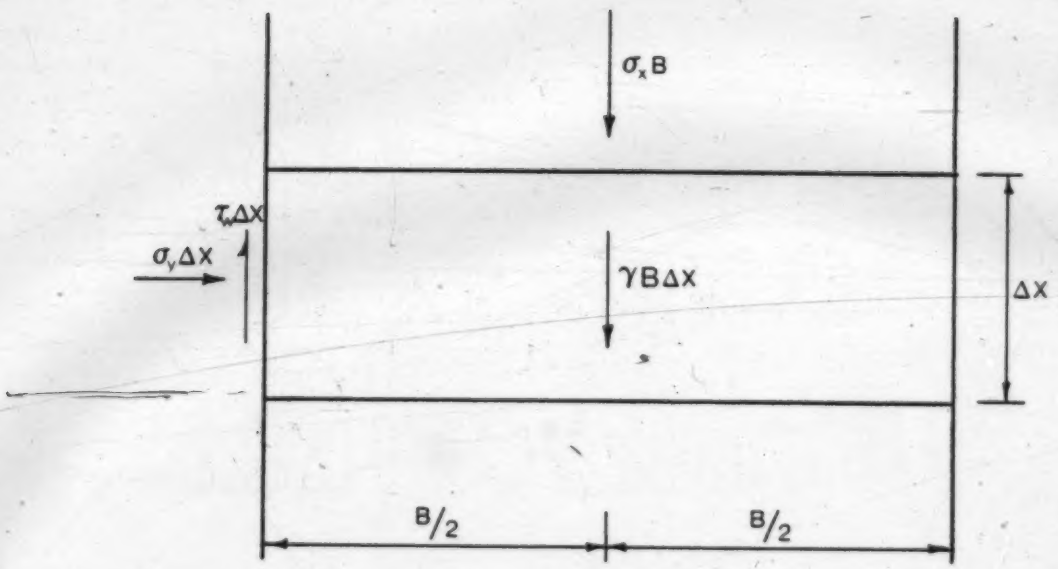

Figure 2.1 Plan view of a rectangular 'Janssen' element.

element',similar to that used by Pariset et al., is shown in Figure 2.1.

Pariset et al. conducted a force balance on this element and, introducing the simplification that the Chezy coefficient of the bed and the jam underside are the same, obtained:

[2.1] $$\frac{BV^2}{\mu C^2 H^2}\left[1 + \frac{\rho' t}{\rho R}\right] = \frac{2c_1 t}{\rho g \mu H^2} + \frac{\rho'}{\rho}\left(1 - \frac{\rho'}{\rho}\right)\frac{t^2}{H^2}$$

where: B = channel width

V = velocity of flow under jam

μ = jam strength parameter

C = Chezy coefficient (of bed and jam underside)

H = overall water depth (ie. waterway plus submerged ice thickness)

t = thickness

R = hydraulic radius

ρ' = ice density

ρ = water density

c_1 = cohesion

g = acceleration due to gravity

In carrying out the analysis, Pariset et al. assumed that the thickness along the accumulation is constant and that uniform flow conditions prevail. Hence Equation [2.1] is valid only

in the equilibrium section of the jam.

Measurements taken on the Beauharnois Canal indicated that μ had a value of 1.28 and that c_i was negligible for all but very thin jams. Assuming $c_i = 0$, $\mu = 1.28$, and a wide, rectangular channel, Pariset et al. derived the familiar bell-shaped curve which results when Equation [2.1] is plotted in the form of $Q/(C^2BH^4)$ (Q being the discharge) is plotted against t/H. A jam which plots above this stability curve will collapse and thicken to a point on or below the curve. It should be noted that this stability criterion is used in some of the present ice jam profile models (see for example Keenhan, Panu and Kartha, 1980; Petryk and Boisvert, 1978) even though the roughness of the bed and jam underside are very different in most cases.

Somewhat parallel to the work of Pariset et al. is that of Michel. Much of Michel's early work was published in French, but more recent summaries of this work are available in English (Michel, 1971, 1978 a). Michel's wide channel jam analysis is very similar to that of Pariset et. al. except that it is based on his interpretation of Caquot and Kerisel's (1956) silo theory. This theory makes use of an element of parabolic planform as shown in Figure 2.2.

Concurrent with the early Canadian research was work done in the Soviet Union, most notably that of Nezhikovskiy (1964) and Berdennikov (1965). Nezhikovskiy's compilation of roughness measurements remains the only comprehensive data

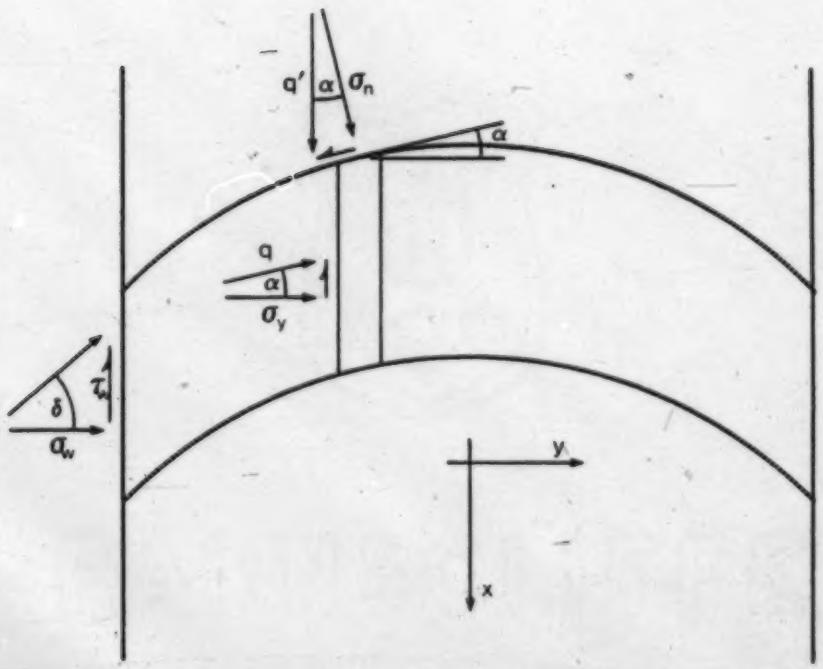

Figure 2.2 Plan view of a parabolic 'Caquot' element.

set applicable to ice jams. The Nezhikovskiy data is a compilation of Manning's n computed for various freeze-up ice cover conditions on Soviet rivers. The pertinent information was gathered from gauging station records and the cross-section properties used were calculated only for the gauging site and so are not 'reach-averaged'. Nezhikovskiy found that the roughness depended on the thickness of the accumulation (a finding consistent with Kennedy's (1958) measurements on laboratory-scale log jams). Nezhikovskiy's proposed relationship between roughness and thickness is shown in Figure 2.3 using the hydraulic roughness height, k, rather than Manning's n (the conversion was made assuming that the hydraulic radius was 1.5 m in each case as suggested in the original text).

Berdennikov (1965) undertook what is believed to be the first laboratory investigation into the mechanical properties of fragmented ice. His apparatus consisted of a small annular flume which could be filled with fragmented ice and then chilled so that the sample would freeze to the walls. By rotating the inner flume wall, a shear failure could be produced within the sample. A confining stress could be applied to the sample by means of air pressure and a rubber membrane. Unfortunately, this is not easily related to the normal stress on the failure plane which is the stress required to define the Mohr failure envelope.

Berdennikov's results indicate that cohesion was large (about 33 Pa) and that the effect of confining stress was

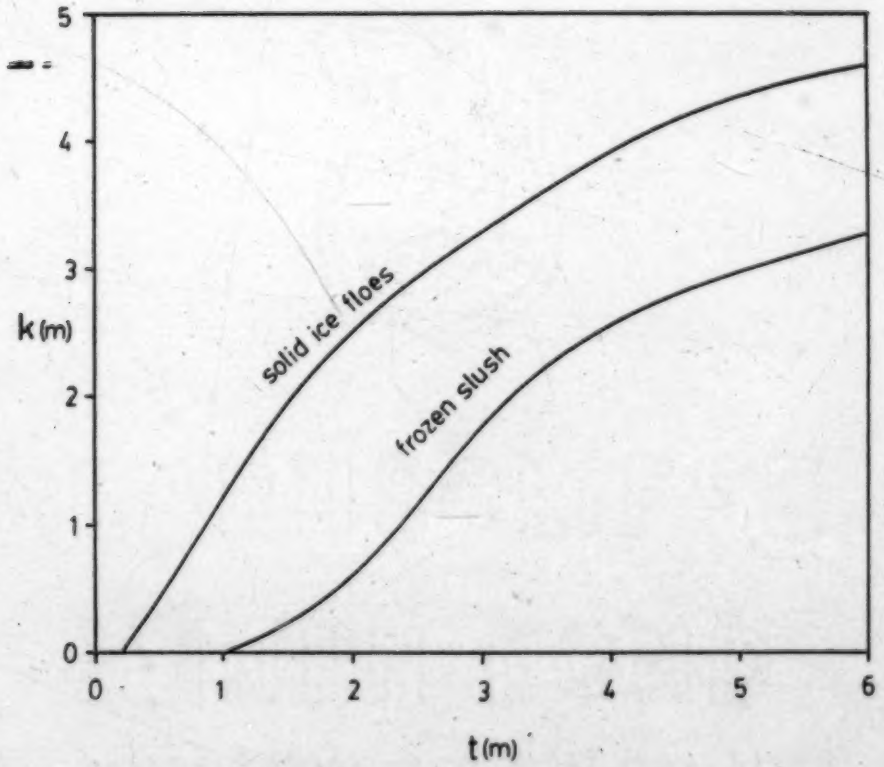

Figure 2.3 Nezhikovskiy's relationship between jam roughness and thickness in terms of roughness height, k.

negligible (ie. $\phi \approx 0$, where ϕ is the angle of shearing resistance). This can perhaps be attributed to experimental conditions which would have promoted refreezing of the particles (ie. ice fragments freezing together at points of contact) with the result that the ice fragments did not behave as a cohesionless granular material.

Also of interest are Berdennikov's measurements of the physical characteristics of fragmented ice. He weighed six samples of fragmented ice, each with a different particle size composition, and found fairly consistent bulk unit weights of between 0.52 and 0.60 g/cm^3. This indicates porosities (assuming that the specific gravity of ice is 0.92) between 0.38 and 0.43.

RECENT DEVELOPMENTS

During the 1970's a significant amount of work was done at the Iowa Institute of Hydraulic Research, aimed primarily at developing a more general theory for wide channel ice jams and establishing the strength characteristics of a fragmented ice cover.

Uzuner and Kennedy (1974, 1976) extended the analysis of Pariset et al. to include non-uniform flow and thickness as well as some time-dependent aspects of jam formation. This led to the development of a computer program for calculating the water surface and thickness profiles in the upstream

transition region of a jam.

The strength characteristics of a fragmented ice cover were investigated by a number of researchers whose results were summarized by Cheng and Tatinclaux (1977). Three experiments were devised, one to measure the compressive strength and two to measure the shear strength.

The compressive strength apparatus consisted of a tank over which a carriage travelled on rails, the entire apparatus being housed in a cold room. Attached to the carriage was a plate instrumented to measure the force applied to it. To conduct the test, the tank was filled with water (chilled to 0°C) and a sample of fragmented ice or ice cubes was placed in the water in a uniformly thick layer. The carriage was then moved at a constant rate so that the plate caused the floating sample to collapse in compression.

The first of their shear experiments was conducted in the same tank as the above experiment. It consisted of a rectangular box divided by an I-shaped partition. A sample of fragmented ice or ice cubes was floated in the box and the I-shaped partition moved at a constant rate so as to produce two shear failure planes in the specimen.

The second shear apparatus was similar to the vane shear test device used in soil mechanics. The apparatus consisted of a cross-shaped vane enclosed in a concentric cylinder. The cylinder was filled with water and a sample of fragmented ice was placed inside. A shear failure was produced by rotating the vane.

Unfortunately, these experiments, as those of Berdennikov, allowed no control over the normal stress on the failure plane and so it is impossible to determine the angle of shearing resistance, Ø. The Iowa researchers also measured very high values of shear strength, much higher than could be obtained by granular material behaviour under plausible normal stresses for the test conditions. This implies that refreezing was taking place and what was in fact being measured is the strength of these bonds. The formation of these bonds is clearly a time dependent process which probably explains the observed marked dependence of the measured shear strength on deformation rate. It also implies that the measured strength is very dependent on test conditions (room temperature, water temperature and so on) and on test procedures (length of time between placement of sample and failure for one). It is not known at present how closely these test conditions model the behaviour of fragmented ice in nature.

Another major research program of the 1970's was initiated by Gerard (1975) at the Alberta Research Council. This program was based on a relatively economic and rapid field observation technique in which ice jams were photographed from the air to show the position of the water surface relative to some identifiable landmark at several locations along the jammed reach. In summer, a field party

returned to establish the elevation of these landmarks and so obtain a relatively accurate 'instantaneous' water surface profile through the jam. These summer surveys also established the open water slope and channel geometry in many cases.

This field program culminated in a paper by Beltaos (1983) in which 13 case studies were analyzed. Beltaos simplified the thickness equation obtained by Uzuner and Kennedy (1976) and showed its similarity to the expression of Pariset et al. (1966) in the equilibrium section. He then rearranged Equation [2.1] into a more meaningful dimensionless depth-discharge relation which has μ (the jam strength parameter) and the bed and jam roughnesses as parameters. Of these, only the bed roughness can be determined independently. To obtain estimates of μ for the various case studies, Beltaos developed a relationship between jam roughness and thickness based on Nezhikovskiy's (1964) data. Using this relationship, along with his depth-discharge equation, Beltaos found that μ varied from 0.6 to 3.5 for the 13 case studies he examined. The two extreme values were based on questionable data and if they were neglected the range was reduced to 0.8 - 1.3 with an average of 1.2 (a value very similar to that found by Pariset et al.).

A somewhat different analysis of one of the Alberta case studies was performed by Andres and Doyle (1984). An ice jam on the Athabasca River near Ft. McMurray in 1978 remained in

place for three days allowing complete profile measurements to be made at three quite different discharges. By assuming the roughness and thickness of the jam did not change between the first two measurements, Andres and Doyle were able to solve for μ and n_i (where n_i = Manning's n of the jam underside) using Manning's equation and equilibrium jam theory. The values they found were $\mu = 1.6$ and $n_i = 0.072$. It should be noted however that these results are very sensitve to the uniform flow equation used and to small errors in the measured stage.

The Cold Regions Research and Engineering Laboratory (CRREL) of the U.S. Army Corps of Engineers has also been active in ice jam research. Calkins (1978) reported the first thickness profile measurements of break-up ice jams. These measurements were made on two small New England streams in which a jam had occurred and then frozen in place. The results indicated the thickness generally decreased in the upstream direction as expected, but that there was considerable scatter. Calkins also noted that the size of floes comprising the jam decreased in the upstream direction. Calkins (1983) addressed the problem of ice jams in channels with floodplains. Like Beltaos, Calkins rewrote the stability equation of Pariset et al., using the hydraulic radius as the length scale to non-dimensionalize the terms.

Sodhi and Weeks (1978) presented a one-dimensional formulation governing the force exerted on an obstacle by an ice jam in a straight channel. The resulting equation is almost identical to that of Pariset et al. (1966) although much less restrictive assumptions were used in its derivation. An important point made by Sodhi and Weeks is that the usual assumption that the full material shear strength is mobilized at the banks provides a lower bound on the thickness, and thereby on the water level, which can be attained by a jam.

Stewart and Daly (1984) performed a series of experiments to better define the relationship between the longitudinal and transverse stresses in an ice jam. Very little is known about this relationship. For example Pariset et al. could only speculate that the ratio of transverse to longitudinal stress is less than or equal to one. Unfortunately, the scatter in the results of Stewart and Daly makes refinement of this relationship difficult.

Recent work by Beltaos, now at the Canada Centre for Inland Waters, has concentrated on conditions near the toe of a jam. Beltaos and Wong (1986) described a computer program which allows the thickness and water surface profiles in the downstream transition to be calculated, taking into account the flow through the pores of the accumulation which was found experimentally to depend on the square root of the

water surface slope. The program is based on the differential thickness equation developed by Uzuner and Kennedy (1976) and on the momentum and continuity equations.

The solution procedure used by Beltaos and Wong is virtually identical to that of Uzuner and Kennedy in that the thickness and depth of flow at equilibrium are used as the starting boundary conditions. The solution proceeds downstream until the underside of the jam and the channel bed intersect. The uniform flow stage downstream of the jam is then compared with the stage at the point of 'grounding' to determine if the jam has a 'floating' or 'grounded' toe.

DISCUSSION

From the above brief review of the literature, it is apparent that current ice jam theory is essentially one-dimensional (ie. variation of thickness or longitudinal stress across the channel is not considered). This relatively simple one-dimensional theory is fairly well developed but the numerical value of some of the parameters can only be crudely estimated. This is mainly due to the difficulties involved in obtaining a complete set of field measurements, measurements which must include either thickness or jam roughness, in addition to the usual

hydraulic parameters, if a closed set of relations is to be obtained.

As such measurements are usually not available, it would be useful if some other means were available to estimate the required parameters. The most fundamental strength parameter in a cohesionless jam is the angle of shearing resistance, Ø. While Ø is a commonly measured quantity in soil mechanics, it is rather difficult to measure for fragmented ice. This is primarily due to the temperature and strain rate dependence of the physical properties of ice. Despite these difficulties, much more effort must be made to understand the mechanical behaviour of fragmented ice because this will lead to a more rational definition of the parameters used in ice jam theory.

One of the most important of these parameters is the ratio of longitudinal to vertical stress, denoted K_v. The vertical stress in a jam is directly related to the thickness and so K_v is the link between streamwise stress and thickness. As a start to a more fundamental investigation of the mechanics of floating packs, the evaluation of this parameter will be considered next. Thereafter, this investigation concentrates on the development of a solution algorithm for calculating the full profile of an ice jam without the necessity for the jam to be fully-developed, as assumed by Uzuner and Kennedy and Beltaos and Wong.

CHAPTER 3: EXPERIMENTAL VERIFICATION OF PASSIVE PRESSURE CONCEPT

INTRODUCTION

Current equilibrium ice jam theory is based on the simple, one-dimensional formulation propsed by Pariset et. al. (1966). As will be shown later, several fundamental parameters describing the properties of fragmented ice are combined in this theory to give a single dimensionless parameter, μ.

The generalization of this theory, to include the non-equilibrium reaches of a jam, requires that the individual components of μ be defined separately so that calculation of an entire ice jam thickness profile is possible. Furthermore, the definition of μ in terms of more fundamental parameters may eventually allow its estimation without resorting to difficult field measurements.

Uzuner and Kennedy (1976) attempted this by estimating the required jam strength parameters from the results of laboratory experiments. However, these investigators did not present their results in terms of the angle of shearing resistance, $\emptyset$, as is usually done in soil mechanics. In the

following, an attempt will be made to define one of the components of μ in terms of ϕ.

THE PASSIVE PRESSURE CONCEPT

As mentioned, one of the most important parameters which is implicit in μ, is K_v, the ratio of longitudinal to vertical stress. Some investigators (eg. Pariset et al., 1966) have noted the similarity between the 'shoving' behaviour of an ice jam and the passive pressure concept in soil mechanics, and so proposed that:

$$\sigma_x = K_v \sigma_z \qquad [3.1]$$

where: σ_x = thickness-averaged longitudinal stress

σ_z = thickness-averaged vertical stress

K_v = passive pressure coefficient = $\tan^2(45 + \phi/2)$

ϕ = angle of shearing resistance

Equation [3.1] is valid only at incipient failure, in which case the relationship holds for both point values and thickness-averaged values of stress. An inherent assumption in the use of [3.1] in the present context is that both σ_x

and σ_z can be considered principal stresses.

In general, the shear stress on the jam underside, τ_i, is small compared to the vertical stress and so σ_z can be approximated as a principal stress. However, the thickness-averaged value of longitudinal stress, σ_x, can only be a principal stress where the shear stress in the horizontal plane is also zero. Since there is a shear stress at either bank, σ_x cannot be a principal stress everywhere. However, it can be shown by symmetry that at the centreline the shear stress is zero and so σ_x will be a principal stress there.

Thickness-averaged values of stress are used in ice jam theory for simplicity. The actual distribution of stress over the thickness has never been measured but it is not likely to be significantly non-linear. This accords with the common assumption made in Geotechnical Engineering whereby retaining walls are designed based on the assumption that soil pressure increases linearly with depth (see for example Bowles, 1982). Given this assumption, the average vertical stress, σ_z, can be calculated from (Uzuner and Kennedy, 1976; Mellor, 1980):

$$\sigma_z = \gamma_e t \qquad [3.2]$$

where: $\gamma_e \cong 0.5\rho' g(1- \rho'/\rho)(1 - e)$

ρ' = ice density

ρ = water density

g = acceleration due to gravity

e = porosity

Versions of [3.1] and [3.2] have been used in the past (eg. Michel, 1970, 1978 a) but their validity has never been checked. The experiments of Uzuner and Kennedy (1974) and Cheng and Tatinclaux (1977) do not allow these relationships to be tested because the value of Ø for the ice fragments they used is unknown. The validity of equation [3.1] can only be confirmed by an experiment in which σ_x, σ_z and Ø are measured independently.

EXPERIMENTAL PROGRAM

An experiment was devised in which a floating, granular mass was caused to fail in compression under conditions similar to those in an ice jam. The force required to cause this failure was then compared to that which was predicted by

Equation [3.1] from the mechanical properties of the test material.

Low density polyethylene beads were chosen as the test material for several reasons. First, they are relatively inexpensive and easily obtained. They also have the appropriate size and shape for the experiment: the beads are small cylinders, about 3 mm in diameter and ranging in length from about 0.5 mm to 5 mm, with a mean length of about 1 diameter. They have a density slightly less than that of water and will therefore float (coincidentally, the specific gravity of low density polyethylene is 0.92, about the same as fresh water ice). The advantage of polyethylene over ice is that the tests can be carried out at room temperature and the refreezing problem is eliminated.

The experimental apparatus is very similar to that used in the crushing strength experiments initiated by Uzuner and Kennedy (1974) and continued by Cheng and Taitinclaux (1977). The apparatus is shown in Figure 3.1. Essentially, the set-up consists of a rectangular plexiglass tank with two walls artificially roughened, over which a carriage rides on aluminium rails. The test section was approximately 0.6 m by 1.5 m and the tank was 0.5 m deep. The carriage supports an array of seven instrumented 'paddles' which are lined up edge to edge to form a barrier. These paddles are rectangular plexiglass sheets attached to an aluminium rod. Each aluminium rod has a flat section milled into it on which two strain gauges are attached, one on either face, forming a

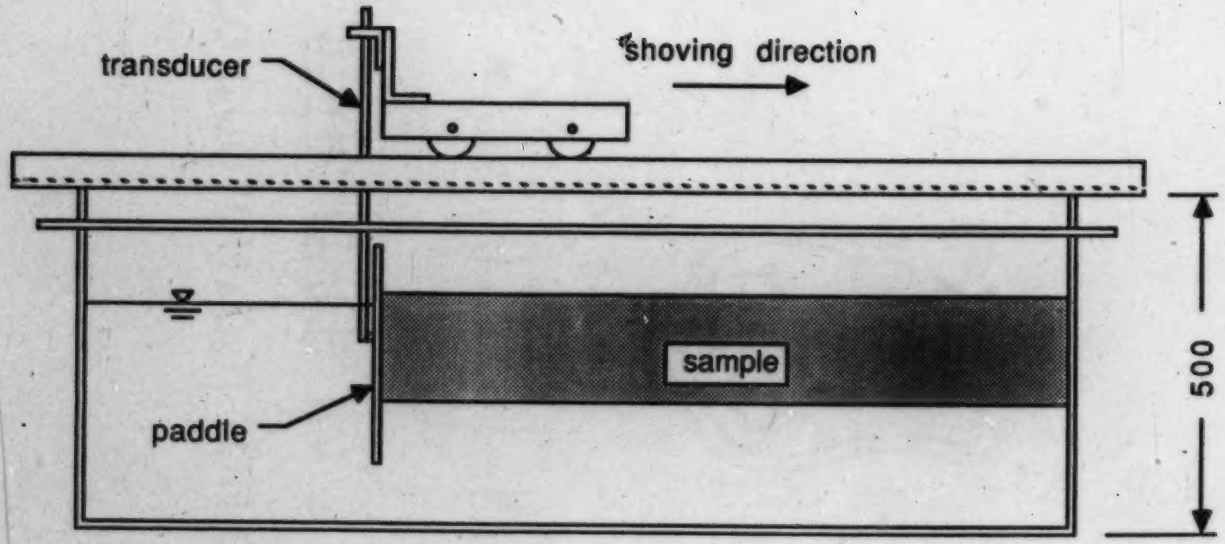

Note: Dimensions in mm

Figure 3.1 a Sketch of experimental apparatus (side view).

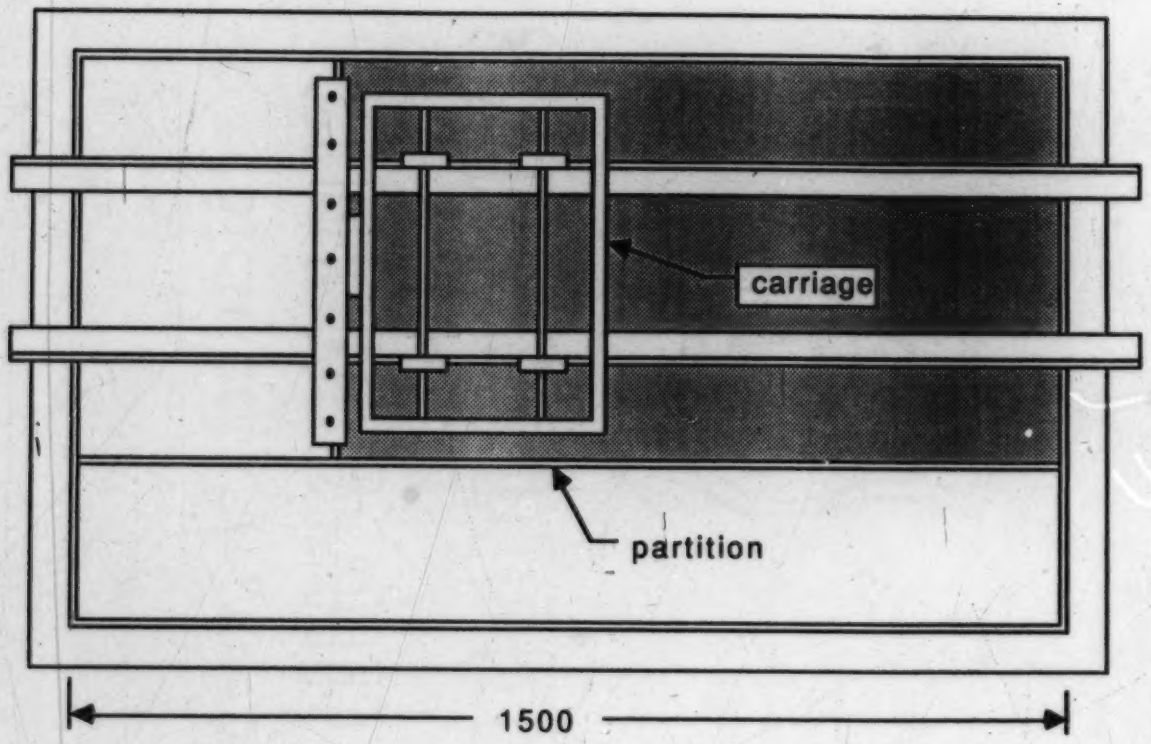

Figure 3.1 b Sketch of experimental apparatus (plan view).

Figure 3.1 c Photo of apparatus (side view).

Figure 3.1 d Photo of apparatus (oblique view).

Figure 3.1 e Close-up view of transducer.

Figure 3.1 f Close-up view of transducer array.

sensitive force transducer. These force transducers were each connected to a Validyne CD19 signal conditioner/ amplifier which was in turn connected to a micro-computer controlled data aquisition system.

Each transducer was calibrated in place by applying a known load and recording the output voltage. The known load was applied by attaching the transducer to a pendulum of known weight and length. The distance that the pendulum was pulled from vertical was related to the force applied. The transducers were found to have a sensitivity better than 0.01 N and were designed to have a capacity of about 10 N.

One end of the carriage was connected to a winch by a thin wire cable. The other end was connected by way of a wire cable and a pulley to a lead weight. In this way the carriage could be moved forward and backward by controlling the speed and direction of the winch. The cable which supported the lead weight was also wrapped around a pulley attached to a potentiometer. This provided the means of relating the carriage position to a voltage which was transmitted to the data aquisition system. The data aquisition system was turned on by a micro-switch attached to the carriage. A small movement of about 2 - 5 mm was required by the carriage to close this switch. Once underway, the data aquisition system recorded a complete set of readings every half second.

The output from the data aquisition system was stored on floppy diskettes and then transferred to a mainframe

computer where the output voltages were multiplied by the appropriate calibration coefficients and a plot was generated. A complete data set for one experiment consisted of a force record for each of the force transducers and a record of the change in carriage position with time.

EXPERIMENTAL PROCEDURE

The tank was filled with water, which contained a small amount of detergent to reduce surface tension, to the desired level and the carriage placed so that the paddles were at the starting position. A sample of polyethylene beads was introduced and stirred to achieve a uniform thickness. The carriage was then started. When the test was complete, the carriage was reversed and the sample re-leveled in preparation for the next test. Tests were performed at one thickness and two different carriage velocities.

EXPERIMENTAL RESULTS

Because of symmetry, the shear stress within the accumulation is zero at the centreline and so, at this point at least, σ_x should be a principal stress. Since there is

no flow of water in the tank, there is no shear on the underside of the sample and so σ_z is a principal stress everywhere. Therefore, the hypothesis to be tested is whether, when σ_x is increased to a level causing failure, σ_x at the centreline and σ_z will indeed be related by Equation [3.1], and γ_e can be calculated from Equation [3.2].

The 'effective' bulk density, γ_e, can be calculated from the expression given with Equation [3.2] if the specific gravity and porosity of the polyethylene beads is known. These quantities were measured using the procedure outlined in Appendix A. The average values were $\rho'/\rho = 0.92$ and $e = 0.38$. Using these, a value of $\gamma_e = 224$ N/m^3 is obtained which, through Equation [3.2] gives σ_z for each experimental run.

In the experiments, the force applied to each of the paddles was calculated by multiplying the output voltage by the appropriate calibration coefficient. The result must then be multiplied by another factor to account for the position of the centroid of the pressure distribution relative to the end of the transducer (the transducers were calibrated assuming the force was applied at the end).

Assuming the triangular pressure distribution shown in Figure 3.2, the centroid is located a distance d_c below the water given by:

[3.3] $$d_c = [2(\rho'/\rho) - 1]t/3$$

where: t = thickness of sample

The true force will depend on how far the centroid of the pressure distribution is from the end of the transducer and can be found by multiplying the measured force by the ratio of assumed and actual moment arms. The assumed moment arm is the distance from the strain gauge to the end of the transducer while the actual moment arm is the distance from the strain gauge to the centroid of the pressure distribution. For the test conditions, this meant that the measured forces had to be multiplied by a factor of 1.115.

Although σ_x is only a principal stress at the centreline it was reasoned that the stress applied to the two paddles on either side of the centre one would not be too different (this was supported by the experimental results) and therefore σ_x was calculated from the average of the three central paddles in an effort to 'smooth out' some of the experimental variability.

As pointed out previously, some 2 - 5 mm (or about one particle diameter) movement of the carriage had already occurred before the data aquisition system was enabled (at T

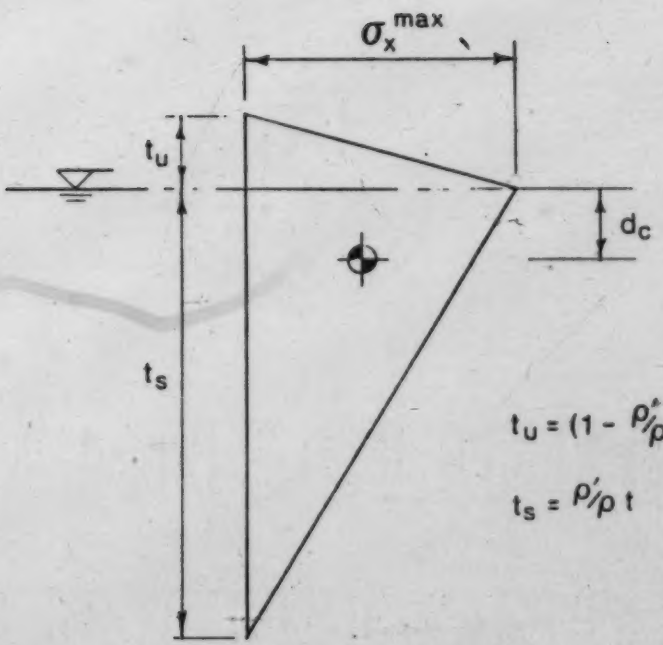

Figure 3.2 Assumed triangular stress distribution.

= 0, T being time into experiment) and so it is not unreasonable to assume that failure had already begun at this point. Using the forces at T = 0 is convenient because the thickness of the sample adjacent to the paddles is known accurately: the sample thickness increases continuously near the paddles as time goes by due to the failure occurring there.

Two series of tests were run with a sample thickness of 50 mm and carriage velocities of 1.42 mm/s and 2.36 mm/s. An example of the force vs. time record obtained is shown in Figure 3.3. A 'best fit' line was drawn through the points by eye and the force corresponding to the T = 0 intercept noted.

The force on each of the paddles is given in Table 3.1 and shown graphically in Figure 3.4 for each of the test runs. From the average force on each of the three central paddles, the value of σ_x was calculated given the paddle width (81 mm) and the measured sample thickness. σ_z can be calculated from Equation [3.2] with the value of γ_e = 224 N/m^3 determined previously. The angle of shearing resistance, Ø, can be determined on the basis of Mohr's circle, an example of which is shown in Figure 3.5. The results are summarized in Table 3.1. The average value was 47.3 .

The measured forces were observed to decrease from a maximum near the centre to a minimum near the walls. This is explained by the rotation of the principal stress axes near

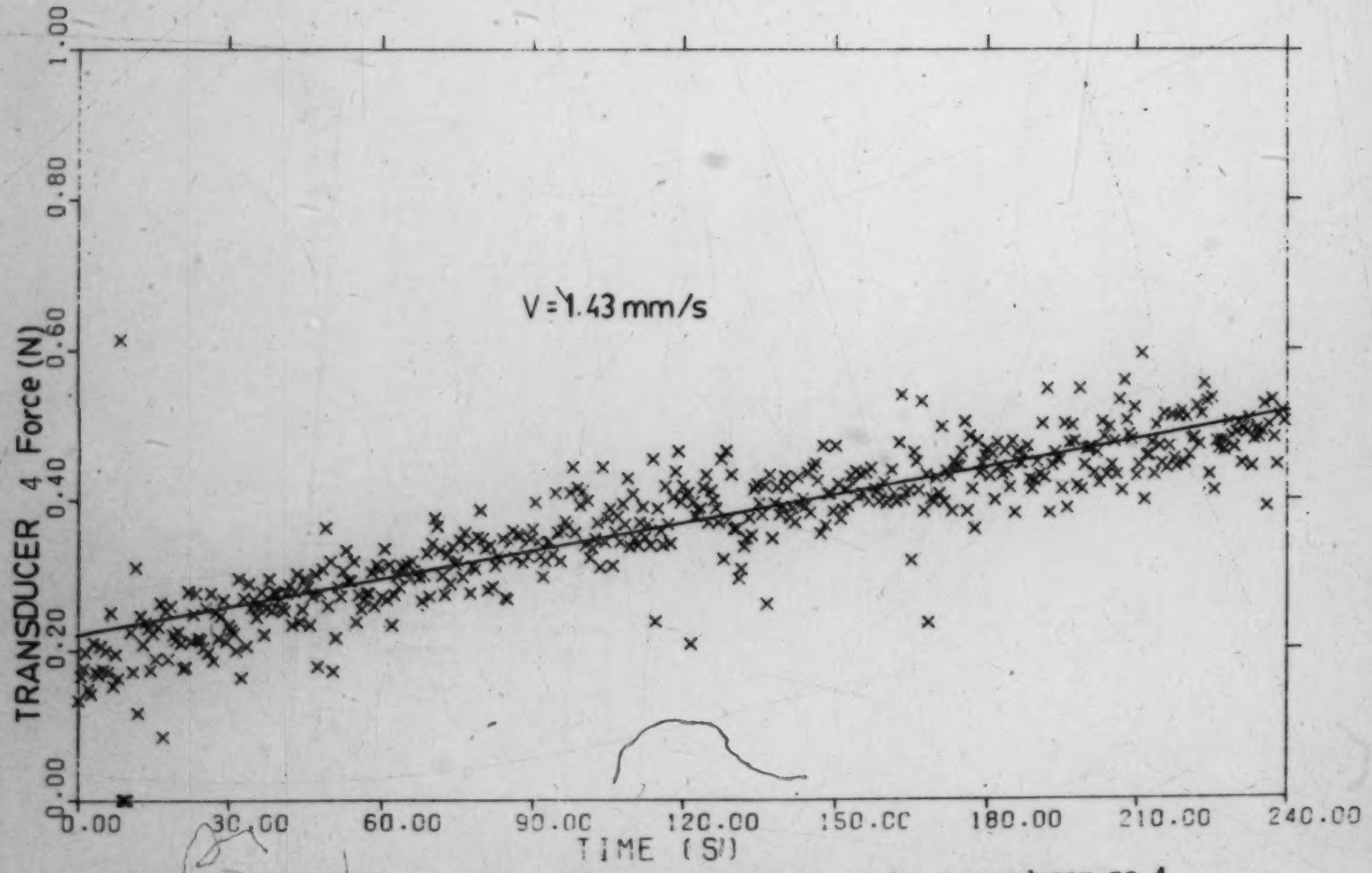

Figure 3.3 Plot of force vs. time record for transducer no.4 (ie. centreline), experiment no.401.

TABLE 3.1

Results of Passive Pressure Experiments

Run	t (mm)	V_c (mm/s)	F (N)	σ_x (Pa)	σ_z (Pa)	ø °
401	50	1.43	0.31	77	11	49
402	50	1.41	0.30	74	11	48
404	50	1.42	0.31	77	11	49
405	50	2.36	0.26	64	11	45
406	50	2.36	0.26	64	11	45
407	50	1.42	0.29	72	11	48
					Average =	47

t = sample thickness
V_c = carriage velocity
F = average corrected force over 3 central paddles
σ_x = average longitudinal stress
σ_z = average vertical stress
ø = shearing angle from Mohr's circle

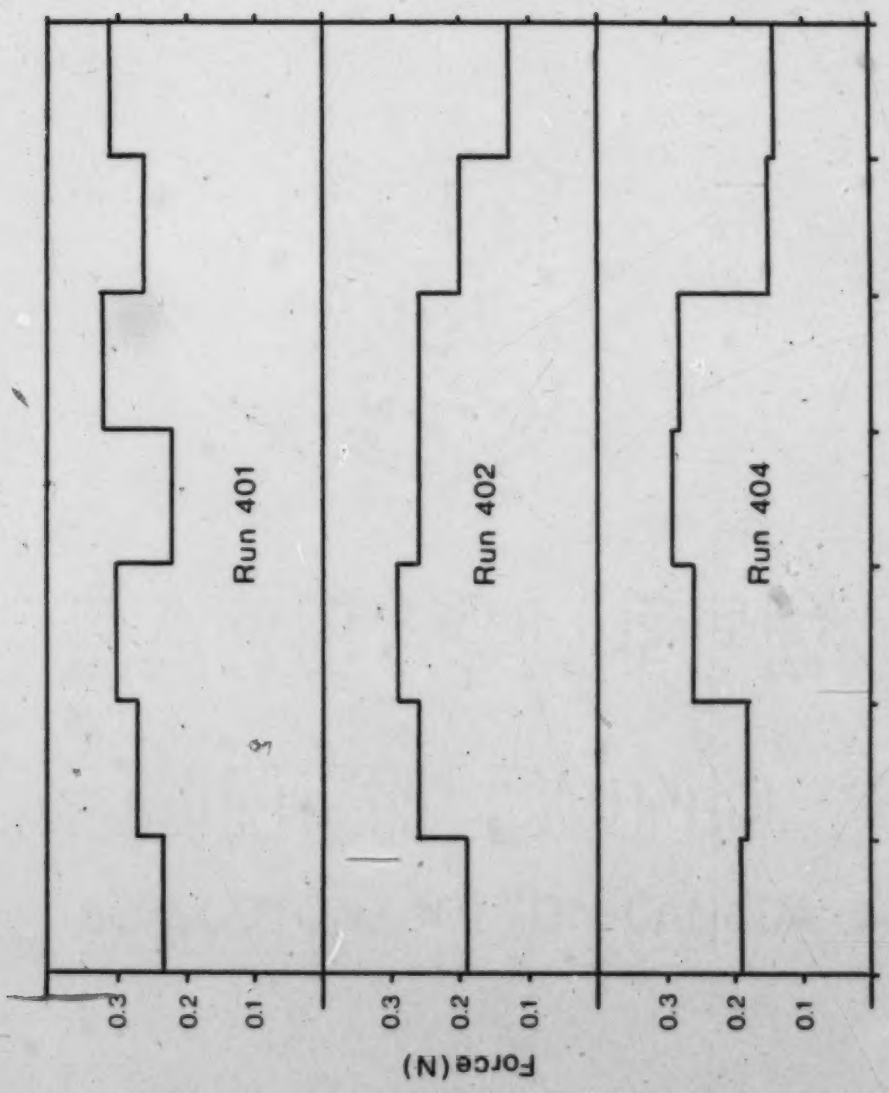

Figure 3.4 Forces measured at T=0 for each experiment.

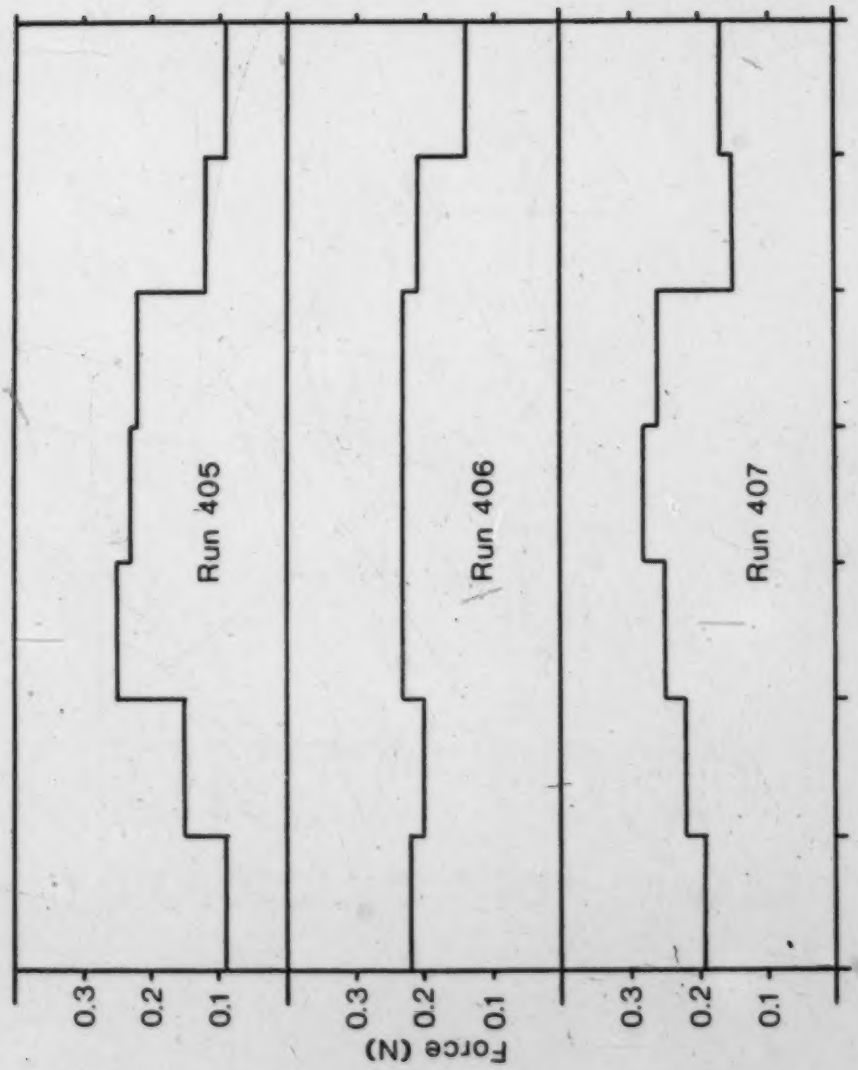

Figure 3.4 Continued.

the walls due to the relatively large shear stress. To determine the extent of the shear failure in the accumulation, the longitudinal deformation pattern was observed by sprinkling rows of coloured confetti perpendicular to the walls prior to one of the tests. The deformation pattern was much like a boundary layer in that little or no slip was observed along the roughened wall and so the initially straight confetti lines became curved. This 'boundary layer' region extended over the width of the test section as shown in Figure 3.6. This indicates that most of the sample experienced shear deformation in the horizontal plane. Also, the sample experienced greater longitudinal deformation near the paddles than near the opposite wall. This was expected since σ_x should decrease with distance from the paddles as the load is shed to shear on the walls.

The angle of shearing resistance found in the experiments can be compared to that measured for the polyethylene beads using the standard shear box test. The details of this test are given in Appendix A. The standard shear box test gave a value of Ø of 48.9° for both wet and dry samples. A small amount of cohesion was observed but was attributed to friction between the two halves of the shear box. It should be noted that shear box tests normally overestimate Ø by 1° - 4° (Lee, 1970, as quoted in Bowles, 1982). The two quite independent measurements of Ø are therefore in very good agreement.

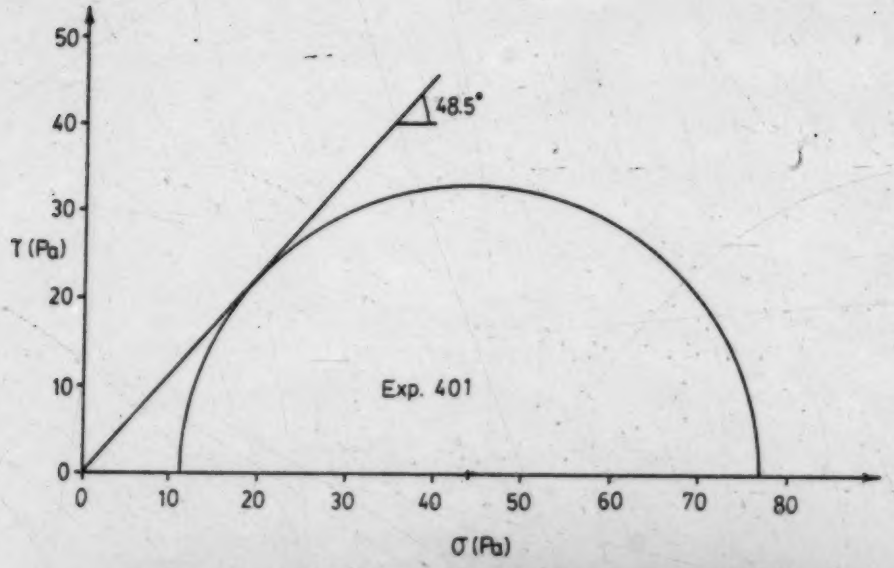

Figure 3.5 Mohr's circle for experiment no.401.

Figure 3.6 Deformation pattern at the end of a test shown by curved lines of confetti.

(note: the longitudinal centreline of the test section is approximately 2/3 of the way up the photo; the rigid wall is at the left edge of the photo; one of the rails and two of the carriage wheels can be seen; the rails are 50mm wide.)

The good agreement found between the measured shear strength (characterized by the angle of shearing resistance) and the value obtained in the shoving apparatus implies that the vertical and horizontal principal stresses in an ice jam can indeed be related by the passive pressure coefficient, given a realistic estimate of the shearing angle. Unfortunately, there is very little published work in which the angle of shearing resistance for fragmented ice has been accurately determined.

CHAPTER 4: ICE JAM THEORY

INTRODUCTION

The theory describing ice jam behaviour in a wide channel has changed little since it was first suggested, for floating log accumulations, by Kennedy (1958). This theory makes use of simplifying assumptions to allow what is really a three-dimensional situation to be approximated as one-dimensional.

The simplification from three dimensions to two is accomplished by averaging the effective stresses over the thickness. Following Janssen (1895), the situation is further simplified from two dimensions to one by assuming that the thickness and longitudinal stress are constant across the width. This assumption has not been verified and is, in fact, inconsistent with the findings reported in the last chapter. It is also inconsistent with the results of a two-dimensional theory based on a more recent silo theory (Flato, in prep.). Therefore, the longitudinal stress used in the theory must be considered a width-averaged value.

Another major assumption that will be used in the following is that the jam behaves as a cohesionless,

granular mass. This allows application of simple soil mechanics principles in the stress analysis and is probably a fair approximation for ice jams evolving in warm weather.

THEORY

The following development is similar to that of Pariset et al. (1966) and is based on the force balance required for stability of a Janssen element like that shown in Figure 4.1. A force balance for this element requires:

$$\frac{d(\sigma_x t)}{dx} = \frac{-2\tau_b t}{B} + \rho' g t S + \tau_i \qquad [4.1]$$

where: σ_x = thickness-averaged and width-averaged longitudinal stress

t = thickness

τ_b = thickness-averaged shear resistance at bank

B = channel width

ρ' = ice density

g = acceleration due to gravity

S = slope of phreatic surface

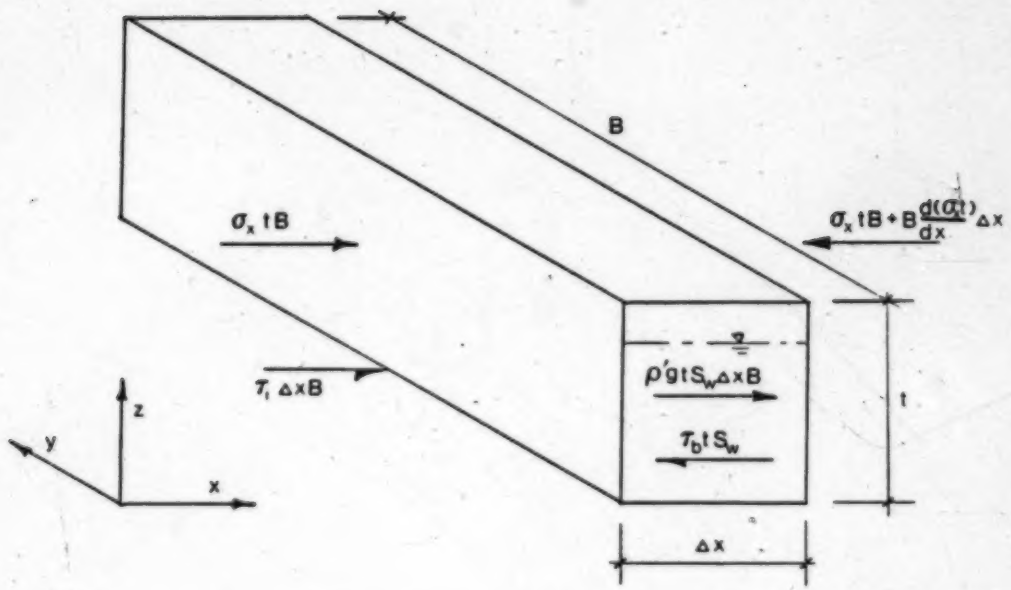

Figure 4.1 Oblique view of ice jam element used in force balance.

τ_i = width-averaged shear stress applied to jam underside

It should be noted that in the above force balance the effect of changing channel width is ignored. A sharply converging channel might provide a significant additional force and may in fact lead to the phenomenon of arching.

The shear stress at the banks, τ_b, can be written as:

[4.2] $$\tau_b = \sigma_y \tan\delta$$

where: σ_y = thickness-averaged normal stress at bank

δ = angle of friction between ice and bank

It is usually assumed that the shear failure takes place along a line within the accumulation (called the shear line): δ may then be approximated by ϕ if it can be assumed that reworking of the sheared surface does not decrease this significantly. The appropriate 'channel width' in [4.1] is clearly the distance between the two shear lines. It is usually assumed that these shear lines form where the bottom of the accumulation meets the bank.

The shear resistance implied by Equation [4.2] can only be mobilized at the point of incipient failure. This requires some streamwise motion of the pack. This motion is provided by the collapse in compression of the accumulation that characterizes the shoving process. As mentioned, Sodhi

and Weeks (1978) pointed out that the assumption that $\delta = \phi$ gives the maximum possible shear resistance at the banks and thus leads to a lower limit on the thickness.

The transverse stress, σ_y, is calculated using an empirical lateral stress transfer coefficient, K_{xy}, which is defined by:

$$\sigma_y = K_{xy}\sigma_x \qquad [4.3]$$

Pariset et al. (1966) explained that this coefficient must be less than or equal to 1.0. It might be noted here that the coefficient relating σ_x and σ_y is similar to the coefficient of earth pressure at rest as used in soil mechanics. This coefficient has a value of between 0.35 and 0.50 for granular soils (Holtz and Kovacs, 1981) and perhaps this can be used as a guide in ice jam situations.

The experiments discussed in Chapter 3 have shown that, at the centreline, the relationship between σ_x and σ_y is given by Equation [3.1]. While it may only be a good approximation near the centre of the channel, Equation [3.1] is also generally assumed to hold over the entire width.

Equations [3.1], [3.2] and [4.1] - [4.3] can now be combined, with $\delta = \phi$, to give:

$$K_v\gamma_e\frac{dt}{dx} = \frac{-K_{xy}K_v\gamma_e\tan\phi t^2}{B} + \rho' gtS_w + \tau_i$$

or:

[4.4] $$\frac{dt}{dx} = \frac{\rho' gS_w}{2K_v\gamma_e} + \frac{\tau_i}{2tK_v\gamma_e} - \frac{K_{xy}\tan\phi t}{B}$$

Where the shear stress on the jam underside can be written as:

$$\tau_i = \gamma R_i S_f$$

where: $\gamma = \rho g$

ρ = density of water

R_i = hydraulic radius of ice-influenced portion of the waterway (ie. distance down to the plane of zero shear)

S_f = slope of energy line

Equation [4.4] is the general one-dimensional formulation of the thickness equation for a prismatic, wide channel, cohesionless jam. Its solution gives the variation in accumulation thickness along the jam. The water surface profile through an ice jam is calculated in much the same way as a gradually varied open water profile. The only difference is that in a jam, the submerged portion of the ice

accumulation increases the wetted perimeter and the overall depth of flow. The height of the energy grade line above the bed at any location is given by:

$$[4.5] \qquad H_T = h + (\rho'/\rho)t + V^2/2g$$

where: H_T = total energy per unit weight of flow

h = depth of flow under jam

V = velocity of flow under jam

The slope of the energy grade line can be approximated using the logarithmic flow equation viz:

$$[4.6] \qquad \frac{dH_T}{dx} = \frac{V^2}{[2.5 \ln(R/k) + 6.2]^2 gR}$$

where: R = hydraulic radius of waterway under jam

x = downstream coordinate direction

Obviously, the solution of Equations [4.5] and [4.6] to find the water surface profile of a jam depends on knowing the thickness profile.

In the equilibrium reach the accumulation thickness is constant and the flow under the jam will be more or less uniform. Hence, $dt/dx = 0$ and $S_w = S_f = S$, where S is the water surface slope under open water conditions. Substitution of these relations into Equation (4.4) reduces it to a simple quadratic which can be solved directly for t. After some algebra, and the usual assumption that $\rho'/\rho = 0.92$, the physically meaningful root of the quadratic gives:

$$[4.7] \qquad \frac{t_{eq}}{SB} = \frac{6.25}{\mu}\left[1 + \sqrt{1 + \frac{0.35\mu R_i}{SB}}\right]$$

where: t_{eq} = equilibrium thickness

μ = jam strength parameter = $K_v K_{xy} \tan\phi (1 - e)$

The various components of the jam strength parameter, μ, merit some comment here. It was determined experimentally in the previous chapter that, in a cohesionless accumulation, K_v is given by the passive pressure coefficient, which is a function of ϕ only. The term, $\tan\phi$, appears as a result of the assumption that the angle of friction at the shear line is equal to ϕ. The value of the lateral stress coefficient, K_{xy}, is also likely a function of ϕ, but it need not be evaluated directly if good estimates of e, ϕ and μ are available.

The hydraulic radius associated with the ice cover, R_i, can be approximated in a wide channel by h_i, the depth to the plane of zero shear stress from the jam underside. An expression for h_i can be developed based on the assumption that $V_b = V_i = V$ (where V_b, V_i, and V are the average velocities in the bed influenced portion of the flow, the ice influenced portion of the flow, and the entire section respectively) yielding (see for example Gerard and Andres, 1982):

[4.8] $$h_i = h\ (k_i/k)^p$$

where: h_i = depth of ice influenced portion of flow

h = depth of flow

k_i = ice roughness

k = composite roughness of waterway

p = coefficient which depends on the ratio R/k

The composite roughness of the section can also be computed based on similar assumptions yielding:

[4.9] $$k = \left[\frac{k_i^p + k_b^p}{2}\right]^{1/p}$$

The coefficient p is equal to 0.25-if the power function equivalent of Manning's equation is assumed valid. Equation [4.9] is then essentially the Sabaneev equation written in terms of hydraulic roughness height rather than Manning's n.

Various versions of Equations [4.7] to [4.9] have been used in the past to calculate water levels and analyze observed jam stages as discussed in Chapter 2. However, the task here is to solve Equations [4.4] and [4.5] to define tha water level and thickness profile over the full length of the jam.

From the above discussion it is evident that the configuration of a jam depends not only on the mechanics of fragmented ice but also on the flow of water beneath it.

Equation [4.4], which governs the thickness profile, can be written as:

[4.10] $$\frac{dt}{dx} = f(t, h, ...)$$

The varied flow equation which governs the depth can be written as:

[4.11] $$\frac{dh}{dx} = f'(t, h, ...)$$

The behaviour of the accumulation and the flow are therefore closely related and can only be uncoupled in the equilibrium section. Hence, a complete thickness and water surface profile requires solving Equations [4.10] and [4.11] simultaneously along with the appropriate boundary conditions.

BOUNDARY CONDITIONS

From the physics of the problem, the boundary condition for Equation [4.10] is the thickness at the head of the jam. This thickness is governed by the process forming the head, which may be simple juxtaposition of floes, underturning and

deposition, or some combination of these.

The boundary condition for Equation [4.11], as for any varied flow calculation in a mild channel, is the water level at the downstream end of the jam. This water level is equal to the depth of flow plus the submerged portion, or draft, of the ice. The only water level that can be calculated a priori is that for flow beneath the solid ice sheet downstream of the toe. However, this can only be used as the downstream boundary condition if some configuration is assumed for the toe because Equation [4.10] is not valid in the toe section.

A plausible toe configuration can be visualized by considering the following sequence of events, illustrated in Figure 4.2. Figure 4.2a shows the solid ice sheet prior to jam formation. In Figure 4.2b, ice floes are beginning to accumulate against the upstream edge of the ice cover. This accumulation will thicken, by underturning and deposition or by small shoving events, and lengthen as more floes arrive. An M2 backwater profile will develop due to the rougher surface presented to the flow by the accumulation. The streamwise force on the accumulation is resisted by friction between the ice floes and the solid ice underside and by bearing directly against the upstream face of the solid ice sheet. This results in a configuration such as that in Figure 4.2c in which the accumulation becomes thinner downstream of the solid ice interface. The downstream slope of the accumulation will presumably correspond to the angle

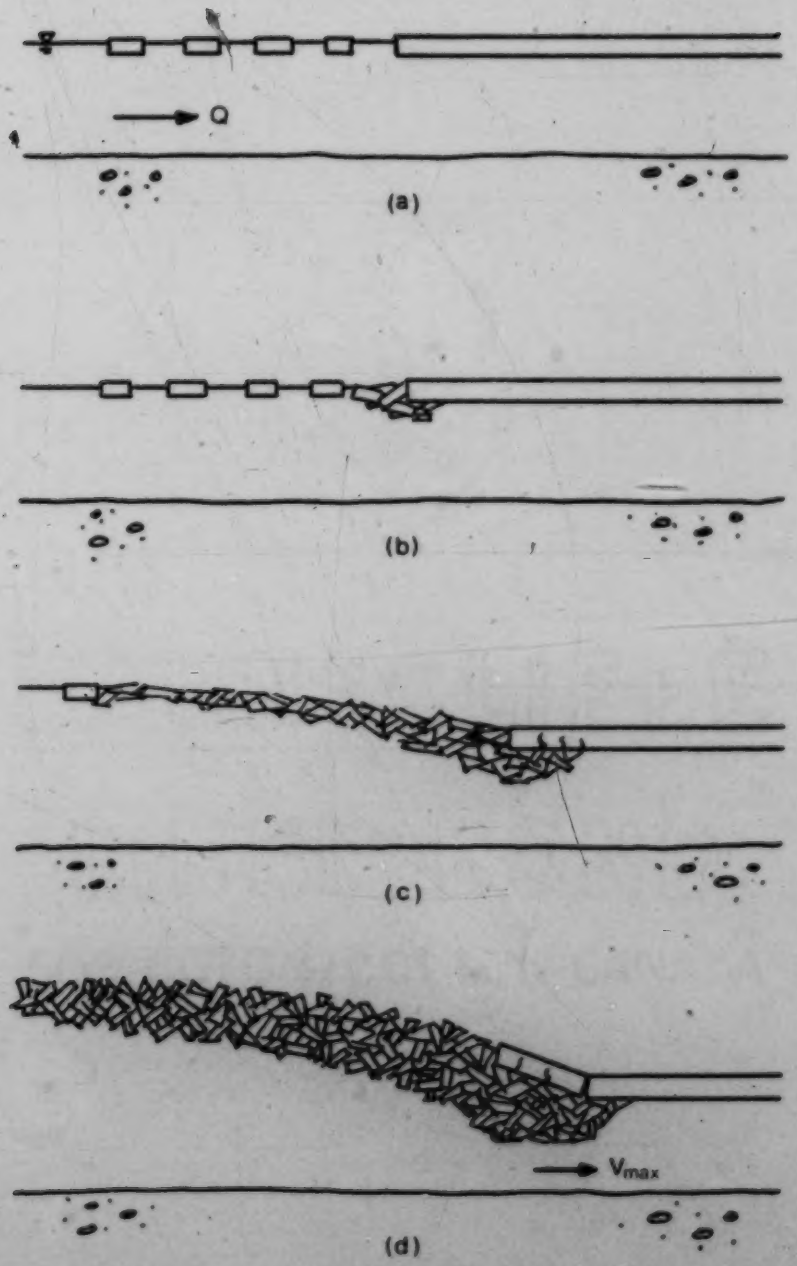

Figure 4.2 Hypothesized developement of jam toe

of repose of the submerged ice blocks, much like the downstream face of a sand dune. The solid ice sheet will be deflected upward due to the buoyancy of the accumulation beneath it.

As described above, the resistance to the streamwise force on the accumulated ice is enhanced by the presence of the solid ice sheet. Therefore, Equation [4.4] is not applicable in the toe. Upstream of the solid ice sheet, however, Equation [4.4] is applicable and so the thickness profile beyond this point can be calculated.

In most cases, the accumulation will become very thick just upstream of the toe because of the steep water surface slope. If the bed is inerodible, then at some point the waterway will become so constricted that the velocity will exceed the erosion velocity of the ice blocks and downstream transport will begin. The situation will then be as shown in Figure 4.2d and the waterway depth over most of the toe region will be governed by the erosion velocity, V_{max}. The process of shoving, erosion, and deposition will continue until the water level through the accumulation is increased enough to produce a stable configuration.

Knowing V_{max}, the water level profile across the toe can be defined; the water level for the solid ice sheet can then be used as the downstream boundary condition. The erosion of ice blocks under a jam has not been thouroughly studied and so obtaining estimates of V_{max} may not be easy.

Uzuner (1975) has reviewed most of the available literature on this subject and has made some recommendations based on laboratory experiments.

The hypothetical toe configuration described above is plausible as long as the floes are small enough to pass through the constricted waterway. Larger floes might become lodged and lead to the development of a grounded jam but on a large river of moderate slope, such grounding is unlikely.

The assumption of an inerodible bed may not be realistic in many cases. The constricted waterway beneath the toe of a jam will lead to high velocity flow and the concomitant potential for scour. The more general problem of sediment transport under an ice cover has received very little attention and this must certainly be addressed in the future. For now, the bed will be assumed inerodible to concentrate on the behaviour of the jam.

To summarize, the 'floating toe' configuration is one in which the thickness profile is governed by the varied flow profile and the erosion velocity V_{max}. The thickness equation is valid to the upstream end of the toe and the internal strength lost below this point, as the accumulation is thinned by erosion, is assumed to be compensated by friction on the solid ice underside. This toe configuration implies that the rise in water level should be apparent some

distance downstream of the solid ice / jam interface, which accords with the observations of Rivard (1985).

Equations [4.10] and [4.11], together with the boundary conditions discussed above, provide the means of calculating the water surface and thickness profiles of a jam throughout its length. This calculation will allow assessment of the accuracy of the common assumption that equilibrium theory is valid at every section, as well as the influence of various parameters on profile shape.

CHAPTER 5: ICE JAM PROFILE MODEL

INTRODUCTION

In the first chapter, the existing schemes for calculating the thickness and water surface profiles of a wide channel jam were discussed. These schemes all employed the assumption that equilibrium theory is applicable at every section, even for the non-equilibrium reaches. A more rational profile calculation would make use of the differential thickness and varied flow equations discussed in the previous chapter. There have been at least two profile models which use these equations and, although other schemes may be in use, in house, by consulting firms and others, only the results of Uzuner and Kennedy (1974,1976) and Beltaos and Wong (1986) have been published.

The solution technique used by these two groups are very similar even though Uzuner and Kennedy calculate the upstream transition profile while Beltaos and Wong calculate the downstream transition profile. Both use equilibrium conditions as a boundary condition from which the calculations proceed and therefore both presume the existence of an equilibrium section. Because all gradients vanish in

an equilibrium section, no solution is immediately possible starting there. Uzuner and Kennedy circumvent this difficulty by invoking l'Hospital's rule and then move the starting point for the solution scheme some arbitrarily small increment away from equilibrium. Beltaos and Wong use the same technique.

In the upstream transition dealt with by Uzuner and Kennedy, it is apparent a priori that the accumulation thickness should decrease upstream. In the downstream transition, the choice of increasing versus decreasing thickness is not so obvious; either one is possible. The situation is analogous to the more common problem of calculating gradually varied flow profiles under open water conditions. There are two possibilities for a mild channel downstream of a region of uniform flow. The profile may be of either the M1 of M2 type depending on conditions further downstream. It is for this reason that gradually varied flow calculations in such a channel usually begin with a downstream boundary condition and proceed upstream.

Beltaos and Wong consider only the case wherein the thickness increases in the downstream direction. This is certainly the accepted shape for the downstream transition and the few documented water surface profiles do indeed exhibit this 'M2-like' shape. However there may be cases where an M1 profile may develop, such as for a jam forming upstream of a control structure or a severely grounded toe of low porosity.

With the technique used by Uzuner and Kennedy and by Beltaos and Wong, the boundary conditions can only be applied after the calculations are complete since the calculations begin at the equilibrium reach and proceed toward the boundary condition location. This is much like beginning a gradually varied flow calculation at the normal depth and proceeding towards the control, which is not normally done. However, the major drawback is that the technique requires an equilibrium section exist in the jam. This is not always the case and is a severe limitation if the model is to be used to track the development of a jam over time or, indeed, in almost any real channel situation. Unless a channel is prismatic, there is no possibility for an equilibrium section to develop and, even in a prismatic channel, the length required for the jam to become fully-developed may not be achieved due to an insufficient supply of ice. A model which requires the existence of an equilibrium section would seem, therefore, to be of limited practical use.

COMPUTER MODEL DEVELOPMENT

The limitations of the existing ice jam models discussed above point out the need for a scheme which allows the

complete water surface and thickness profile of a jam to be calculated regardless of jam length or channel geometry. This requires the simultaneous solution of two equations whose general form is given by [4.10] and [4.11] and satisfaction of boundary conditions such as those described in the previous chapter.

An appropriate numerical algorithm would seem to be an iterative one which solves [4.11] upstream, as is usually done for varied flow calculations in a mild channel, with an initial estimated accumulation configuration and then, as suggested by the physics of the situation, solves [4.10] downstream with the flow depth profile just computed. This iterative cycle would continue until convergence was attained.

Such an algorithm was developed and its main elements are shown in the flowchart of Figure 5.1. This algorithm has been coded in the program ICEJAM ver.1.5 which is described in detail in Appendix B. The program starts by reading constant data like discharge, porosity, density and jam strength parameters. Next, data for each cross-section is read: the program can handle arbitrarily shaped cross-sections at irregular intervals so that surveyed channel data can be used. The ice and bed roughness must be specified for each cross-section as well as a reasonable water surface elevation.

The solution procedure begins by calculating the normal

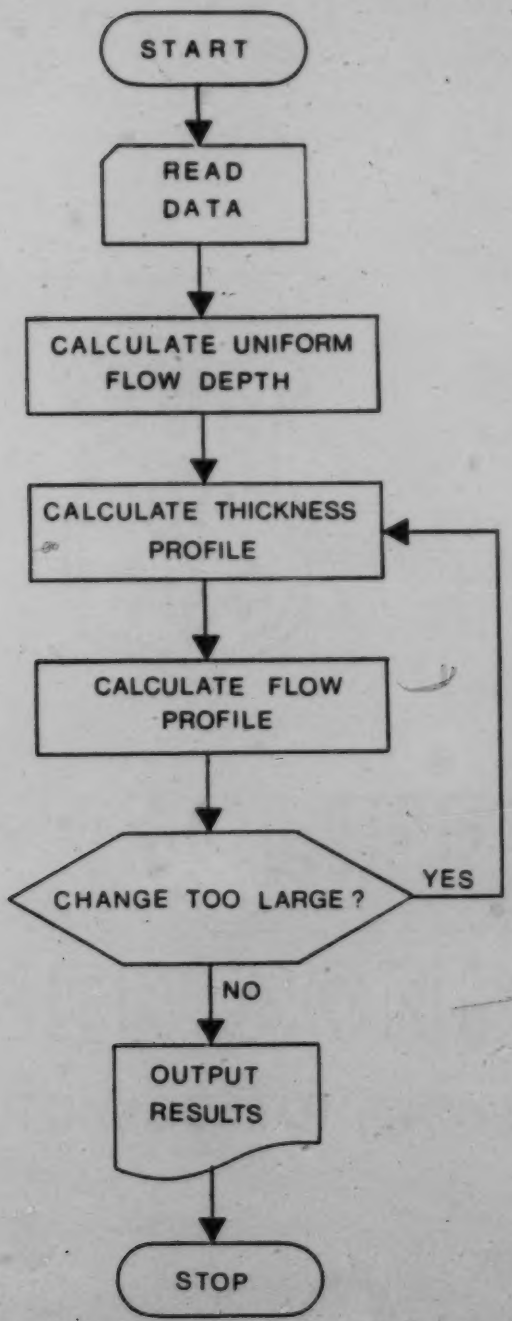

Figure 5.1 Flowchart of ICEJAM program.

depth at each cross-section assuming an ice cover of uniform thickness exists. The slope used to calculate the normal depth is calculated from the given water surface elevations. Using the flow profile so determined, a first estimate of the thickness profile is obtained by solving Equation [4.4] with a simple, forward difference scheme. The thickness calculations begin at the head of the jam, with a specified initial thickness, and proceed downstream. Then, keeping this thickness profile fixed, a new depth profile is obtained using the 'standard step' method of varied flow calculation to solve Equation [4.6]. The depth calculations begin at the downstream end of the jam toe and proceed upstream. Using this depth profile, a new thickness profile is then calculated and so on.

After each iteration, the change in flow depth is compared to a specified tolerance. When all the cross-sections have met this tolerance, the calculations stop and the profile is displayed in tabular and graphical form.

The forward difference method was chosen to solve the thickness equation because it is simple to apply and can conveniently handle variable step sizes (ie. distance between cross-sections). A factor was introduced to limit the change in thickness for each iteration to 1/3 of the calculated change. It was found that without this damping factor, the profile would oscillate on either side of the solution and not converge in some cases. The solution of the differential thickness equation was attempted using a more complicated

predictor-corrector method. This method proved to be somewhat unstable, particularly at locations where the step size changed, and was therefore abandoned.

The 'floating toe' configuration is introduced in the algorithm in the following manner. During the accumulation thickness calculation, which begins at the upstream end of the accumulation, the accumulation thickness is allowed to become as high as necessary for 'geotechnical' stability. Then, during the gradually varied flow 'sweep', which starts at the given downstream end of the toe, the waterway depth at each section is checked against that which would give the specified erosion velocity. If it is less, the accumulation thickness is reduced to simultaneously satisfy the gradually varied flow constraint and the erosion velocity constraint. It is presumed that the reduction in accumulation strength caused by this reduction in thickness can be provided by the solid ice sheet (ie. the force applied directly to the upstream vertical face of the solid ice sheet, and the shear between the accumulation and the underside of the solid ice). Hence the end of the solid ice will be near the section where no reduction in accumulation thickness is required to satisfy the erosion velocity constraint, as indicated in Figure 4.2 (d). In other words, the thickness in the downstream transition region is governed by Equation [4.4], while that in the toe is governed by the gradually varied flow profile and the erosion velocity.

DISCUSSION

The main advantage of the above algorithm is the ability to calculate a jam profile without presupposing an equilibrium section exists. This allows profiles to be determined in cases where the jam is too short to be fully-developed and for the development of a jam over time to be traced. Moreover, it provides a means of estimating the length required for a jam to be fully-developed, which is an important piece of information if equilibrium theory is to be used at all.

Another advantage is the ability to calculate a profile with realistic channel geometry. This may prove useful in deducing jam strength and roughness parameters from field measurements of water surface profiles. The ability to use real cross-section data also makes it a practical tool for estimating ice jam induced flood level profiles.

The major limitation to calculating the profile throughout the full length of a jam is the current poor understanding of the circumstances that exist at the toe. For the present calculations, a situation has been presumed that is plausible for large rivers with an essentially inerodible bed. Questions remain, however, as to the effect of an erodible bed and the possibility of partial or complete grounding in small streams.

A further limitation is imposed by the present inability

to accurately predict various input data. For example, the discharge at the time of jam formation and the volume of ice that can be supplied play a dominant role in determining the size and flooding potential of a jam, yet only rough bounds can be placed on their value. As well, parameters that affect the size and shape of a jam (eg. μ, $\emptyset$, e and k_i) can only be crudely estimated.

CHAPTER 6: MODEL DEVELOPMENT AND EVALUATION

INRODUCTION

The profile model discussed in the previous chapter was first applied to a simple, rectangular, prismatic channel. This simplified ice jam situation was used to:

a) evaluate the numerical procedure and assess its performance
b) evaluate, at least qualitatively, the influence of various parameters
c) develop some appreciation for the length required for a fully-developed jam

The situation assumed would be reasonably representative of a wide and deep, slow-moving, relatively flat river. The Mackenzie River at Norman Wells is such a situation, and detailed field documentation of ice jams at this location could be used in evaluating the model results.

The characteristics of this reach are reported in Rivard,Kemp, and Gerard (1984) and Rivard (1985). The average channel characteristics of this reach are: open water

slope S = 0.0000976; channel width B = 2000 m; and bed roughness k_b = 50 mm. Rivard et al. (1984) documented a long ice jam through this reach and found the following parameters provided a reasonable description of the circumstances: ice accumulation roughness, k_i = 3.3 m; solid ice roughness k_s = k_b; and the solid ice thickness, t_s = 1.7 m. Rivard et al. also found that values of μ = 1.6 and Q = 15,000 m^3/s allowed the observed 'equilibrium' water level to be reproduced by equilibrium theory. It is of interest to note however, that a similar water level is predicted using Q = 10,000 m^3/s and μ = 1.2 (this discharge is the lower bound estimate obtained by Rivard et al. and the value of μ is the average value found by Beltaos, 1983).

PRELIMINARY TESTS

One measure of the 'ruggedness' of a computational scheme is its ability to maintain reasonable accuracy with increasing step size (the step size is the distance between computational nodes - in this case, the distance between cross-sections). Several runs were made using the data listed in Table 6.1 (this is the same as that labelled M6 in Table 7.1) and the results are shown in Figure 6.1.

TABLE 6.1

Quantities Used to Examine Examine Effect of

Changes in Node Spacing

Slope (S)	0.000098
Width (B)	2000 m
Discharge (Q)	10,000 m^3/s
Jam roughness (k_i)	3.3 m
Bed roughness (k_b)	0.05 m
Jam strength parameter (μ)	1.2
Vertical stress coefficient (K_v)	4.32

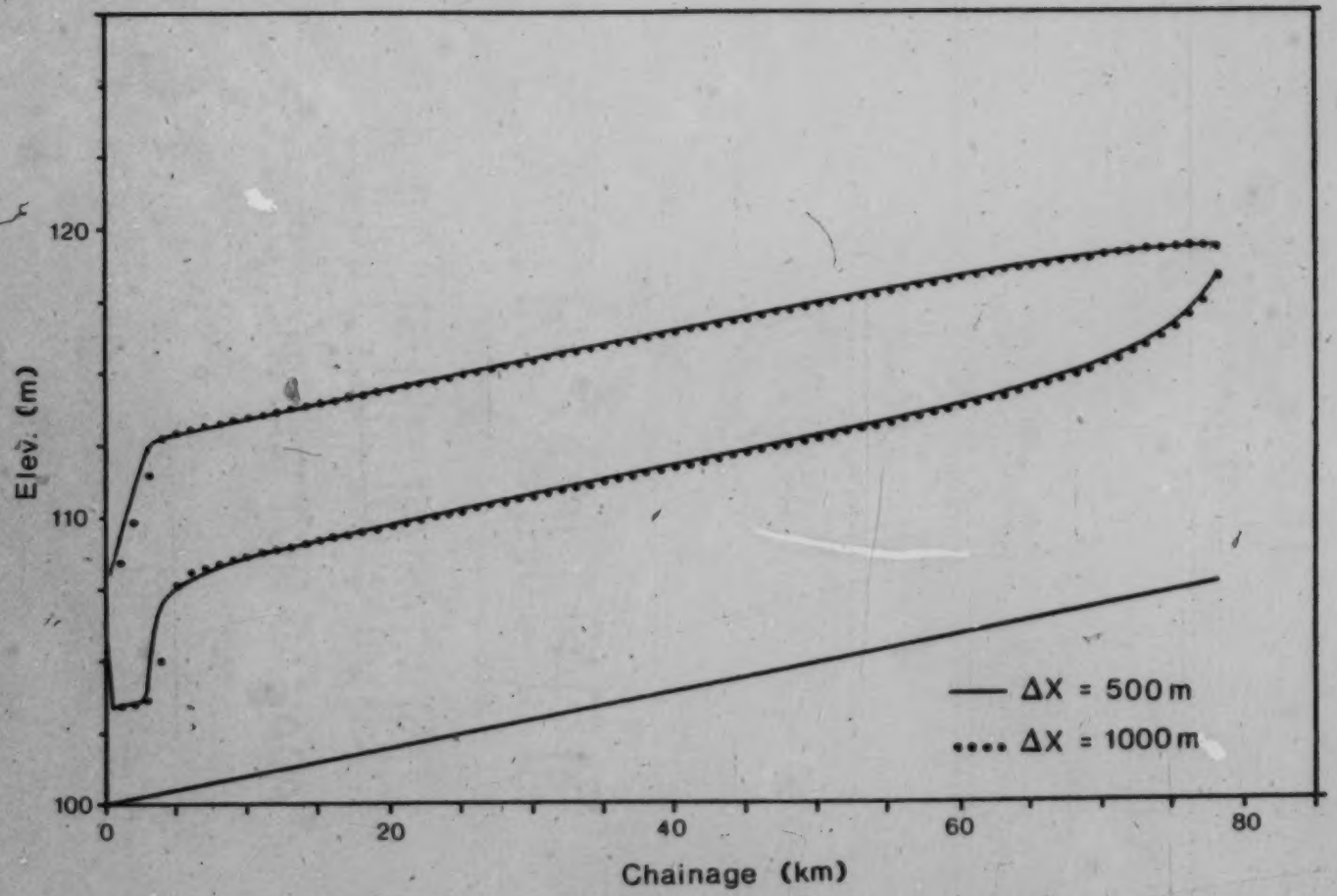

Figure 6.1 a Comparison of calculated profiles with step sizes of 500m and 1000m.

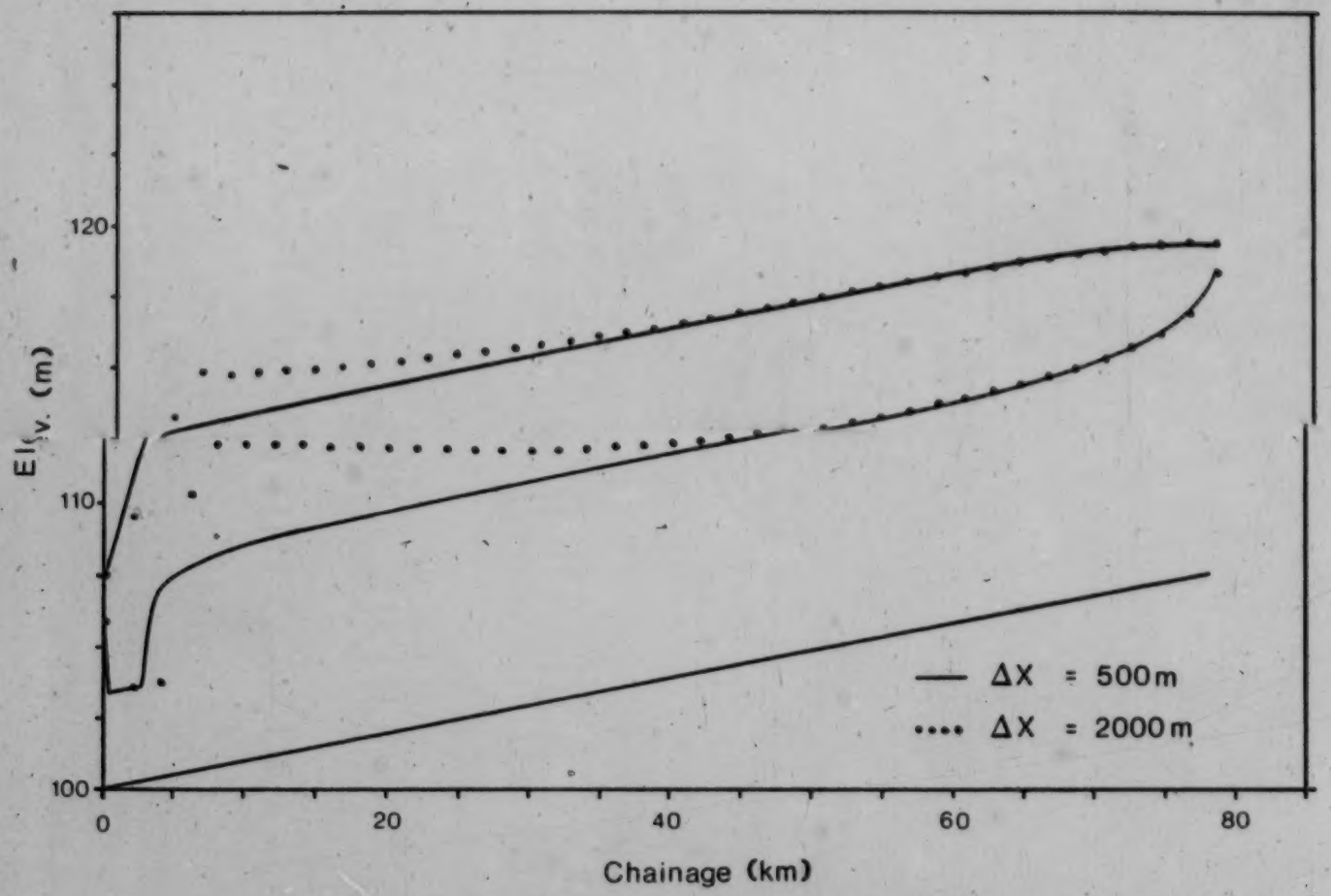

Figure 6.1 b Comparison of calculated profiles with step sizes of 500m and 2000m.

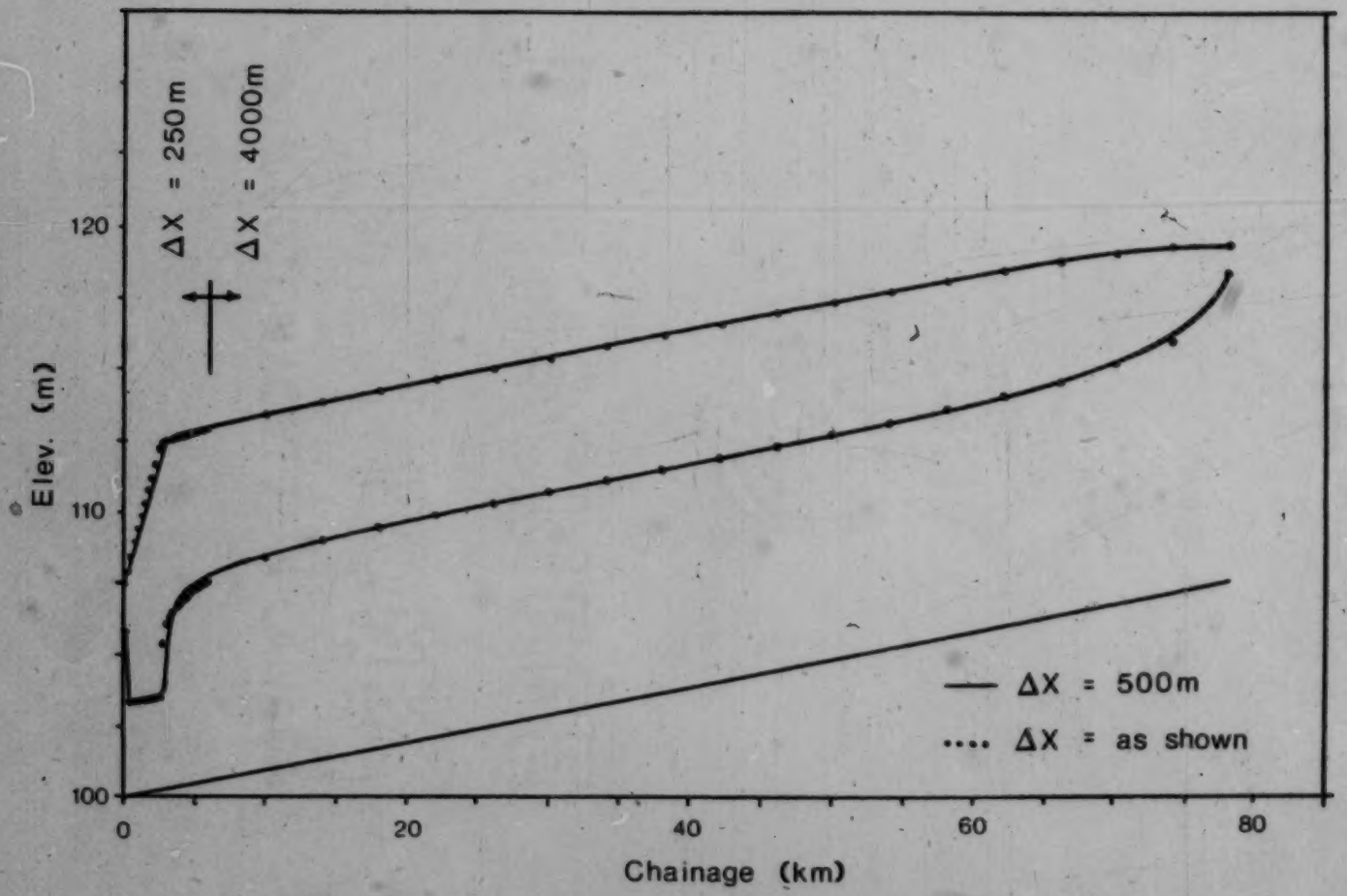

Figure 6.1 c Comparison of calculated profiles using variable step sizes.

Figure 6.1a shows calculated ice jam profiles in which very little difference is observed when the step size (Δx) is doubled from 500 m to 1000 m. However, when the step size is again doubled to 2000 m, the shape of the downstream transition is very different as shown in Figure 6.1b. This behaviour can be explained by the fact that there are two mathematically possible shapes for the downstream transition. These two shapes correspond to the M1 and M2 water surface profiles observed in open channel flow. When the step size is too large, the steep energy gradient in the toe causes the water level to 'overshoot' the normal flow depth and the numerical scheme then converges to the M1-like solution as shown.

To avoid this problem, the step size in the toe region can be reduced. The results are then as shown in Figure 6.1c. In this case the step size is 250 m for the 6 km furthest downstream, and 4000 m for the remainder of the reach. The small step size in the toe has allowed the calculation to proceed through the steep energy gradient and maintain the desired M2 shape. The remainder of the profile shows that even a relatively large step size allows an accurate profile to be calculated.

INFLUENCE OF PARAMETERS

For the numerical experiments described herein, the following parameter values were used: Q = 10,000 and 15,000 m^3/s; μ = 1.0, 1.6, 2.0; K_{xy} = 0.5 and 1.0; k_i = 1.5, 3.3, 10.0 m; L (jam length) = 15,30, 59.5 km; and e = 0.4.

Table 6.2 shows the combinations used in the various test runs. In all cases the erosion velocity was specified as 1.5 m/s (a reasonable value based on the recommendations of Uzuner, 1975) and the initial thickness as 1.0 m. This may be somewhat thinner than the actual head thickness but was chosen to evaluate model performance for steep initial thickness gradients.

Figure 6.2 shows some examples of the calculated ice jam profiles (these correspond to, from top to bottom, runs 01, 20, and 30). The various zones indicated in Figure 1.1 are clearly evident. It is noteworthy that the toe region extends for some 4 km in each case, which accords with the observations of Rivard (1985). All of the parameters, except the length of the jam, were kept constant in these runs to show the development of a jam toward its fully-developed state. The upstream and downstream transition zones of the calculated profiles obviously overlap for the 15 and 30 km cases. It is only when the jam is about 60 km long (Figure 6.2 a), that the transition regions appear to be separated by an equilibrium section.

TABLE 6.2
Quantities Used in Preliminary Test Runs

Run	Q (m^3/s)	k_i (m)	K_{xy}	ø	μ	L (km)	h (m)	R_i (m)	t_{eq} (m)	H_{eq} (m)
01	15000	3.3	1.0	35	1.6	59.5	9.83	7.28	4.41	13.9
02	10000						7.78	5.76	4.03	11.5
03	15000		0.5	44	1.61		9.83	7.28	4.31	13.8
05			1.0	30	1.04				5.65	15.0
07			0.5	38	0.98				5.87	15.2
09			1.0		1.97				3.82	13.3
11			0.5	46.5	1.99				3.80	13.3
13		10.0	1.0	35	1.55		11.1	8.75	4.75	15.5
14			0.5	44	1.61				4.64	15.4
15		1.5	1.0	35	1.55		9.16	6.42	4.20	13.0
16			0.5	44	1.61				4.11	12.9
20		3.3	1.0	35	1.55	30	9.83	7.28	4.41	13.9
21			0.5	44	1.61				4.31	13.8
22		1.5					9.16	6.42	4.11	12.9
23		10.0					11.1	8.75	4.64	15.4
24		3.3		38	0.98		9.83	7.28	5.87	15.2
25				46.5	1.99				3.80	13.3
30			1.0	35	1.55	15			4.41	13.9
31			0.5	44	1.61				4.31	13.8
32		1.5					9.16	6.42	4.11	12.9
33		10.0					11.1	8.75	4.64	15.4
34		3.3		38	0.98		9.83	7.28	5.87	15.2
35				46.5	1.99				3.80	13.3

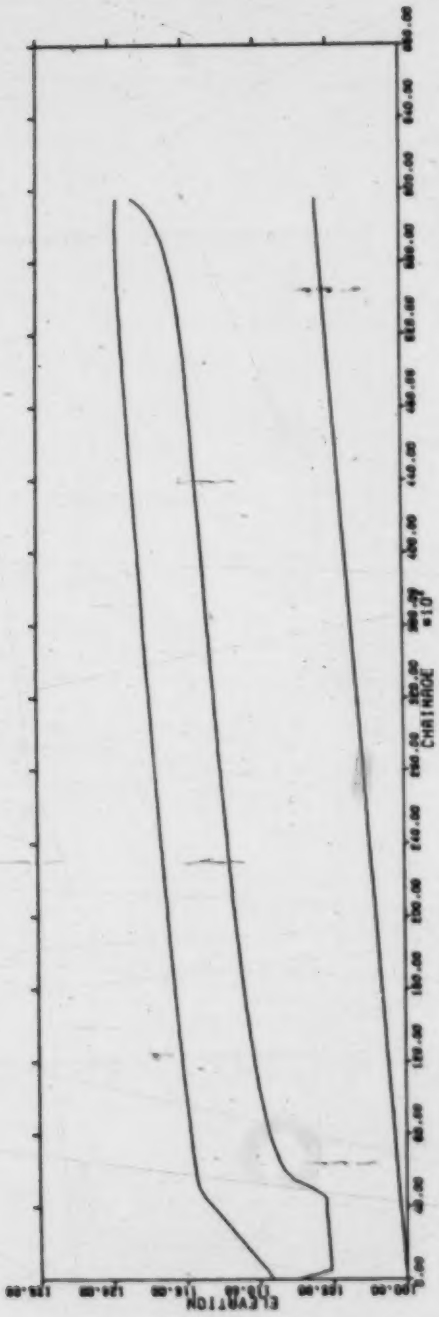

Figure 6.2 a Calculated profile for run no. 01.

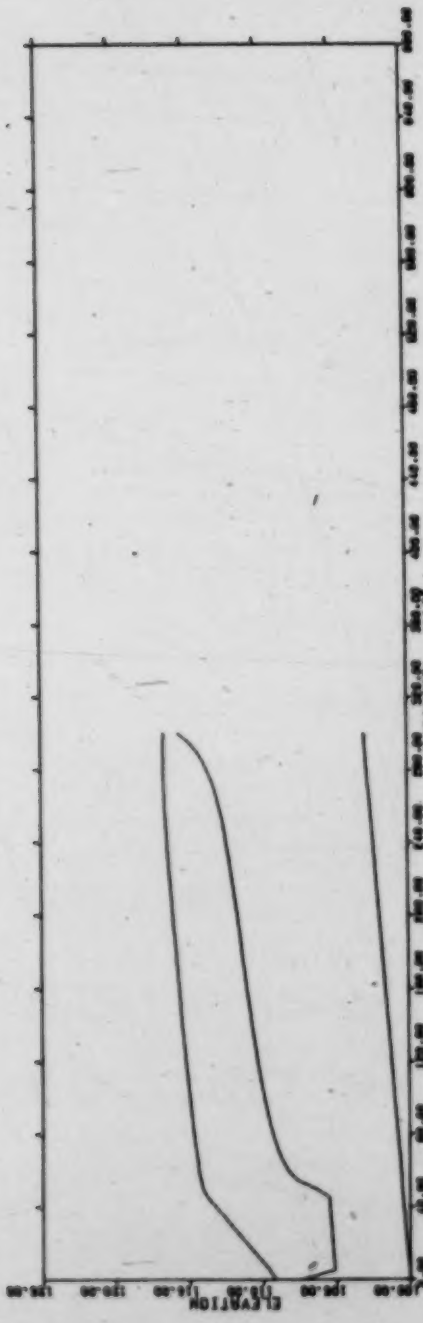

Figure 6.2 b Calculated profile for run no. 20.

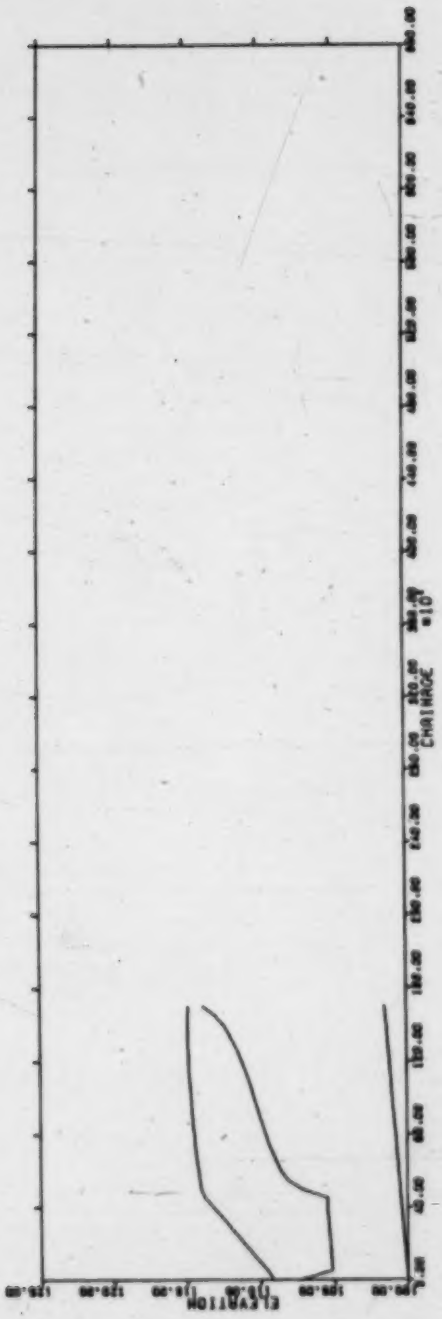

Figure 6.2 c Calculated profile for run no. 30.

In Figures 6.3 and 6.4, thickness profiles are shown in which the thickness has been non-dimensionalized using the equilibrium thickness calculated from Equation [4.7]. Non-dimensionalizing the thickness in this manner allows the effect of various parameters on the shape of the jam profile to be separated from their more obvious effect on the thickness. The abscissa in these figures is the distance upstream from the downstream end of the toe non-dimensionalized by the river width. The thickness in the toe portion of the profile has not been plotted.

The top portion of Figure 6.3 shows the variation of profile shape with discharge, all other parameters being kept constant. The shape of the profiles are very similar with the main difference being the upstream extent of the toe. The thickness gradient in the downstream transition zone seems to be somewhat steeper for the larger discharge. This is not unreasonable given that the increasing thickness in this reach is profoundly influenced by the shape of the varied flow profile.

The bottom portion of Figure 6.3 shows the influence of the lateral stress coefficient, K_{xy}, on the profile shape. It can be seen that the transition regions are slightly shorter for $K_{xy} = 1.0$ than for $K_{xy} = 0.5$. The lateral stress coefficient can be thought of as the ratio of bank shear to streamwise stress and therfore influences the rate of 'load shedding'.

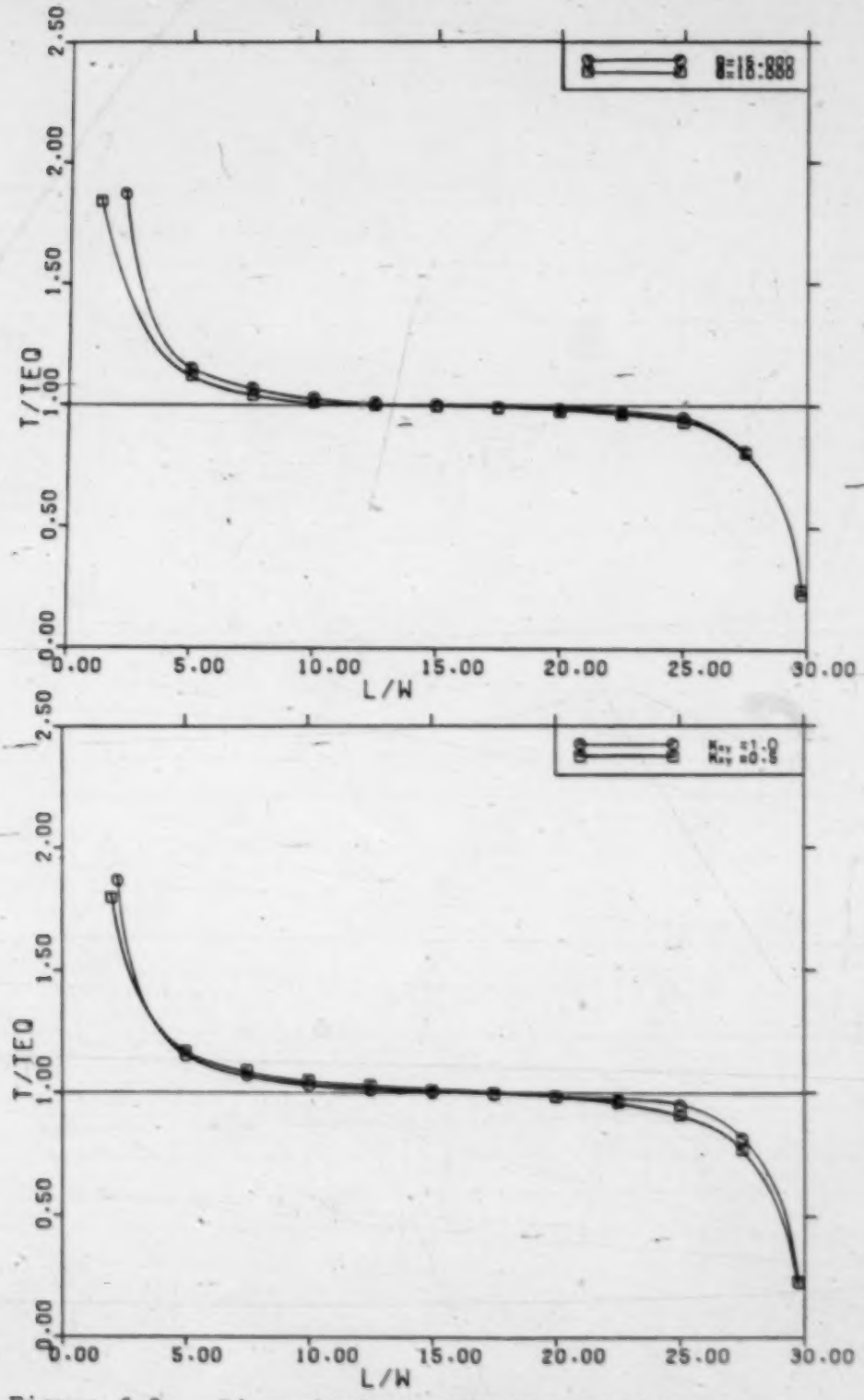

Figure 6.3 Dimensionless calculated thickness profiles for differing values of Q and K_{xy}.

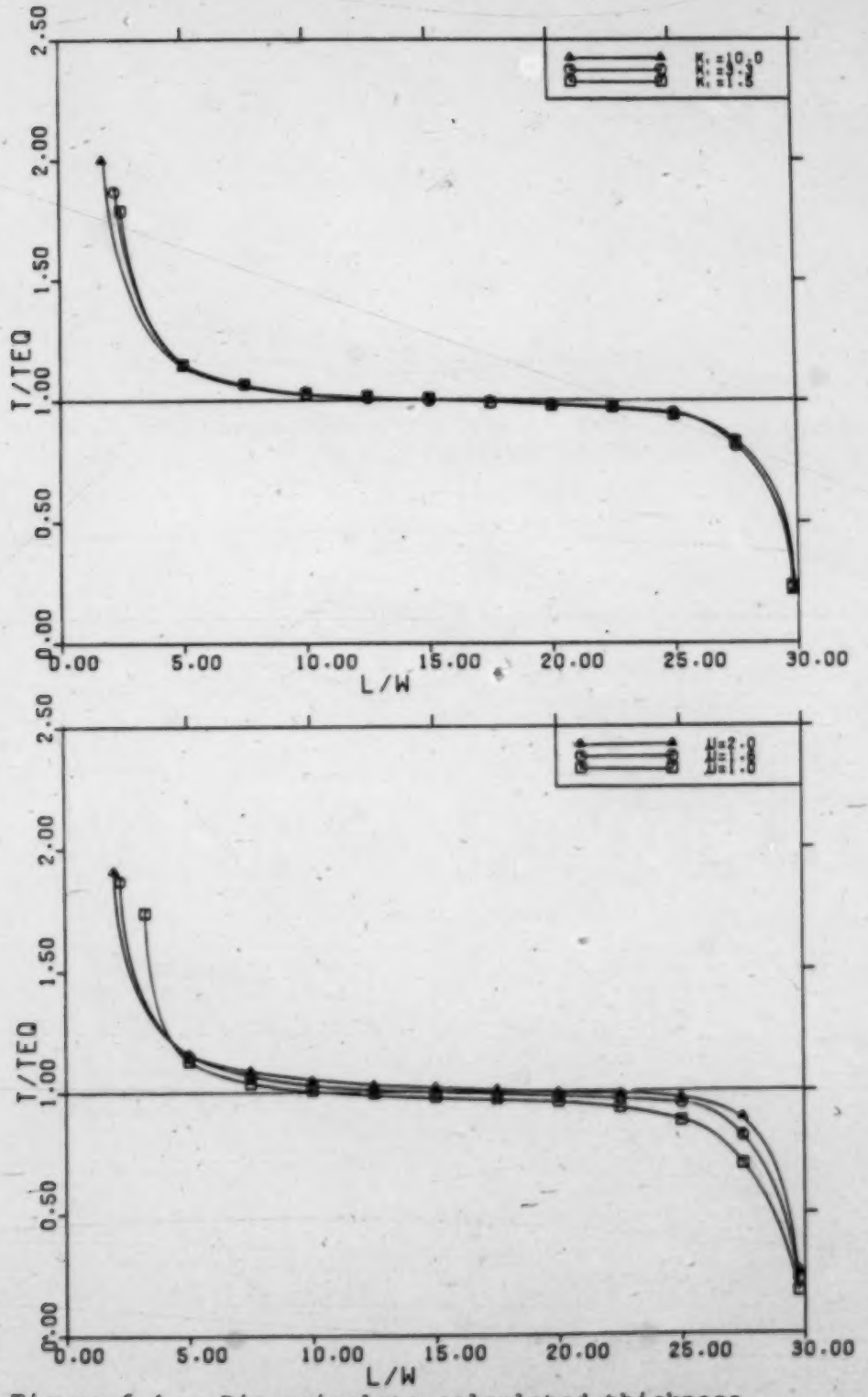

Figure 6.4 Dimensionless calculated thickness profiles for differing values of k_1 and μ.

In Figure 6.4, the top portion shows the effect of ice jam roughness height, k_i, on profile shape. As in the case of discharge, the influence of roughness height is primarily confined to the toe and downstream transition regions. This influence is quite small, considering the large change in assumed roughness. It was explained earlier that the thickness in these two sections of the jam is strongly affected by the gradually varied flow profile. Therefore, the influence of hydraulic parameters on the shape of the thickness profile is to be expected.

The jam strength parameter, μ, is essentially an index of the ability of a jam to resist the streamwise forces applied to it. The bottom half of Figure 6.4 shows the influence of this parameter on the profile shape. It has the largest influence of all. In this case the lateral stress coefficient, K_{xy}, was kept constant and μ was varied by changing the value of $\emptyset$. The most obvious influence of is on the length of the upstream transition. As μ becomes larger (ie. the jam becomes stronger), the upstream transition becomes shorter, reflecting the increased ability of the jam to resist the streamwise forces. Increasing μ also decreases the length of the toe. Recalling the discussion of the development of a jam toe, it is not surprising that a weaker jam (ie. lower μ) requires a longer toe for a stable configuration.

It is of interest to examine the relative magnitude of the terms in the differential thickness equation (ie. Equation [4.4]). This can be written as:

[6.1] $$\frac{dt}{dx} = a\bar{t} + \frac{b}{\bar{t}} + c$$

where: $\bar{t}$ = average thickness of two computational nodes in forward difference scheme

$$a = \frac{-K_{xy}\tan\phi}{B}$$

$$b = \frac{\rho g R_i S_f}{2K_v\gamma_o}$$

$$c = \frac{\rho' g S_w}{2K_v\gamma_o}$$

(note: the rest of the variables are as defined in Chapter 4)

The magnitude of the terms in Equation [6.1] are shown graphically in Figure 6.5 for the same data used to compute the profile shown in Figure 6.1. As intuition would suggest, the term 'at', which represents the streamwise resistance of the jam, is the dominant term throughout, with the other terms playing different roles in different reaches. The sum of 'b/t' and 'c' is essentially constant in the upstream reach. This means that in this region:

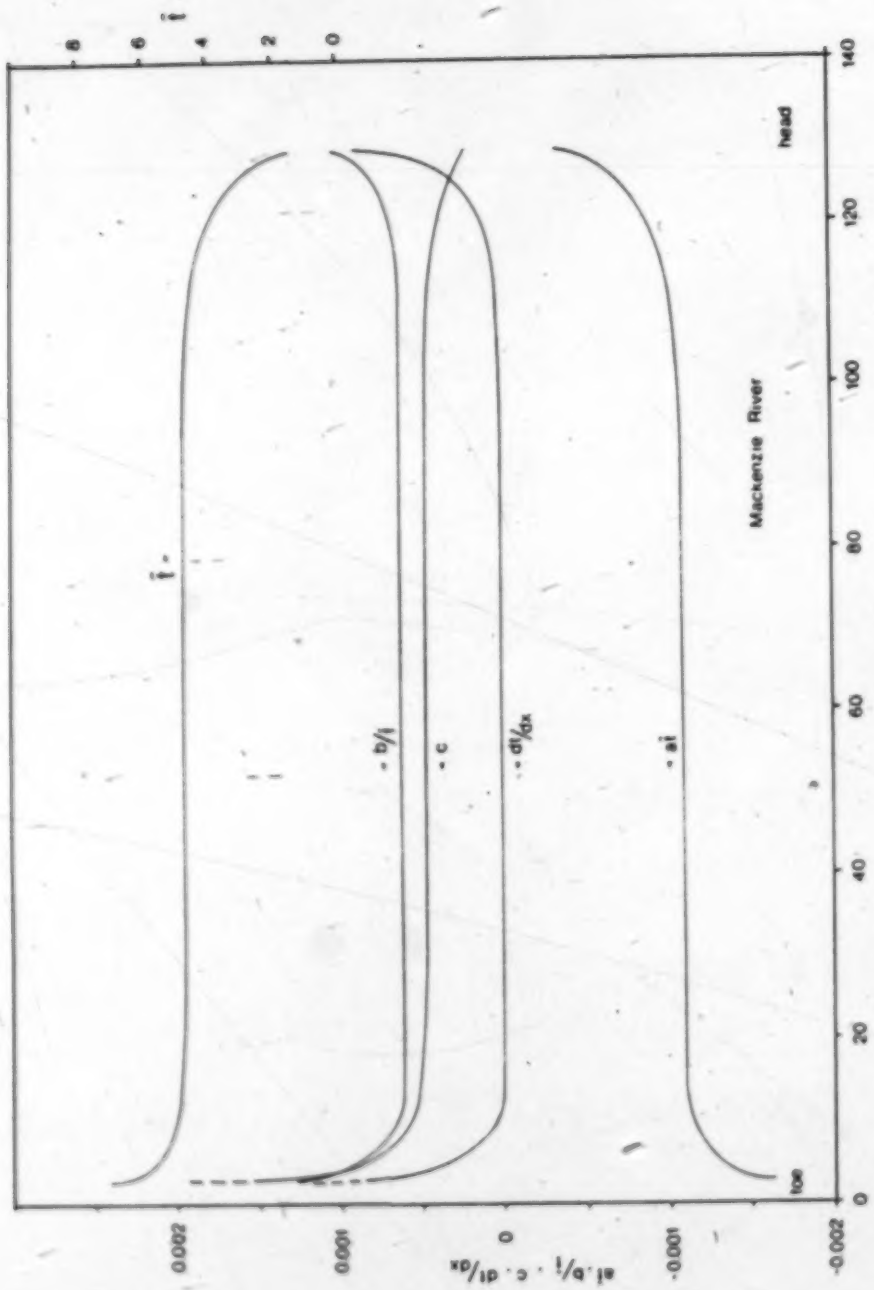

Figure 6.5 Magnitude of terms in differential thickness equation over length of jam.

[6.2] $$\frac{dt}{dx} \alpha 1 - kt$$

where: k = constant

In the downstream transition, the sum of 'b/t' and 'at' is essentially constant so that:

[6.3] $$\frac{dt}{dx} \alpha S_w$$

where: S_w = water surface slope

In other words, the thickness profile in the transition regions could be approximated using the simple relationships above. Of particular note is the observation that the thickness profile in the upstream transition reach is well-approximated by a simple, linear O.D.E. and is virtually independant of the water surface profile.

Figure 6.6 shows the dimensionless depth profiles (in which the overall depth has been non-dimensionalized by the overall depth in the equilibrium section) obtained with K_{xy} = 0.5 for various values of μ. There is no discernible difference in the profiles. However, they do show that over almost the entire length of the jam the depth obtained from equilibrium calculations is a very close approximation to the actual depth. This implies that it would be very difficult to determine the extent of the equilibrium section of a jam from water level observations alone.

The program also calculates the total volume of solid

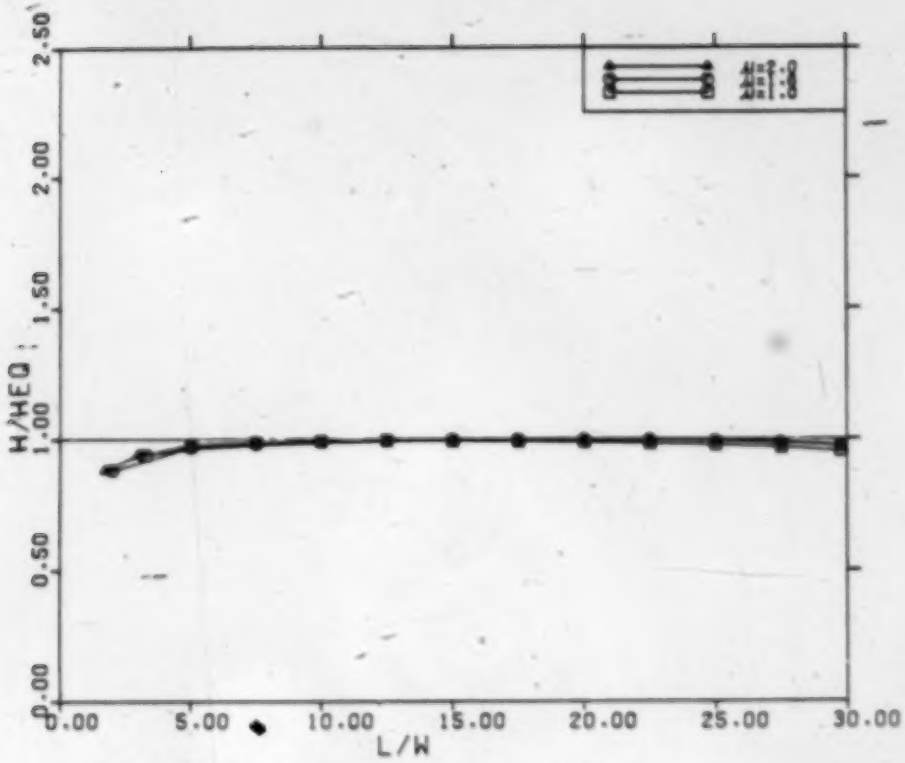

Figure 6.6 Dimensionless calculated overall depth profiles for various values of μ.

ice in the jam (V), including the toe region, and these values have been compared with the volume of solid ice obtained by assuming the equlibrium thickness exists over the full length of the jam, including the toe. This latter volume is termed the equilibrium volume, V_{eq}. Table 6.3 shows the results of these calculations for three runs. Evidently the volume calculated assuming equlibrium thickness throughout is not far from the actual volume.

Application of the profile model to a simple prismatic channel situation has allowed the calculation procedure to be evaluated and refined. The stability of the numerical scheme was demonstrated by its tolerance to increasing node spacing and widely varying parameters. In the following chapter, the profile model will be applied to several case studies to allow comparison with measured ice jam profiles and previously developed computational schemes.

TABLE 6.3

Comparison of Calculated Ice Volumes

Run	L (km)	t_{eq} (m)	V (km^3)	V_{eq} (km^3)	V/V_{eq}
01	59.5	4.41	0.325	0.315	1.03
20	30	4.41	0.169	0.159	1.07
30	15	4.41	0.086	0.079	1.08

CHAPTER 7: APPLICATION OF MODEL TO CASE STUDIES

INTRODUCTION

The 'Mackenzie River' application showed that the model is capable of calculating an ice jam profile for a wide, flat, prismatic channel. To further evaluate model performance, four additional case studies were carried out. The first three were rectangular, prismatic approximations of the Thames River (narrow and flat), the Athabasca River (wide and steep), and the Smoky River (narrow and steep). The first two channels were approximated using the same data used by Beltaos and Wong (1986) to allow comparison between the downstream transition profiles calculated by their model and those calculated by the present model. The Smoky River data was a combination of that given by Beltaos (1978) and that of Kellerhals et al. (1972). The fourth case study makes use of the actual surveyed cross-sections reported by Doyle and Andres (1978) for the Athabasca River at Ft. McMurray.

The application of the model to the first three channels

served two purposes. The first was to evaluate model performance for various realistic situations. The second was to compare the transition profiles calculated by the present model, particularly the transition lengths, with those of previous investigators. The Athabasca River case study allowed the computed water surface profile to be compared with an accurately measured one.

APPLICATION TO RECTANGULAR, PRISMATIC CHANNELS

As discussed previously, the main body of a jam may be composed of upstream and downstream transition sections and an equilibrium section. The equilibrium section, required for the jam to be fully-developed, will exist if the jam is long enough that the upstream and downstream transitions do not overlap. It was shown in the previous chapter that the shape of the upstream transition is governed primarily by the interaction of the streamwise forces on the jam and the resistance offered by the banks. On the other hand, the downstream transition is strongly influenced by the change in depth caused by the M2 water surface profile. This fundamental difference implies that the two transition lengths should be considered separately.

The transition sections in a jam approach equilibrium asymptotically and so the length of the transition regions

must be based on some arbitrary definition. As in previous investigations, the transition length has been defined as the length required for the thickness to be within 1% of the equilibrium thickness. Therefore the upstream transition length, L_{US} is defined as the length from the head of the jam to a point where the thickness is 99% of the equilibrium thickness. The downstream transition, L_{DS} length is defined as the length from the upstream end of the toe to a point where the thickness is 101% of the equilibrium thickness.

Several runs were made using the profile model and the data summarized in Table 7.1. Most of the runs were made with $\mu = 1.2$, $K_v = 4.32$ and $e = 0.4$ to allow direct comparison with the results of Beltaos and Wong (1986) regarding the downstream transition length. Two runs were also made using the data for the test case of Uzuner and Kennedy (1976), with $\mu = 1.8$ and $e = 0.4$, to allow comparison with the upstream transition lengths calculated by these investigators. From the results of these runs the upstream and downstream transition lengths were determined based on the above definitions and are presented in Table 7.1.

The downstream transition lengths calculated in the present study and by Beltaos and Wong (1986), are almost identical for the Athabasca River case (run A4). The agreement is very poor, however, for the Thames River case (run T6), for which the downstream transition calculated in

TABLE 7.1

Results of Test Runs on Rectangular Channel Data

Run	Description	S	B (m)	Q (m^3/s)	k_i (m)
T6	Thames River	0.00027	109	330	0.05
S7	Smoky River	0.00052	250	375	5.0
A4	Athabasca River	0.00036	560	1120	6.3
M6	Mackenzie River	0.000098	2000	10000	3.3
U1	Uzuner and Kennedy Test Data	0.0004	305	1120	0.57
U2	" " "	0.0004	305	800	0.57

TABLE 7.1 Cont'd

Run	k_b (m)	μ	K_{xy}	H_{eq} (m)	H_t (m)	t_{init} (m)	t_{eq} (m)
T6	0.05	1.2	4.32	5.33	4.48	0.25	1.16
S7	0.50	1.2	4.32	5.31	5.03	0.40	2.48
A4	2.2	1.2	4.32	7.95	7.52	0.75	3.66
M6	0.05	1.2	4.32	12.1	11.2	1.0	4.71
U1	0.0014	1.8	20	5.10	4.80	0.20	1.95
U2	0.0014	1.8	20	4.36	3.95	0.20	1.81

TABLE 7.1 Cont'd

Run	L_{US} (m)	L_{DS} (m)	Notes
T6	750	12600	Beltaos and Wong (1986) find L_{DS} = 957 m
S7	6000	300	
A4	12900	1100	Beltaos and Wong (1986) find L_{DS} = 1164 m
M6	34000	16500	
U1	8500	-	Uzuner and Kennedy (1976) find L_{DS} = 1850 m
U2	9000	-	Uzuner and Kennedy (1976) find L_{DS} = 1850 m

the present study is more than 10 times longer than that calculated by Beltaos and Wong. The reason for this discrepency is unknown but recent measurements of an actual (although perhaps not fully-developed) jam on the Thames (Beltaos and Moody, 1986) indicate that the downstream transition region may extend much further upstream than the 9 river widths calculated by Beltaos and Wong (1986).

The results of two runs using the test data of Uzuner and Kennedy (1976) allow comparison of the calculated upstream transition lengths. Uzuner and Kennedy included a cohesive strength of 96 Pa which was also used in the present calculations. The total channel discharge given by Uzuner and Kennedy is about 1120 m^3/s; however, the model they use reduces the discharge under the jam by the amount lost to storage as the jam lengthens upstream. Therefore, the two runs in the present study were made using discharges of 800 and 1120 m^3/s. The discharge under the jam used in the calculations of Uzuner and Kennedy should fall in this range. In both cases, the upstream transition computed by the present model is significantly shorter than that computed by Uzuner and Kennedy. The reason for this discrepency is also unknown.

APPLICATION TO ATHABASCA RIVER CASE STUDY

The Athabasca River near Ft. McMurray is a site which experiences nearly annual ice jams. Andres and Doyle (1984) reported observations and documentation of several ice jams in this reach. Of particular interest here is the documentation of the 1978 ice jam for which an accurate water surface profile was measured. Doyle and Andres (1978) and Andres (1980) provide additional information about channel geometry and ice jam conditions, making this an ideal case study to test the present profile model.

Measured channel cross-sections were given by Doyle and Andres (1978) and were converted to Geodetic elevation using the longitudinal thalweg profile given by Andres (1980). This yielded five measured cross-sections in the ice-jammed reach. Additional intermediate cross-sections were obtained by eye as a 'compromise' of the two closest measured cross-sections. A total of 22 cross-sections were used in the calculations.

The bed roughness of the jammed reach, reported by Andres and Doyle (1984) as $n_b = 0.021$, can be expressed in terms of roughness height as $k_b = 0.02$ m. This value is applicable in the wide, flat reach downstream of the jam (Kellerhals et al., 1972) but may be somewhat low for the relatively steep and narrow reach in which the jam formed. Therefore, a value of $k_b = 0.15$ m was used, a reasonable

value for a gravel bed river (see for example, Limerinos, 1970).

The profile model was run using the above channel geometry and bed roughness for various values of discharge and ice jam parameters, and profiles were computed. However, a relatively good estimate of discharge is required if a meaningful comparison between observed and computed water surface profiles is to be made. The estimate of Q = 1850 m^3/s used by Andres (1980) and Andres and Doyle (1984) may be too high (Beltaos, pers. comm.) and so a value of Q = 1200 m^3/s was adopted. It should be noted that this latter value is close to the original estimate of Doyle and Andres (1978).

An example of a computed profile is shown in Figure 7.1 along with the observed water surface elevations reported by Andres (1980). The parameters used for this run were: Q = 1200 m^3/s, k_i = 10 m, e = 0.4, $\emptyset$ = 50°, and K_{xy} = 0.24 (ie. μ = 1.3). The jam roughness, k_i, was obtained by trial and error to achieve the best agreement between the observed and computed water levels for the given discharge and jam strength parameters. A roughness height of 10 m is not unreasonable based on photographs of the jam's upper surface (Andres and Doyle, 1984), when it is remembered that the roughness height is 2 - 3 times the size of the larger roughness elements (eg. Limerinos, 1970, Kamphuis, 1974, Gladki, 1975).

The agreement between the observed and computed water

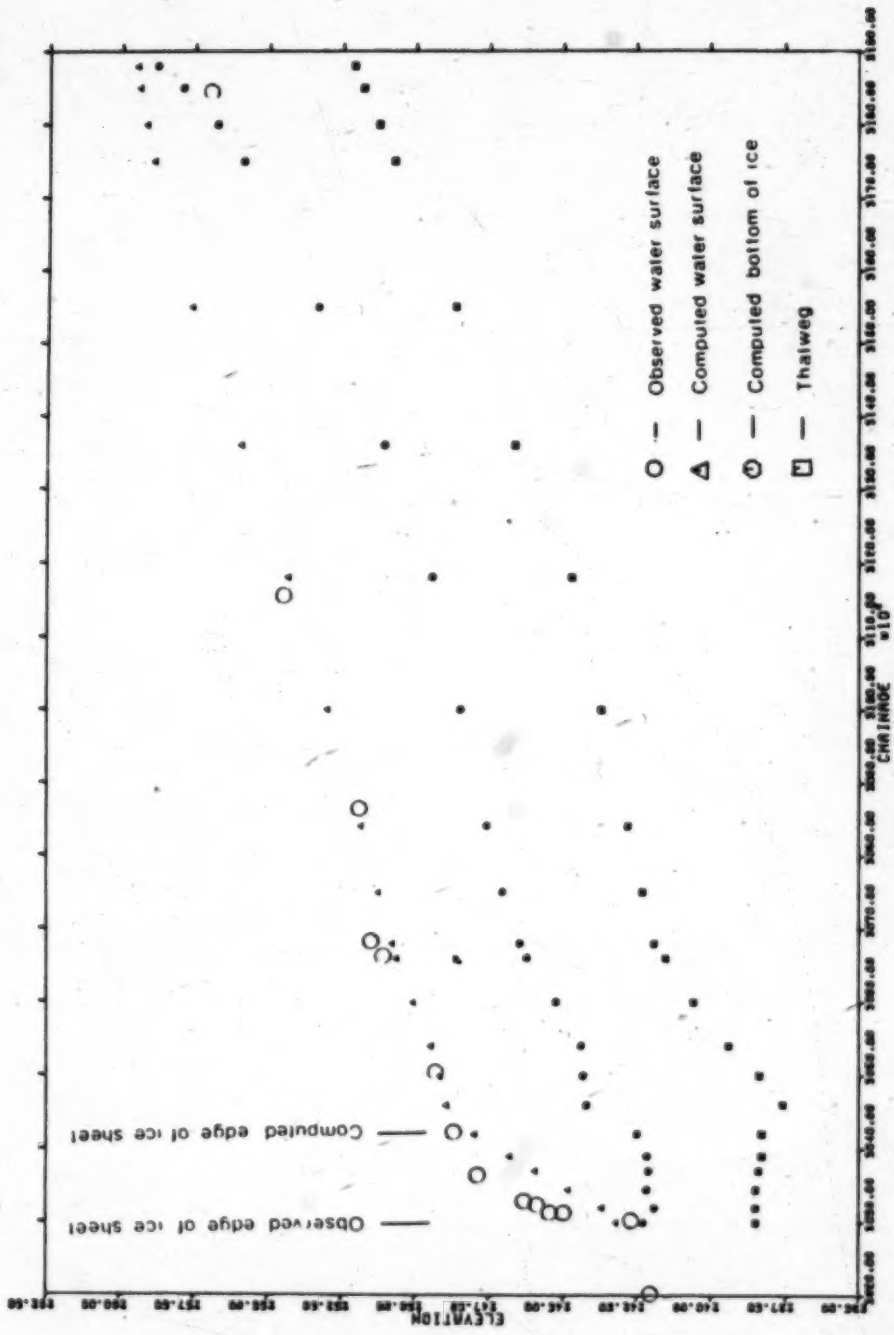

Figure 7.1 Comparison of observed and calculated water surface profiles for Athabasca River case study.

surface profiles is very good over most of the jam. The disagreement between the water levels at the head is probably explained by a lower roughness in the actual jam in the upstream reach. This accords with the observations of, for example, Calkins (1978), wherein the size of ice floes comprising a jam (and hence the roughness) decreased in the upstream direction.

At the toe, the disagreement between the two profiles may be attributable to partial grounding of the prototype jam. This is supported by the sharp rise in water level beginning at the solid ice / jam interface, which is contrary to the floating toe configuration assumed in the calculations. The agreement between the observed and computed water surface profiles is very good upstream of the computed toe region (ie. upstream of the solid ice sheet).

The computed length of the toe was found to be very sensitive to the choice of V_{max}, the erosion velocity. In this case, V_{max} was specified as 1.25 m/s because larger values prompted a switch to an M1 type of varied flow profile in the downstream transition whereas a lower value of V produced a longer toe, worsening the agreement between the observed and computed water surface profiles, and raising the depth of flow under the toe above that for the solid ice-covered reach.

The application of the present model to the Athabasca River case study has shown that it is capable of reproducing

observed ice jam water surface profiles in non-uniform channels. However, if the model is to be used as a predictive tool, techniques for estimating the various required parameters must be improved.

COMPARISON BETWEEN PRESENT MODEL AND EQUILIBRIUM ASSUMPTION

As discussed previously, there are calculation procedures available that have been used for non-uniform channel reaches, but which are based on the assumption that equilibrium theory is applicable at every section. One such method uses the gradually varied flow model, HEC-2.

Current releases of HEC-2 contain an 'ice-option' which allows a varied flow profile to be calculated when an ice cover is present (Calkins, Hayes, Daly, and Montalvo, 1982). The user specifies the thickness and roughness of the ice cover along with the cross-section geometry and hydraulic parameters.

For the present investigation, HEC-2 was used to calculate the varied flow profile for the Athabasca River, given an initial estimate of the thickness, and then the thickness at each section was calculated from Equation [4.7], the equilibrium thickness equation. The calculated thickness was then used to run HEC-2 and the cycle repeated until convergence was attained. Problems of stability, encountered

while running HEC-2, were overcome by using the average water surface slope of three neighbouring cross-sections in the thickness calculations.

The measured cross-section data for the Athabasca River was used to compare the ice jam profile calculated by this method with that of the profile model described previously. However, to avoid having to use the HEC-2 model in the strong transition regions for which it is not suited, a prismatic extension of the upstream and downstream cross-sections was made, allowing the thickness profile to approach equilibrium at each end. The thickness at each end was specified in the present model, based on trial and error, to acheive a smooth transition toward equilibrium conditions (rather than the usual solid ice and head thickness). The comparison is therefore confined to the non-uniform reach containing the real cross-section data.

As seen in Figure 7.2, the two schemes calculate very similar water surface and thickness profiles. It should be noted though, that the channel width and slope are quite uniform in this reach and so this agreement is not surprising. The agreement is not likely to be as good in very non-uniform channels.

The Athabasca River case study has shown that the present model is capable of reproducing observed water levels caused by a jam in a natural channel. However, the accuracy

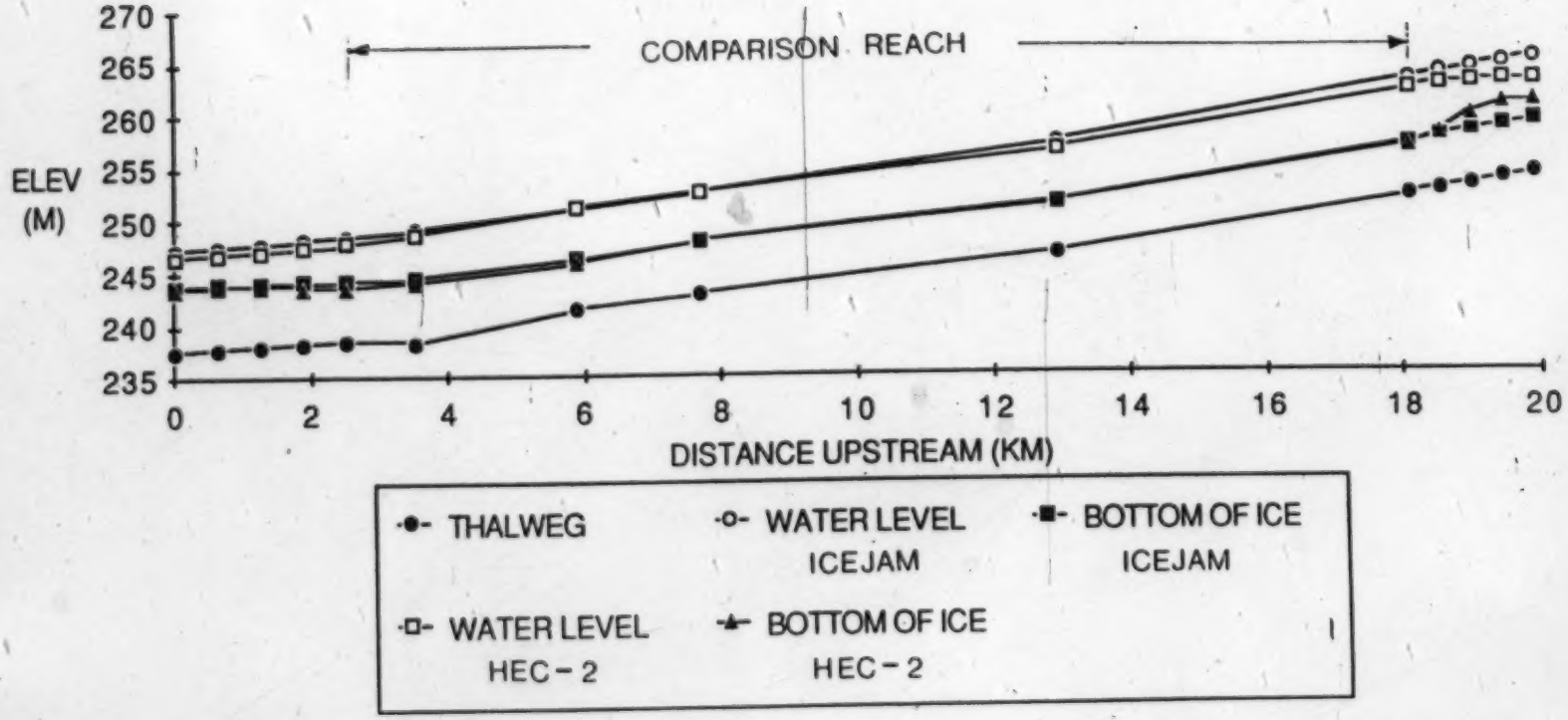

Figure 7.2 Comparison of present model with HEC-2 for Athabasca River case study.

of the calculated thickness profile cannot be tested because thickness measurments were not made. The case study has also shown that for a relatively uniform channel, the thickness and water surface profiles calculated by assuming equilibrium theory is applicable at each section are very similar to those calculated by the present model. However, the equilibrium assumption cannot be used to calculate profiles for the transition reaches of a jam.

CHAPTER 8: CONCLUSIONS

In this investigation, the problem of calculating the thickness and water surface profile along an ice jam in a natural channel was considered. Some of the relevant literature was reviewed and it was shown that only crude methods are presently available to calculate ice jam profiles. One method assumes that the jam thickness at each cross-section can be calculated based on equilibrium theory and local hydraulic and geomorphic conditions. It was not known whether this is a valid simplification in all cases. The second method makes use of the differential thickness equation which is solved numerically starting at the equilibrium section. It was argued that such a method may have limited practical application because it can only be applied to jams which do have an equilibrium section.

It has become customary in ice jam mechanics to combine several fundamental parameters into a single 'jam strength' parameter, μ. If a profile model is to be based on the differential thickness equation, the various components of μ must be specified separately. One of these components is the ratio of longitudinal to vertical stress, K_v. The coefficient K_v has been assumed by some to equal the passive pressure coefficient used in soil mechanics, but this

assumption has not been tested for ice jam situations. An experiment was conducted in which a floating sample of polyethylene beads could be 'shoved' (collapsed in compression) and the stresses measured. It was found that the passive pressure coefficient, $\tan^2(45 + \emptyset/2)$, is indeed an appropriate expression for K_v, at least near the centreline of a channel.

A computer program was developed which uses the differential thickness equation to calculate the thickness and water surface profiles over the entire length of a jam at any stage of development. It was shown that the program can tolerate large variations in parameter values and node spacing and calculates reasonable ice jam profiles for both uniform and non-uniform channels. However, the assumed 'floating toe' configuration, which is plausible for large deep rivers, may not yield an accurate profile over the (relatively short) toe region.

Test runs made with a rectangular, prismatic approximation to the Mackenzie River, allowed a qualitative assessment of the effect of various parameters on profile shape. Furthermore, the influence of the individual terms in the differential thickness equation was assessed in both the upstream and downstream transition regions. It was found that the upstream transition is most affected by the jam strength parameters, while the downstream transition is most affected by the varied flow profile, although none of these effects were large compared to the changes in the equilibrium

thickness.

Application of the model to several prismatic channels (approximations of reaches in which ice jams have been observed), allowed the length of the upstream and downsteam transitions to be calculated. It was found that the length required for a fully-developed jam to develop varied substantially but was on the order of 10 - 100 stream widths.

A realistic case study, the Athabasca River at Ft. McMurray, allowed a comparison between observed and computed water surface profiles. The agreement between the two was very good except near the head and toe of the jam. This was explained by changing roughness and inapplicability of the assumed toe configuration respectively.

This case study was also used to compare the profile calculated by the present model with that calculated assuming the validity of equilibrium theory at every section. The latter calculation was performed using the HEC-2 varied flow model. The two schemes yielded very similar profiles, but the width and slope of the channel were very uniform throughout the test reach, and so this result cannot be generalized.

FUTURE DIRECTIONS

The ice jam profile model developed herein, represents only a small step toward complete understanding of this

complex phenomenon. In particular, the model can be used to assess, at least qualitatively, the influence of various parameters on the profile shape. It is hoped that such information can be used to direct future research.

In the short term, there are several things that can be done to improve the usefulness of the model as a predictive tool, both for flood zone delineation and for design of flood protection works. The first is to test the model more thoroughly by comparing calculated profiles with those measured in the field. Such testing would require the collection of field data, which is both difficult and costly to obtain. However, this kind of comparison is essential, not only as a means of improving the model itself, but also to instill confidence in its predictive capabilities.

Another improvement would be to change the input format so that the same data set could be used for the ice jam model and HEC-2. This would make the profile model more convenient to use, since most consulting firms and government agencies already have data sets which are formatted for use with HEC-2.

In the long term, it is envisaged that the profile model would be a module in a larger 'river ice regime' model which would allow simulation of the entire freeze-up and break-up process. Such a model would include hydrologic and meteorological elements as well as unsteady flow capabilities. While such a model is only a hope for the future, it would provide a useful aid in the operation

planning and impact evaluation of hydro-power developments and flood protection works and allow more rational flood risk assessment.

LIST OF REFERENCES

Andres, D.D. 1980,'The breakup process and the documentation of the 1978 ice jams on the Athabasca River at Ft. McMurray', Proc. Workshop on Hydraulic Resistance of River Ice, Burlington, Ont.

Andres, D.D. and Doyle, P.F. 1984,'Analysis of breakup and ice jams on the Athabasca River at Ft. McMurray, Alberta,' Can. J. Civ. Eng., Vol. 11, No. 3, pp 444-458.

Barnes, H.T. 1928,'Ice engineering', Renouf, Montreal.

Beltaos, S. 1978,'Field investigations of river ice jams',IAHR Symp. on Ice Problems, Lulea, Sweden, pp 355-371.

Beltaos, S. 1983,'River ice jams: theory, case studies and applications', ASCE J. Hyd. Div., Vol. 109, No. 10, pp 1338-1359.

Beltaos, S. and Moody, W.J. 1986,'Measurements of the configuration of a breakup jam', Environment Canada, NWRI Contribution 86-123.

Beltaos, S. and Wong, J. 1986,'Downstream transition of river ice jams', ASCE J. Hyd. Div., Vol 112, No. 2, pp 91-110.

Berdennikov, V.P. 1965,'Physical characteristics of the ice in ice jams and ice gorges', Soviet Hydrology, No. 4, pp 384-402.

Bowles, J.E. 1982,'Foundation analysis and design', McGraw-Hill, 816 p..

Calkins, D.J. 1978,'Physical measurements of river ice jams', Wat. Resour. Res., Vol. 14, No. 4, pp 693-695.

Calkins, D.J. 1983,'Ice jams in shallow rivers with floodplain flow', Can. J. Civ. Eng., Vol. 10, No. 3, pp 538-548.

Calkins, D.J., Hayes, R., Daly, S.F. and Montalvo, A. 1982, 'Application of HEC-2 for ice-covered waterways', ASCE J. Tech. Councils, Vol. 108, No. 2, pp 241-248.

Caquot, A. and Kerisel, J. 1956,'Traite de mechanique des sols', Gauthier-Villars, Paris.

Cheng, S.T. and Tatinclaux, J.C. 1977,'Compressive and shear strengths of fragmented ice covers - a laboratory study', IIHR rep. No. 206.

Clement, F. and Petryk, S. 1980,'Limitations to numerical modelling of ice in rivers', Proc. Workshop on Hydraulic Resistance of River Ice, Burlington, Ontario.

Doyle, P.F. and Andres, D.D. 1978,'1978 breakup in the vicinity of Ft. McMurray and investigation of two Athabasca River ice jams', Alberta Research Council rep. SWE 78-5.

Gerard, R. 1975,'Preliminary observations of spring ice jams in Alberta', IAHR Symp. on Ice, Hanover, New Hampshire.

Gerard, R. 1979,'River ice in hydrotechnical engineering: a review of selected topics', Proc. NRCC Canadian Hydrology Symp., Vancouver.

Gerard, R. and Karpuk, E.W. 1979,'Probability analysis of historical flood data', ASCE J. Hyd. Div., Vol 105, No. 9, pp 1153-1165.

Gerard, R. and Andres, D.D. 1982,'Hydraulic roughness of freeze-up ice accumulations: North Saskatchewan River through Edmonton', Proc. Workshop on Hyd. of Ice Covered

Rivers, Edmonton.

Gerard, R. and Calkins, D.J. 1984,' Ice-related flood frequency analysis: application of analytical estimates', Proc. Cold Reg. Engineering Spec. Conf., CSCE, Montreal, Quebec.

Gladki, H. 1975,'Discussion of "Determination of sand roughness for fixed beds" ', J. of Hyd. Res., Vol. 12, pp 193-203.

Henshaw, G.H. 1887,'Frazil ice: on its nature, and the prevention of its action in causing floods', Trans. CSCE, No.1, pp 1-7.

Holtz, R.D. and Kovacs, W.D. 1981,'An introduction to geotechnical engineering', Prentice-Hall, New Jersey, 733 p.

Howells, R. 1982,'Subroutine Graph (preliminary version)', Program Documentation, Department of Civil Engineering, University of Alberta, Edmonton, Alberta.

Janssen, H.A. 1895,'Versuche uber getreidruck in silozellen', Z. Ver. Dt. Ing., pp 1045-1050.

Kamphuis, J.W. 1974,'Determination of sand roughness for fixed beds', J. Hyd. Res., Vol. 12, pp 193-203.

Keenhan, T., Panu, U.S., and Kartha, V.C. 1980,'Observation and analysis of freeze-up ice jams on the Peace River near Taylor', Proc. Workshop on Hyd. of River Ice, Burlington, Ontario.

Kellerhals, R., Neill, C.R., and Bray, D.I. 1972,'Hydraulic and geomorphic characteristics of rivers in Alberta', Research Council of Alberta, River Engineering and Surface Hydrology Report 72-1.

Kennedy, R.J. 1958,'Forces involved in pulpwood holding

grounds', Engineering Journal, Vol. 41, January, pp 58-68.

Lee, K.L. 1970,'Comparison of plane strain and triaxial tests on sand', ASCE J. Soil Mech. and Found. Div., Vol. 96, No. 3, pp 901-923.

Limerinos, J.T. 1970,'Determination of Manning coefficient from measured bed roughness in natural channels', Geological Survey Water-Supply Paper 1898-B, 47p.

Mellor, M. 1980,'Ship resistance in thick brash ice', Cold Reg. Sci. and Tech., Vol. 3, pp 305-321.

Michel, B. 1971,'Winter regime of rivers and lakes', USA-CRELL Monograph.

Michel, B. 1978 a,'Ice mechanics', Les Presse de l'Universite Laval, Que. 499 p.

Michel, B. 1978 b,'Ice accumulations at freeze-up or break-up', Proc. IAHR Int. Symp. on Ice, Lulea, Sweden, pp 303-317.

Nezhikovskiy, R. A. 1964,'Coefficients of roughness of bottom surface of slush-ice cover', Soviet Hydrology, pp 127-150.

Pariset, E. and Hausser, R. 1961,'Formation and evolution of ice covers on rivers', Trans. EIC, Vol. 5, No. 1, pp 41-49.

Pariset, E., Hausser, R., and Gagnon, A. 1966,'Formation of ice covers and ice jams in rivers', ASCE J. Hyd. Div., Vol. 92, No. 6, pp 1-25.

Peterson, A.W., and Howells, R.F. 1981,'Users manual for HYEPOL a hydraulic engineering problem oriented library', Department of Civil Engineering, University of Alberta, Edmonton, Alberta.

Petryk, S. and Boisvert, R. 1978,'Simulation of ice conditions

in channels', Conf. on Computer App. in Hydrotechnical and Municipal Eng., Toronto, Ontario.

Petryk, S., Panu, U., and Clement, F. 1980,'Recent improvements in numerical modelling of river ice', Proc. Workshop on Hydraulic Resistance of River Ice, Burlington, Ontario.

Rivard, G., Kemp, T., and Gerard, R. 1984,'Documentation and analysis of the water level profile through an ice jam, Mackenzie River, N.W.T.', Proc. Workshop on Hyd. of River Ice, Fredericton, N.B., pp 141-155.

Rivard, G. 1985,'Analysis of a Mackenzie River ice jam', M.Sc. thesis, University of Alberta, Edmonton, Alberta.

Sodhi, D. S. and Weeks, W. F. 1978,'Ice arching and the drift of pack ice through channels', IAHR Symp. on Ice, Lulea, Sweden.

Stewart, D. and Daly, S. F. 1984,'Force distribution in a fragmented ice cover', USA-CRELL report 84-7.

US Army Corps of Engineers 1982,'HEC-2 water surface profiles - users manual', Hydrologic Engineering Center, Davis, California.

Uzuner, M. S. 1975,'Stability of ice blocks beneath an ice cover', IAHR Symp. on Ice Problems, Hanover, New Hampshire.

Uzuner, M. S. and Kennedy, J. F. 1974,'Hydraulics and mechanics of river ice jams', IIHR report No. 161.

Uzuner, M. S. and Kennedy, J. F. 1976,'Theoretical model of river ice jams', ASCE J. Hyd. Div., Vol. 102, No. 9, pp 1365-1383.

APPENDIX A: MEASUREMENT OF MATERIAL PARAMETERS FOR POLYETHYLENE BEADS

MEASUREMENT OF Ø FOR POLYETHYLENE BEADS

The shear strength of the polyethylene beads was determined using a standard shear box test. The tests were conducted at the University of Alberta using a shear box apparatus measuring about 60 mm x 60 mm x 42 mm deep. Two test series were run, one with a dry sample and one with a wet sample, to see if the presence of water affected the shear strength. The wet samples were obtained by rinsing the beads with water and allowing them to drain.

As in the standard shear box apparatus, a normal load was applied to the sample through a platten supporting removeable weights as shown in Figure A1. The bottom half of the box was then displaced at a constant rate by an electric motor (in all the experiments this rate was 0.020 mm/s). The reaction on the top box was measured by an aluminium proving ring fitted with a linear variable displacement transducer (LVDT). The displacement of the bottom half of the box was measured by another LVDT. The signals from the two LVDTs were sent to a data aquisition system

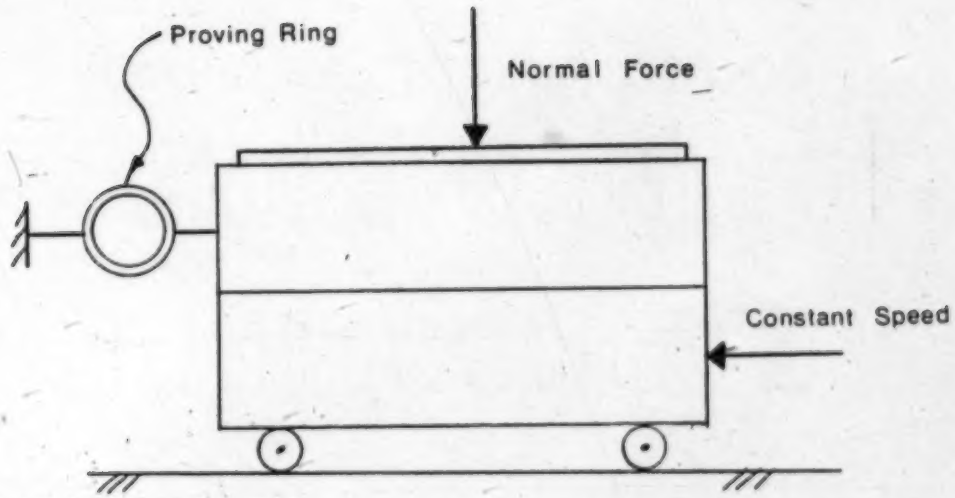

Figure A1 Sketch of shear box apparatus.

which logged the output voltage of the transducers along with the time on a strip chart recorder.

Unfortunately, the shear box apparatus did not allow normal stresses below about 1 kPa to be applied: it was expected that the stresses in the shoving experiments to follow would only be of the order of 10's of Pa. However, if the Mohr-Coulomb failure envelope can be assumed linear, the results of these tests can be applied at a lower stress level.

For each test the shear box was filled with a known (dry) mass of beads (80 g for all tests), the normal load applied and then the sample sheared. After the test, the sample was removed, mixed and weighed in preparation for the next test.

The data from the strip chart recorder was reduced to the load-displacement curves shown in Figure A2 by multiplying the voltages by a calibration coefficient. These coefficients were:

Horizontal LVDT - 4.6076 mm/Volt

Proving ring - 210.1 N/Volt

As the sample was sheared in the shear box, the area over which the shearing took place was reduced due to the displacement of the two halves of the box. This did not affect the normal stress, but the shear stress calculations must take cognizance of the reduced area. An attempt was made to use the displacement corresponding to the peak lateral load on the load-displacement curves but this was made difficult due to the lack of a distinct peak in many of the curves. For this

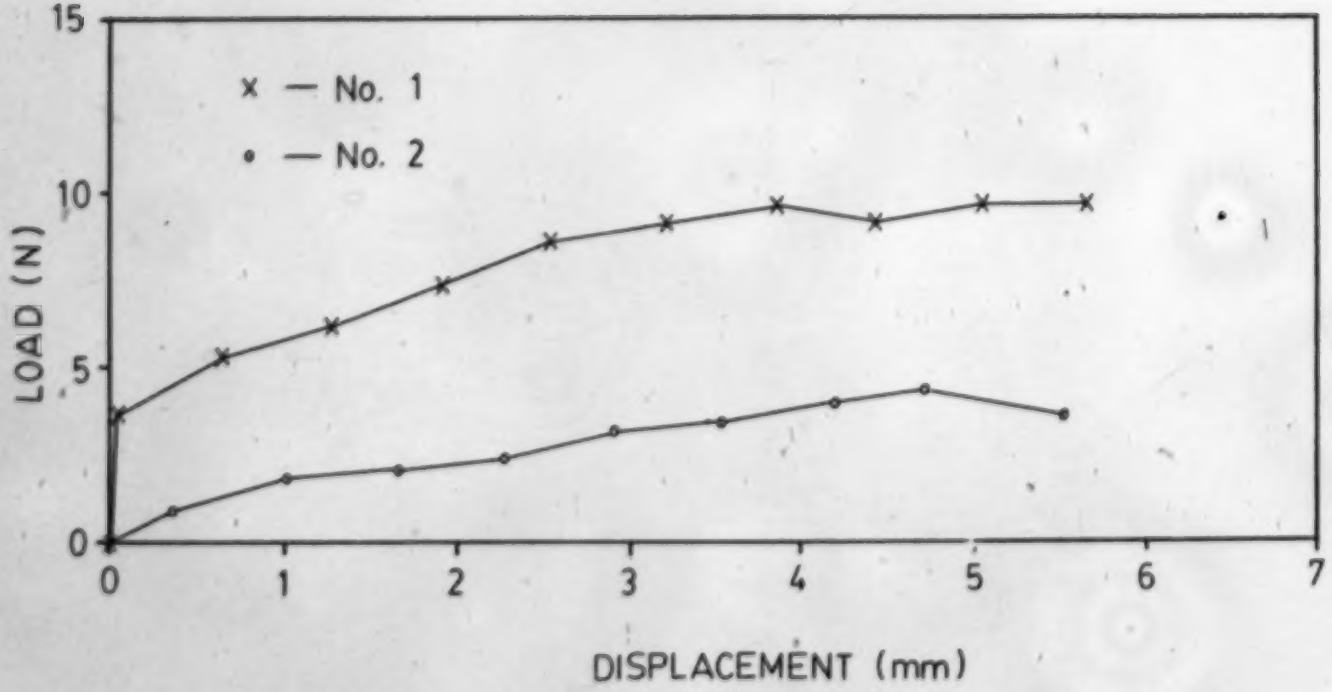

Figure A2 Load displacement curves for shear box tests on polyethylene beads.

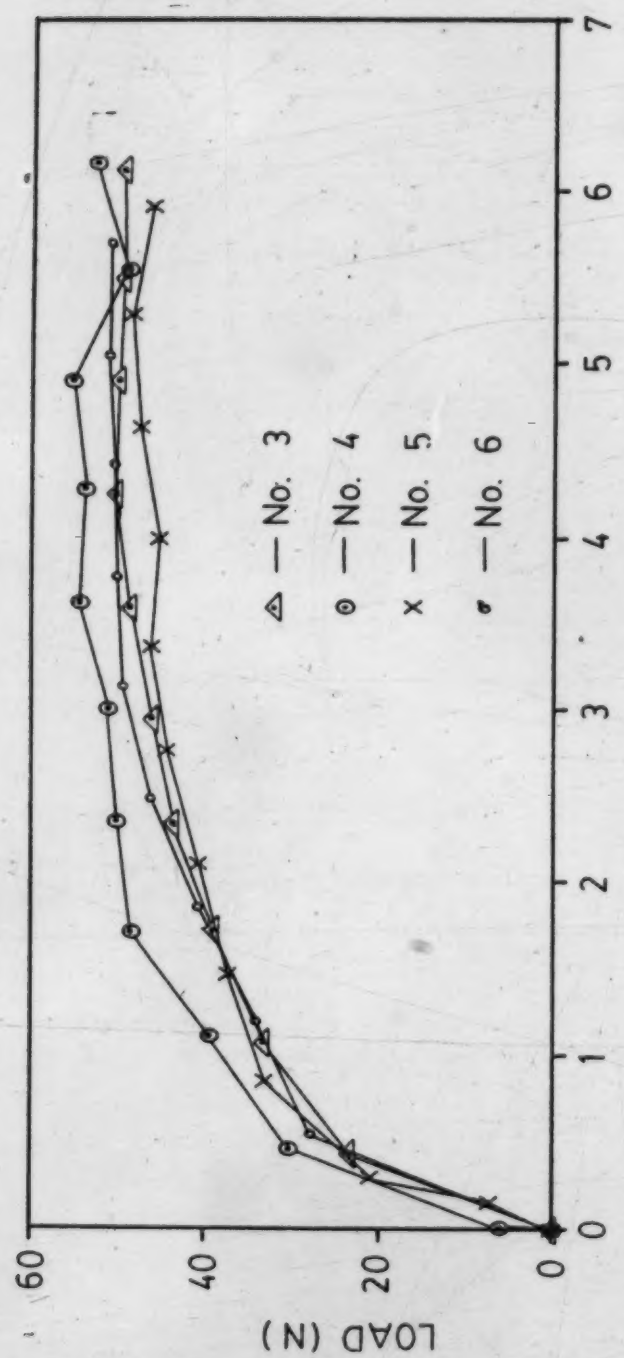

Figure A2 Continued.

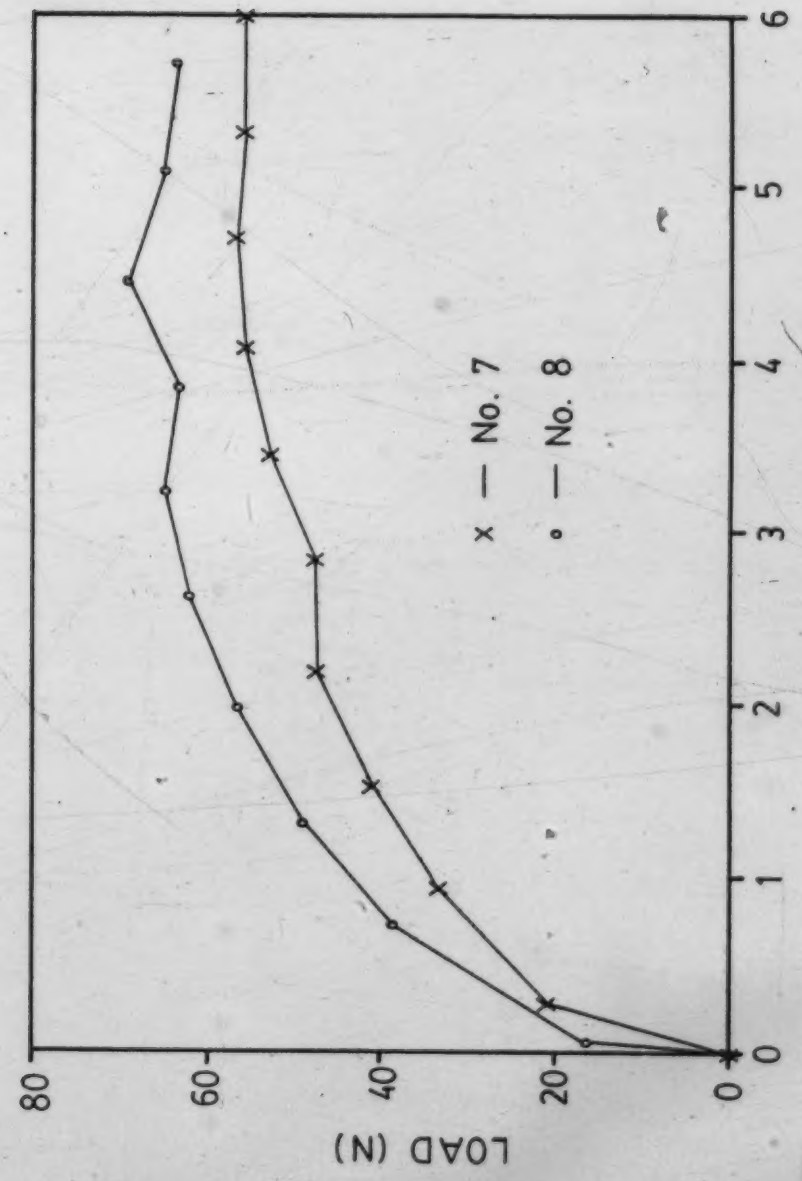

Figure A2 Continued.

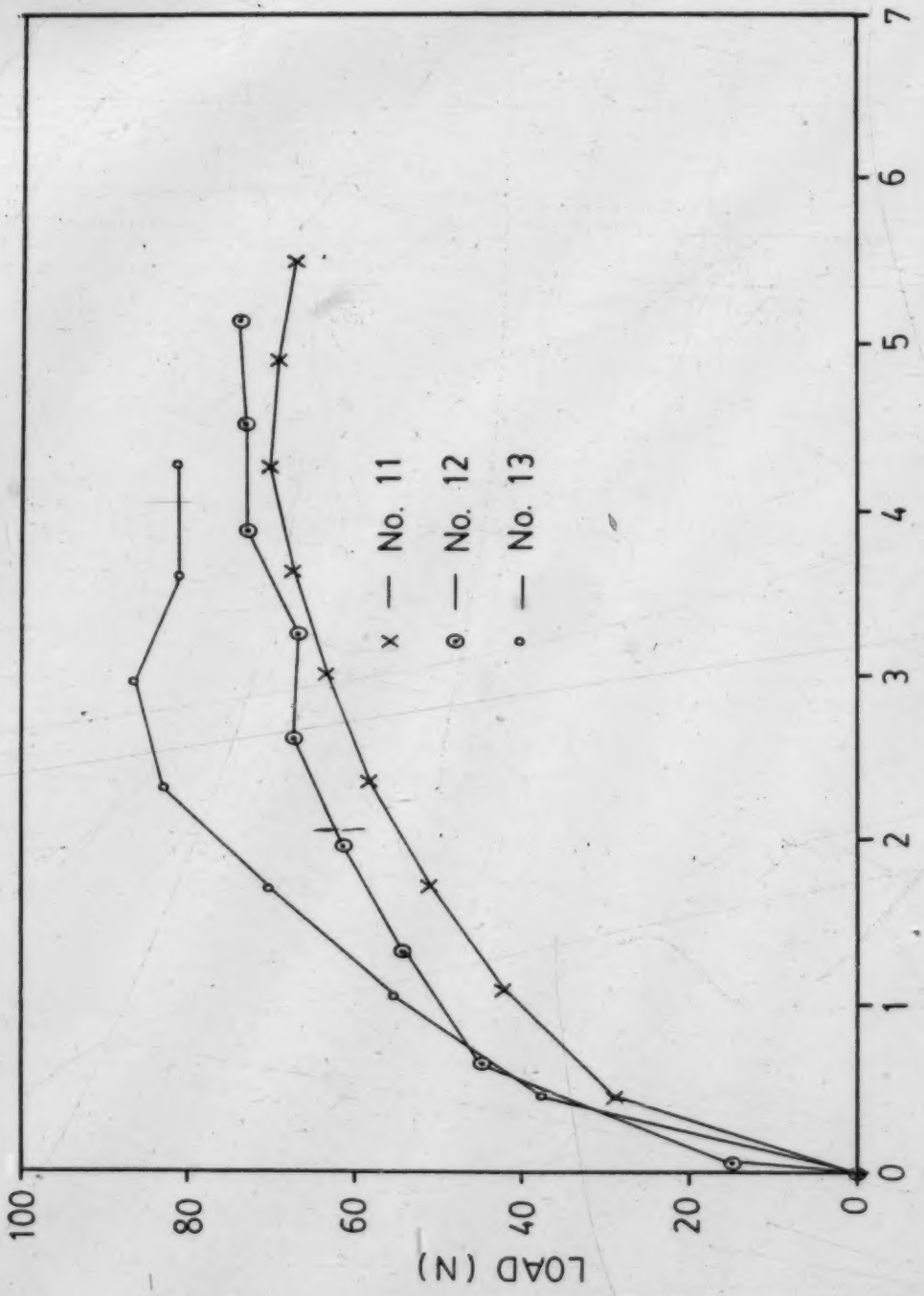

Figure A2 Continued.

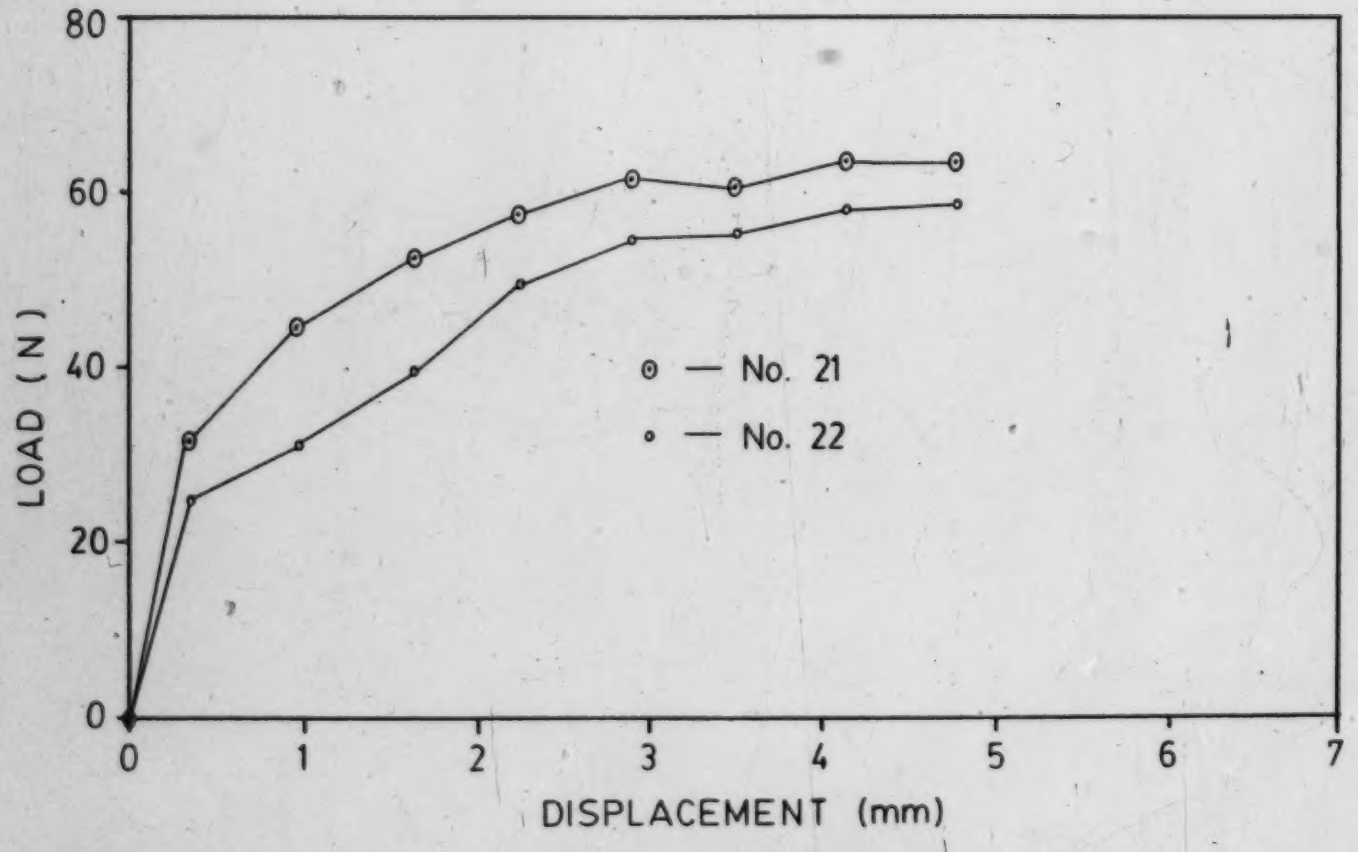

Figure A2 Continued.

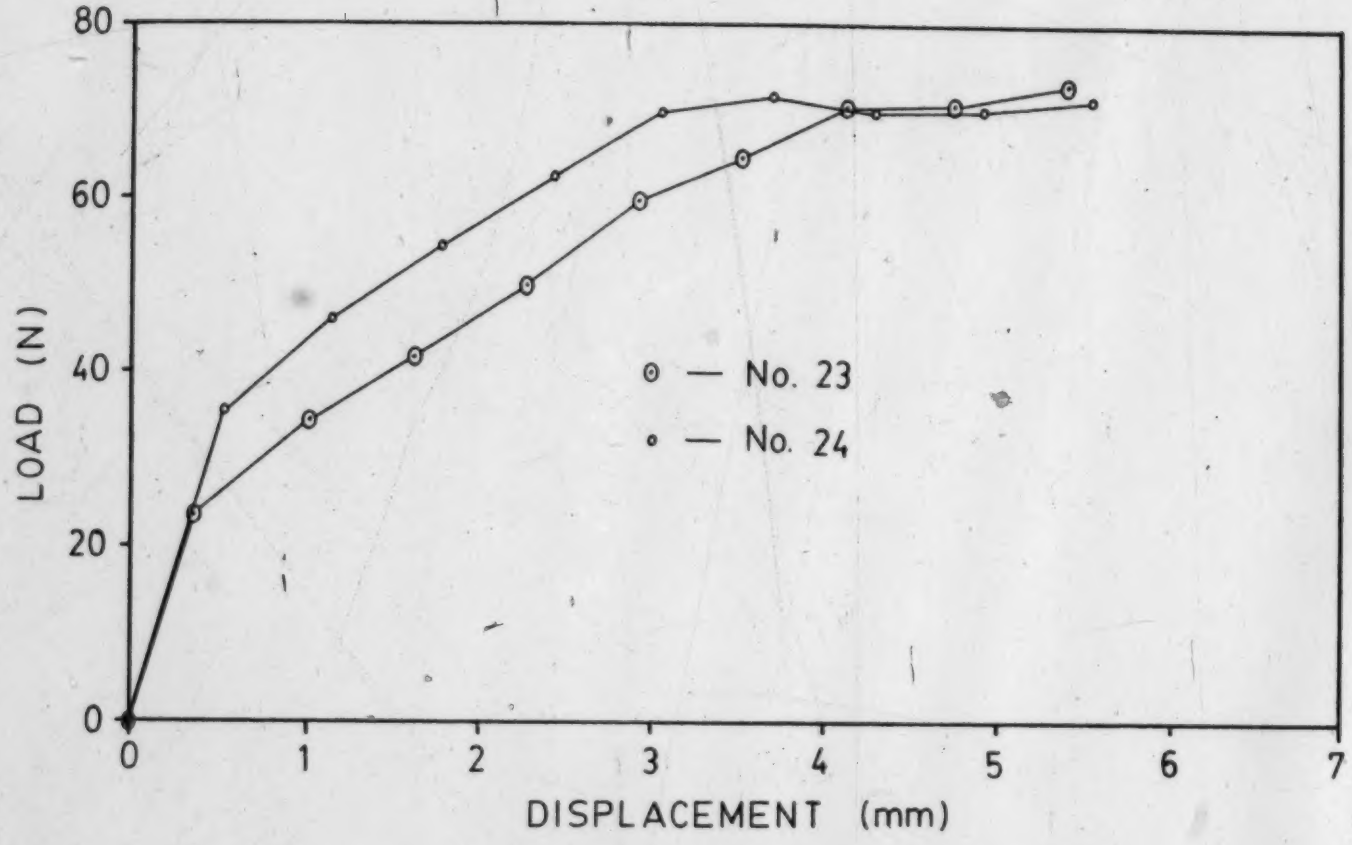

Figure A2 Continued.

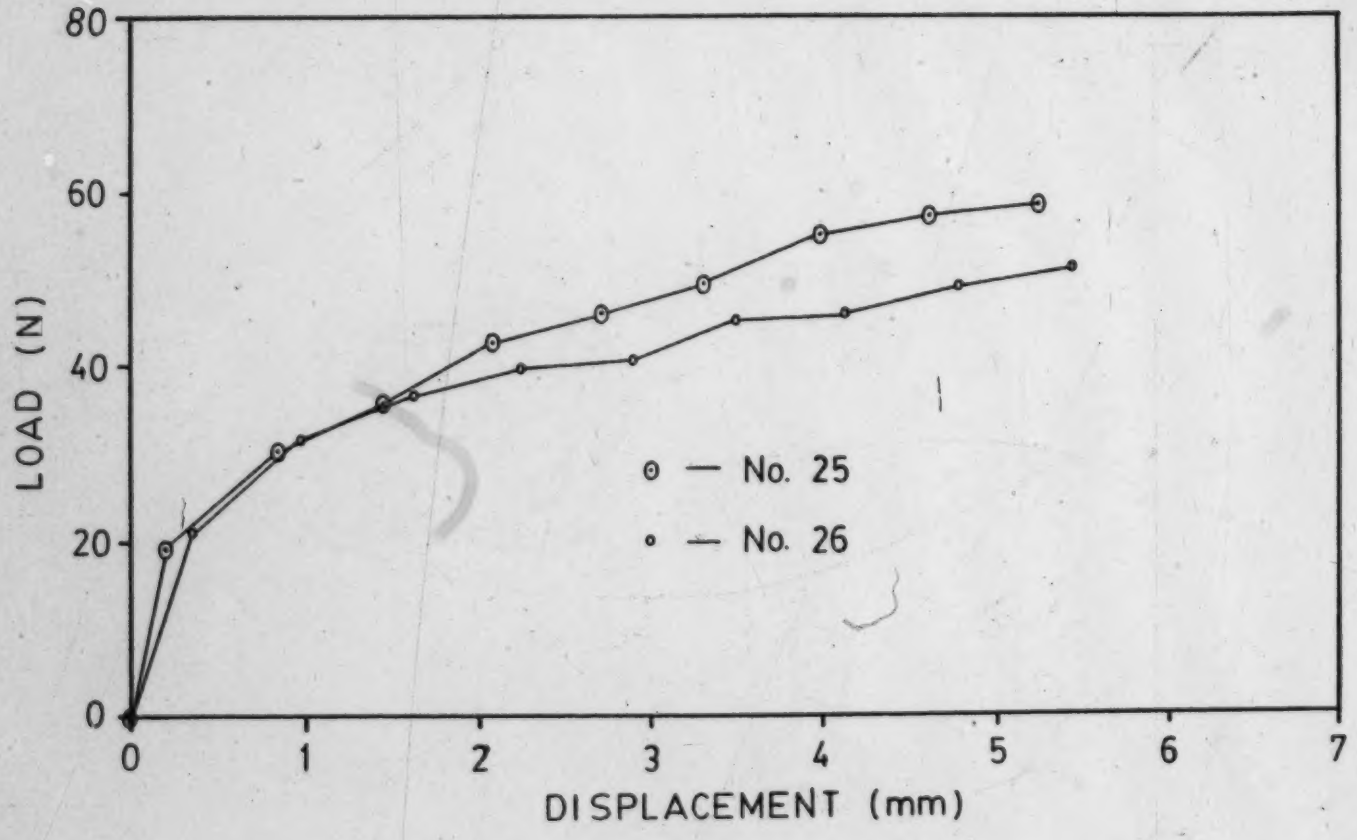

Figure A2 Continued.

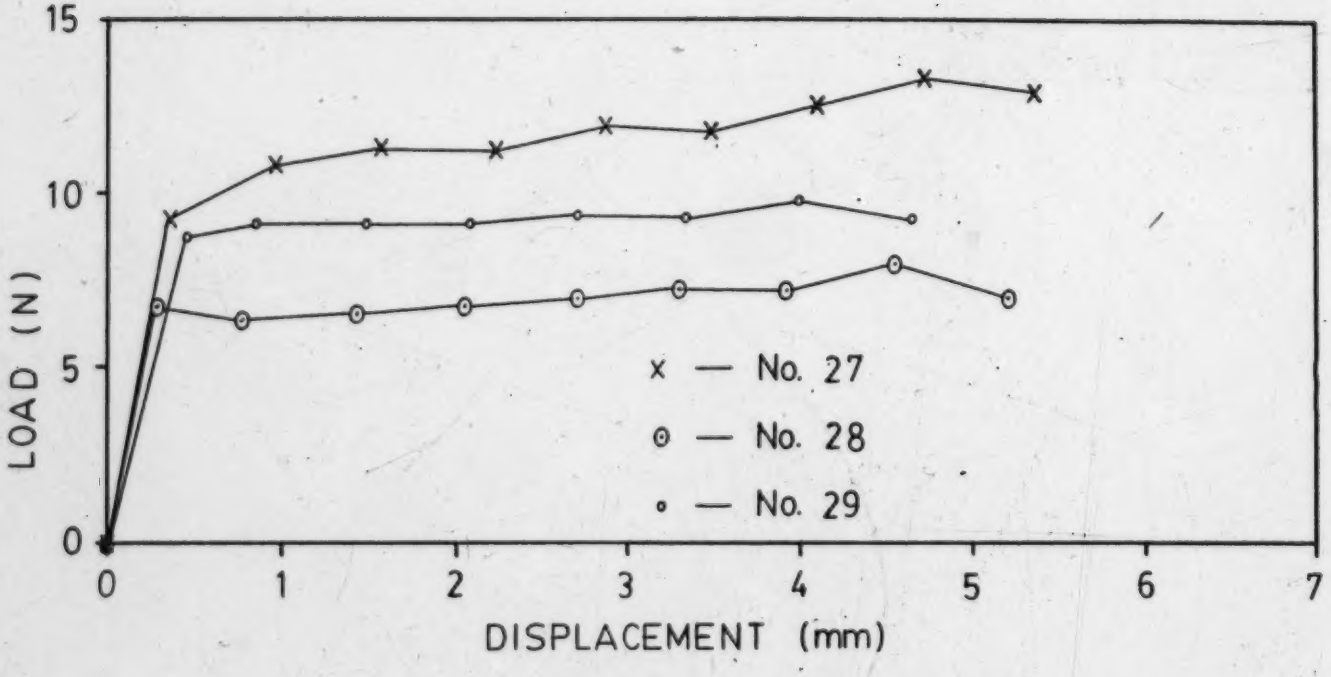

Figure A2 - Continued.

reason a displacement of 4.2 mm (slightly over one grain diameter) was chosen as representative of failure conditions and used throughout for the reduced area calculations (except for tests 27 - 29 in which 3.2 mm was used).

The results of these calculations are given in Table A1. The Mohr-Coulomb failure envelope was determined by linear regression and is shown in Figure A3. The angle of shearing resistance so obtained is 48.9° However it should be remembered that shear box tests normally overestimate Ø by 1° - 4° (Lee, 1970 as quoted in Bowles, 1982). The apparent cohesion is likely due to friction between the two boxes.

MEASUREMENT OF SPECIFIC GRAVITY AND POROSITY

The specific gravity was found by pouring a sample of beads into a graduated cylinder partially filled with water. The cylinder was weighed before and after to obtain the mass of the sample. The volume displaced by the sample was determined by the increase in volume indicated on the cylinder's graduations. Fortunately the friction between the sample and the glass walls of the cylinder was sufficient to overcome almost all of the sample's buoyancy and so, with a little care, virtually all of the sample could be submerged for the volume measurement. The specific gravity of the

TABLE A1
Shear box test results

Test No	'Peak' Displacement (mm)	Area (mm^2)	σ (kPa)	τ (kPa)
1	4.2	3330	1.06	2.90
2	4.2	3330	1.06	1.20
3	4.2	3330	11.34	15.02
4	4.2	3330	11.34	16.22
5	4.2	3330	11.34	14.11
6	4.2	3330	11.34	15.02
7	4.2	3330	12.89	16.82
8	4.2	3330	12.89	18.32
11	4.2	3330	18.37	20.87
12	4.2	3330	18.37	21.86
13	4.2	3330	18.37	21.86
21	4.2	3330	12.89	17.48
22	4.2	3330	12.89	19.07
23	4.2	3330	18.37	21.02
24	4.2	3330	18.37	21.02
25	4.2	3330	11.34	13.87
26	4.2	3330	11.34	16.67
27	3.2	3389	1.06	2.07
28	3.2	3389	1.06	2.72
29	3.2	3389	1.06	3.51

Tests 1 - 13 Dry
Tests 21 - 29 Wet

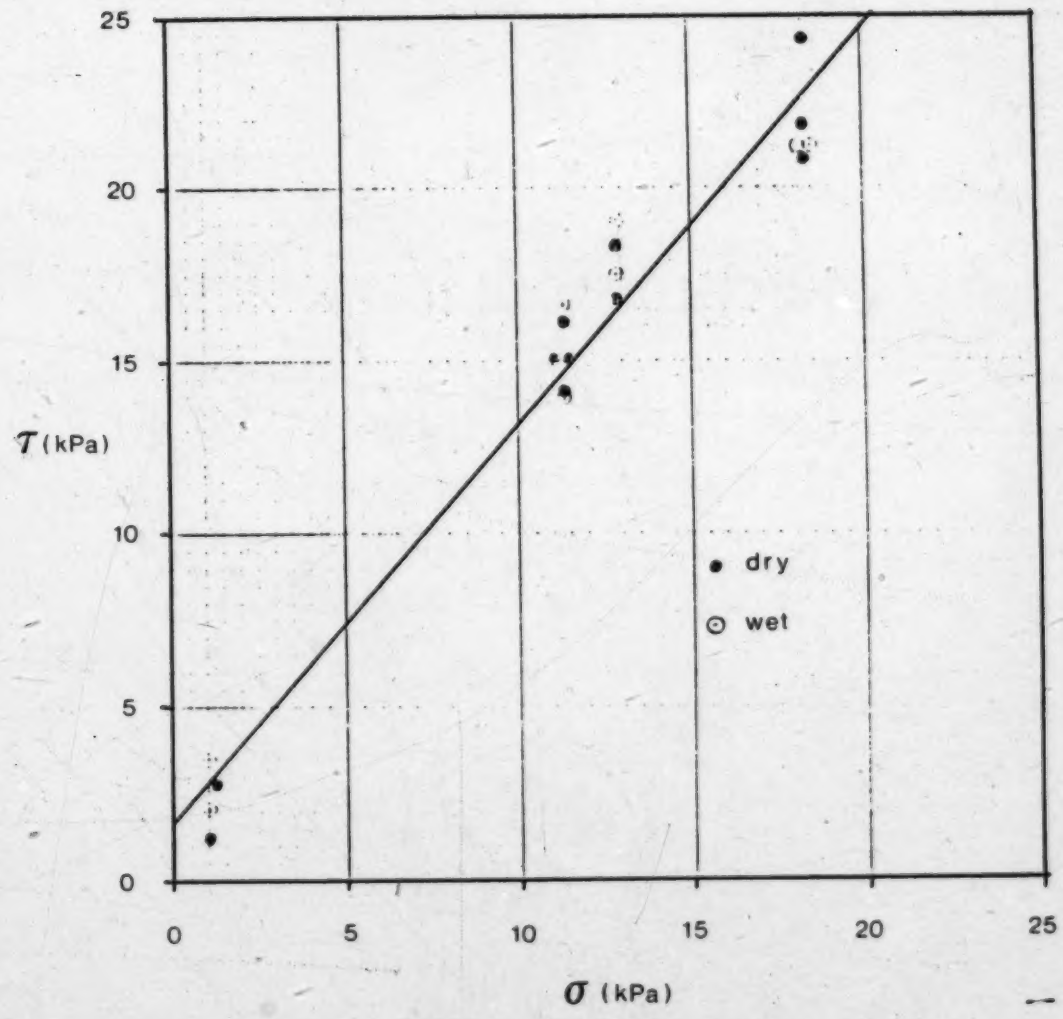

Figure A3 Failure envelope for shear box tests on polyethylene beads.

polyethylene beads was found to be 0.920.

The porosity of the beads was determined using the same graduated cylinder. In this test, the sample was again poured into the cylinder which was partially filled with water. As before, the volume displaced by the sample could be read directly from the graduations on the cylinder's side. The bulk volume of the sample could be determined by subtracting the volume corresponding to the top surface from the volume corresponding to the bottom surface (the sample was carefully leveled to ensure an accurate measurement). The porosity was calculated by subtracting the displacement from the bulk volume and dividing the result by the bulk volume.

The porosity was determined for two extreme conditions: the 'loose' condition was achieved by 'plunging' the sample with a plastic ruler and allowing it to float freely to the surface while the 'dense' condition was achieved by stirring and tapping the sample so that it compacted. The porosity was found to vary between 0.41 for the loosest possible state to 0.34 for the densest state that could be achieved with a 100mm deep sample.

APPENDIX B: DETAILS OF ICE JAM PROFILE MODEL

INTRODUCTION

The basic logic of the program has been discussed in Chapter 5. This Appendix contains details of the two important subroutines namely: THICK - the subroutine responsible for calculating the thickness profile; and GVF - the subroutine responsible for calculating the gradually varied flow profile. Following this is a complete listing of ICEJAM ver. 1.5 which is the version of the program used in all of the applications in Chapters 6 and 7. As well, a sample data file is presented containing typical data for the Athabasca River application discussed in Chapter 7.

SUBROUTINE THICK

This subroutine calculates the thickness profile of an ice jam by solving Equation [4.4] using a forward difference scheme. Equation [4.4] can be written as:

[1] $$\left(\frac{dt}{dx}\right)_i^{j+1} = \bar{a}\,\bar{b} + \frac{\bar{b}}{\bar{t}} + \bar{c}$$

where:

$$\bar{a} = (K_{xy}\tan\emptyset)/\bar{B}$$

$$\bar{b} = \bar{\tau}_i/(2K_v\gamma_e)$$

$$\bar{c} = (\rho' g\bar{S}_w)/(2K_v\gamma_e)$$

$$\bar{t} = \text{thickness}$$

The bars over the variables indicate that they are averages of values for the two computational nodes. The subscript i indicates the computaional node while the superscript j is an iteration index. The remainder of the terms are as defined in Chapter 4.

A forward difference algorithm (based on the defintion sketch of Figure B1) which can be used to solve this equation is as follows, beginning with a known value of t.

Step 1) Estimate t_i^{j+1} (after the first iteration, this is taken as the value from the last cycle)

Step 2) Calculate:

$$a = (a_i + a_{i+1})/2$$

$$b = (b_i + b_{i+1})/2$$

$$c = (c_i + c_{i+1})/2$$

$$t = (t_i + t_{i+1})/2$$

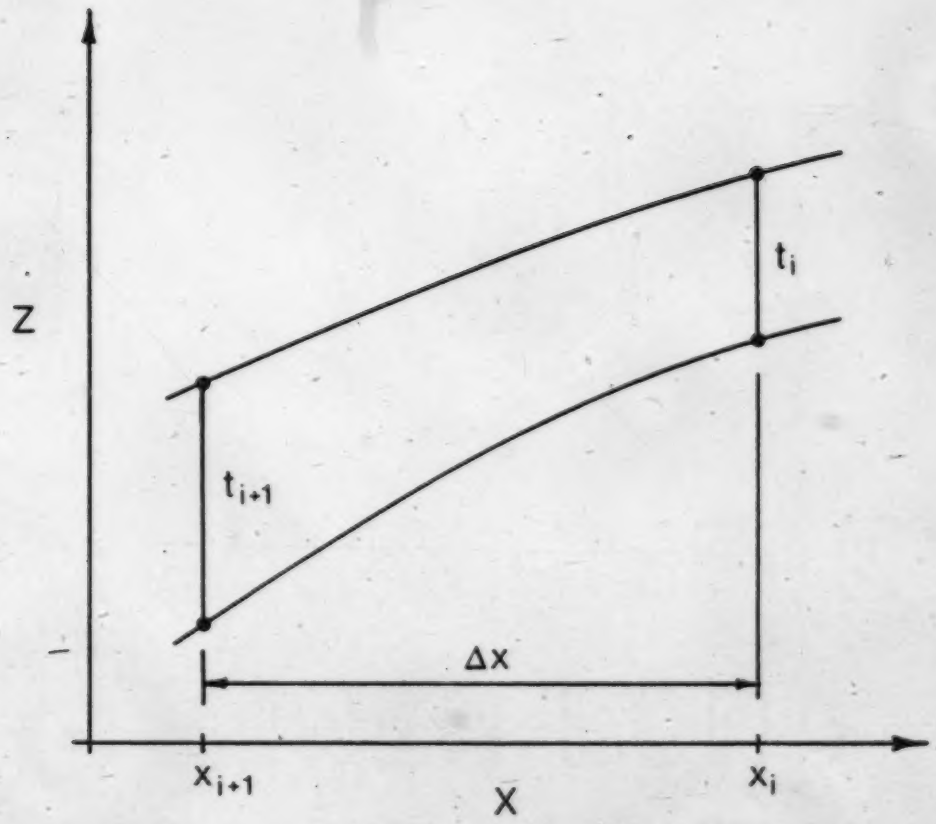

Figure B1 Definition sketch for forward difference algorithm used in thickness calculations.

step 3) Calculate $(dt/dx)_i^{j+1}$ from Equation (A1)

step 4) Calculate: $t_i^{j+1} = t_i + (dt/dx)_i^{j+1} \Delta x$

step 5) IF: $(t_i^{j+1} - t_i^{j}) > \text{tolerance}$

THEN: $t_i^{j+1} = t_i^{j} + D(t_i^{j+1} - t_i^{j})$

GO TO step 2

ELSE: GO TO next node (ie. i = i + 1)

A 'damping factor', D, was introduced in step 5 of the algorithm to ensure that the procedure would converge to a solution unconditionally. This factor has been set at 0.33 in the program. The possible reduction in accuracy caused by this damping has been offset by specifying a small tolerance (equal to 0.0001 m).

SUBROUTINE GVF

The 'standard step' algorithm used to calculate the gradually varied flow profile is somewhat more complicated. In general, this algorithm can be stated as follows (based on

the definition sketch of Figure B2).

Step 1) WSAVE = h_i^{j+1}

Step 2) Estimate h_i^{j+1} (taken as the value from the previous cycle)

Step 3) Calculate H_{Ti}^{j+1} and S_{fi}^{j+1} using equations [4.5], [4.6], and [4.9]

Step 4) Calculate: $S_f^j = (S_f^j + S_{fi}^{j+1})/2$

Step 5) Calculate: $H_{Ti}^{j+1+1} = H_{Ti} + S_f^j \Delta x$

step 6) IF: $(H_{Ti}^{j+1+1} - H_{Ti}^{j+1}) >$ tolerance

THEN: refine estimate of h_i^{j+1}

GO TO step 3

ELSE: $h_i^{j+1+1} = WSAVE + D'(h_i^{j+1+1} - h_i^{j+1})$

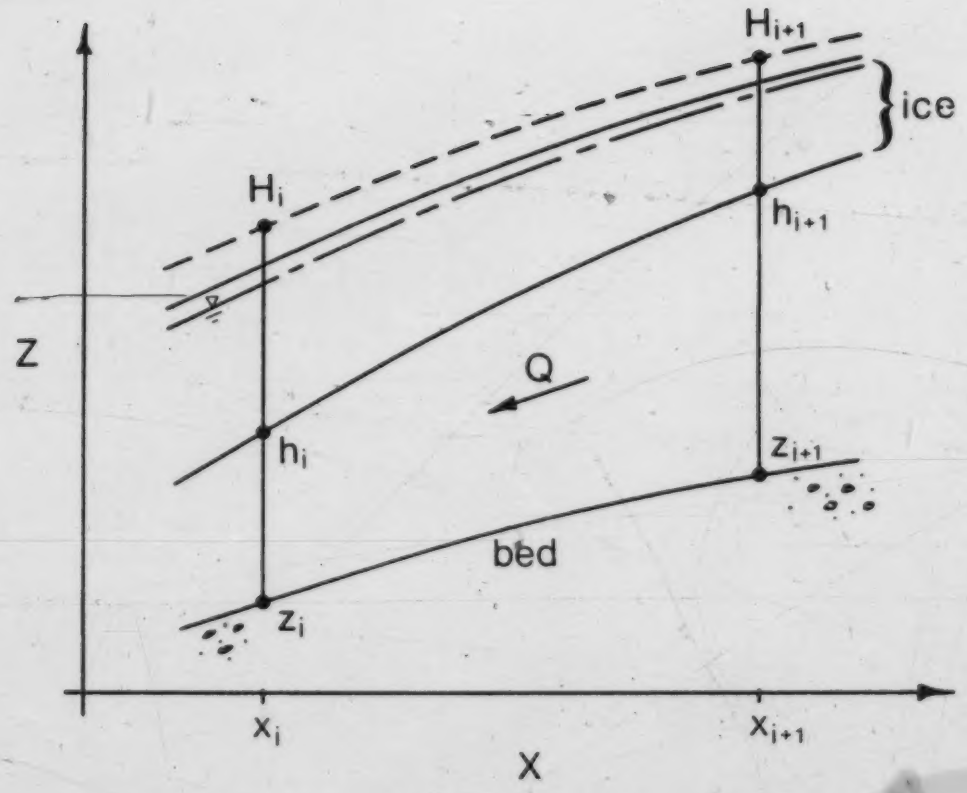

Figure B2 Definition sketch for 'standard step' algorithm used in depth calculations.

GO TO next node

The procedure used in step 6 to refine the estimate of h_i^{j+1} is simply to examine the difference between H_i^{j+*1} and H_i^{j+1} and to add or subtract a fraction (about 1/3) of this difference to or from H_i^{j+*1} so as to make this difference smaller. Although this seems to be a very inefficient procedure, it usually finds a solution in less than five iterations. A rugged procedure like this was necessary because the slope in the toe region is so steep that other methods have difficulty obtaining a solution.

The 'damping factor' D' (which is the one mentioned in Chapter 5) is required so that the entire profile does not oscillate on either side of the solution (which was found to occur in some cases with D' =1).

PROGRAM ICEJAM ver. 1.5

DEFINITION OF IMPORTANT VARIABLES AND ARRAYS IN THE PROGRAM

ARRAYS:

A	- array containing x-sect. areas
B	- array containing horizontal x-sect. coordinates
DFLAG	- array containing diagnostic information
FSLOPE	- array containing friction slope at each x-sect.
H	- array containing vertical x-sect. coordinates
IERR	- array containing diagnostic information
MYPTS	- array containing number of coordinate points describing x-sect.
P	- array containing wetted perimeter for each x-sect.
R	- array containing hydraulic radius for each x-sect.
RKR	- array containing ratio of ice roughness to bed roughness
ROUGHI	- array containing roughness of ice underside
ROUGHB	- array containing roughness of bed
ROUGHC	- array containing domposite roughness of x-sect.
SLOPE	- array containing open water surface slope used for normal depth calculations
TCK	- array containing ice thickness at each x-sect.

THALW - array containing thalweg elevation at each x-sect.

TW - array containing width of jam underside at each x-sect.

WMIN - array containing minimum depth of flow calculated from specified maximum (erosion) velocity

WSEL - array containing elevation of ice underside

WSLOPE - array containing water surface slope with ice cover in place

X - array containing chainage of each x-sect.

VARIABLES:

CI - cohesion (Pa) [note: this is included only to allow comparison with other models - it is not theoretically correct]

E - porosity (dimensionless)

KERR - counter used for diagnostic messages

MAXIT - specified maximum number of iterations

NX - number of cross-sections

NUMBER - run identification number

PK	- vertical stress coefficient (K , dimensionless)
Q	- discharge (m /s)
RHO	- ice density (kg/m)
SERR	- counter used for diagnostic messages
TANPHI	- tangent of shearing angle (dimensionless)
TAT	- thickness of solid ice sheet at toe (m)
TINIT	- thickness at head (m)
TOLERH	- specified tolerance on depth of flow (m)
VMAX	- maximum erosion velocity (m/s)
XK	- lateral stress coefficient (dimensionless)

PROGRAM LISTING:

The following pages contain a listing of the program ICEJAM ver. 1.5. This listing also contains subroutine GRAPH which is the program segment that generates a graphical display of the output on a CALCOMP plotter. Note that the word processor which was used to produce this document uses proportional spacing and so the line numbers in the FORTRAN code do not appear to be in the first 6 columns as is usually the case.

Two of the subroutines used in this program (NORMD and XSPROP are adapted from subroutines bearing the same (or similar) names in the HYEPOL library of subroutines (Howells and Peterson, 1981).

The concept and call format for the GRAPH plotting subroutine are similar to those of a program by the same name (Howells, 1982) which the author had used previously at the University of Alberta. The source code for Howell's version of GRAPH was not available and so a new, somewhat limited version was written for use on the CYBER computer at the Canda Centre for Inland Waters.

```
C
C
C
      PROGRAM ICEJAM(TAPE5,TAPE6)
C*****************************************************************
C                                                                *
C                     ** ICEJAM **                               *
C                                                                *
C        VERSION: 1.5    LAST REVISION:  MAR 16/87               *
C                                                                *
C                                                                *
C          WRITTEN BY: GREG FLATO                                *
C                                                                *
C        DEPARTMENT OF CIVIL ENGINEERING                         *
C          UNIVERSITY OF ALBERTA                                 *
C                                                                *
C*****************************************************************
C                                                                *
C                                                                *
C* THIS PROGRAM CALCULATES THE THICKNESS                         *
C* PROFILE OF AN ICEJAM IN A NATURAL CHANNEL.                    *
C                                                                *
C*****************************************************************
C
C  SECTION: MAIN
C
C*****************************************************************
C
C  MAIN PROGRAM
C
      DIMENSION MYPTS(199),X(199),ROUGHI(199),ROUGHB(199),B(199,25)
      DIMENSION H(199,25),THALW(199),A(199),TW(199),P(199)
      DIMENSION R(199),SLOPE(199),ROUGHC(199),RKR(199),DFLAG(199)
      DIMENSION FSLOPE(199),TCK(199),TP(199),WSLOPE(199),EWAT(199)
      DIMENSION OPTN(12),ADUMMY(2,2),BDUM(8,199),IERR(199)
      DIMENSION TT(5),XSERR(199),XT(5),Y(5),C(5),TSAVE(199)
      DIMENSION IDUM(3,3),LABEL(6),WMIN(199)
      COMMON/ONE/SLOPE,ROUGHC,FSLOPE,RKR,WSLOPE
      COMMON/TWO/WSEL,MYPTS,B,H,XSERR
      COMMON/THREE/A,P,R,TW
      COMMON/FOUR/TINIT,TANPHI,RHO,E,XK,PK,CI
      COMMON/FIVE/TCK,X
      DOUBLE PRECISION WSEL(199)
C
C  INPUT DATA AND ECHO CHECK
C
      READ(5,50) NUMBER,MAXIT
   50 FORMAT(I8)
      READ(5,100) TINIT,TAT,Q,TANPHI,RHO,E,XK,PK,CI
      READ(5,100) TOLERH,VMAX
  100 FORMAT(F10.3)
      READ(5,51) NX
      WRITE(6,40)
   40 FORMAT(//' *** OUTPUT FROM: ICEJAM *** ')
   51 FORMAT(I3)
```

```
      WRITE(6,98) NUMBER
   98 FORMAT(/' -- RUN NUMBER ',I8,' --')
      WRITE(6,101) Q
  101 FORMAT(//'DISCHARGE = ',F10.3)
      WRITE(6,99) TINIT
   99 FORMAT(/'INITIAL THICKNESS GIVEN AT HEAD OF JAM.... ',F10.3)
      WRITE(6,97)TAT
   97 FORMAT('THICKNESS GIVEN AT TOE OF JAM..... ',F10.3)
      WRITE(6,102) TANPHI
  102 FORMAT('TANGENT OF SHEARING ANGLE..... ',F10.3)
      WRITE(6,103) RHO
  103 FORMAT('ICE DENSITY..... ',F10.3)
      WRITE(6,104) E
  104 FORMAT('POROSITY..... ',F10.3)
      WRITE(6,105) PK
  105 FORMAT('PASSIVE PRESS. COEFF. ..... ',F10.3)
      WRITE(6,106)XK
  106 FORMAT('SHEAR COEFFICIENT..... ',F10.3)
      WRITE(6,107) CI
  107 FORMAT('COHESION..... ',F10.3)
      WRITE(6,109) TOLERH
  109 FORMAT('TOLERANCE ON DEPTH OF FLOW..... ',F10.3)
      WRITE(6,110) MAXIT
  110 FORMAT('MAXIMUM NUMBER OF ITERATIONS..... ',I6)
      WRITE(6,111) VMAX
  111 FORMAT('MAXIMUM VELOCITY UNDER JAM ..... ',F10.3)

C
      CALL INPUT(NX,THALW,X,ROUGHI,ROUGHB)
C
C  CALCULATE WATER SURFACE SLOPE AT EACH CROSS-SECTION
C
      CALL SLOP(NX,X,THALW,WSEL)
C
C  CALCULATE COMPOSITE ROUGHNESS OF EACH CROSS-SECTION
C
      CALL COMPR(NX,ROUGHI,ROUGHB)
C
C  CALCULATE THE UNIFORM FLOW DEPTH
C
C
C  CALCULATE MINIMUM DEPTH BASED ON VMAX
C
      CALL MINDEP(NX,Q,KERR,THALW,VMAX,WMIN)
      IF(KERR.EQ.5) GO TO 204
C
      SERR=0.0
      CALL NORMD(NX,Q,WSEL,SERR,THALW)
      IF(SERR.LT.0.01) GO TO 998
      WRITE(6,666)
  666 FORMAT(/'****MAXIMUM NUMBER OF ITERATIONS EXCEEDED
     <'/'IN SUBROUTINE: NORMD
     <'/'****EXECUTION TERMINATED****')
      STOP
C
```

```
C  CALCULATE THE THICKNESS PROFILE USING THE
C  FLOW DEPTHS FROM THE GRADUALLY VARIED FLOW
C  CALCULATIONS. (FOR THE FIRST TRIAL, USE
C  THE UNIFORM FLOW DEPTHS)
C
  998 KSTEP=0
  999 KERR=1
      DO 997 I=1,NX
      IERR(I)=0
  997 DFLAG(I)=0.
      KSTEP=KSTEP+1
      CALL THICK(NX,Q,DFLAG,FLAG,KSTEP,KERR,TAT,TSAVE)
      IF(KERR.NE.1) GO TO 202
   55 CONTINUE
C
C  CALCULATE THE GRADUALLY VARIED FLOW DEPTHS,
C  GIVEN THE THICKNESS PROFILE FROM THE PREVIOUS
C  STEP, USING THE 'STANDARD STEP METHOD'.
C
C  CHANGE IN CALCULATED DEPTH IS TESTED AGAINST
C  TOLERANCE AND KERR IS SET EQUAL TO 4 IF THE
C  CROSS-SECTION DOES NOT MEET TOLERANCE
C
      CALL GVF(NX,Q,TOLERH,KSTEP,KERR,THALW,ROUGHB,RHO,IERR,VMAX,WMIN)
C
C  CHECK FOR ERRORS, IF NONE, CONTINUE
C
      IF(KERR.NE.4) GO TO 202
      IF(KSTEP.LT.MAXIT) GO TO 999
      DO 199 I=1,NX
      IF(IERR(I).EQ.1) WRITE(6,198) I
  199 CONTINUE
  188 FORMAT(/'***THICKNESS CHANGED TO FIT BACKWATER AT SECTION(S): ')
  198 FORMAT(/'**GVF DID NOT CONVERGE FOR SECT. ',I3,' AND WAS
     <'/'SET EQUAL TO MINIMUM')
      DO 300 I=1,NX
      IF(IERR(I).EQ.2) GO TO 301
  300 CONTINUE
      GO TO 302
  301 WRITE(6,188)
      DO 303 I=1,NX
      IF(IERR(I).EQ.2) WRITE(6,197) I
  303 CONTINUE
  197 FORMAT(10X,I3)
  302 CONTINUE
C
      WRITE(6,200) MAXIT
  200 FORMAT(/'***MAXIMUM NUMBER OF ITERATIONS (',I3,') EXCEEDED')
  888 WRITE(6,201)
  201 FORMAT(/' THE PROFILE AT THIS POINT IS AS FOLLOWS:')
      GO TO 204
  202 DO 203 I=1,NX
      IF(IERR(I).EQ.1) WRITE(6,198) I
  203 CONTINUE
      DO 400 I=1,NX
```

```
      IF(IERR(I).EQ.2) GO TO 401
  400 CONTINUE
      GO TO 204
  401 WRITE(6,188)
      DO 403 I=1,NX
      IF(IERR(I).EQ.2) WRITE(6,197) I
  403 CONTINUE
  204 CALL OUTPUT(Q,NUMBER,KSTEP,KERR,NX,THALW,ROUGHI,R,DFLAG,IERR)
      STOP
      END
C
C*************************************************************
C
C  SECTION: INPUT
C
C*************************************************************
C  SUBROUTINE TO INPUT CROSS-SECTION DATA AND FIND THALWEG
C  STARTING AT TOE OF JAM AND WORKING UPSTREAM.
C
      SUBROUTINE INPUT(NX,THALW,X,ROUGHI,ROUGHB)
      COMMON/TWO/WSEL,MYPTS(199),B(199,25),H(199,25),XSERR(199)
      DIMENSION X(NX),ROUGHI(NX),ROUGHB(NX)
      DIMENSION THALW(NX)
      DOUBLE PRECISION WSEL(199)
C
      DO 20 I=1,NX
      READ(5,101) X(I)
  101 FORMAT(F10.3)
      READ(5,*) MYPTS(I)
      NP=MYPTS(I)
      READ(5,103) ROUGHI(I),ROUGHB(I)
  103 FORMAT(F6.3)
      READ(5,113) WSEL(I)
  113 FORMAT(D7.3)
      THALW(I)=10000.
      DO 10 J=1,NP
      READ(5,104) B(I,J),H(I,J)
      IF(H(I,J).LT.THALW(I)) THALW(I)=H(I,J)
   10 CONTINUE
  104 FORMAT(2F10.3)
   20 CONTINUE
      RETURN
      END
C
C*************************************************************
C
C  SECTION: SLOP
C
C*************************************************************
C  SUBROUTINE TO CALCULATE OPEN WATER SLOPE AT EACH CROSS-SECTION
C
      SUBROUTINE SLOP(NX,X,THALW,WSEL)
      COMMON/ONE/SLOPE(199),ROUGHC(199),FSLOPE(199),RKR(199),WSLOPE(199)
      DIMENSION X(NX),THALW(NX)
      DOUBLE PRECISION WSEL(199)
```

```
C
C  SLOPE CALCULATIONS WORKING UPSTREAM FROM TOE.
C
  20 SLOPE(1)=(WSEL(2)-WSEL(1))/(X(2)-X(1))
     NN=NX-1
     DO 21 K=2,NN
  21 SLOPE(K)=(((WSEL(K+1)-WSEL(K))/(X(K+1)-X(K)))+
    <((WSEL(K)-WSEL(K-1))/(X(K)-X(K-1))))/2
     SLOPE(NX)=(WSEL(NX)-WSEL(NX-1))/(X(NX)-X(NX-1))
     DO 22 J=1,NX
  22 FSLOPE(J)=SLOPE(J)
     RETURN
     END
C
C*************************************************************
C
C  SECTION: XPROP
C
C*************************************************************
C  SUBROUTINE TO CALCULATE CROSS-SECTION PROPERTIES
C
     SUBROUTINE XPROP(NCS)
     COMMON/TWO/WSEL,MYPTS(199),B(199,25),H(199,25),XSERR(199)
     COMMON/THREE/A(199),P(199),R(199),TW(199)
     DOUBLE PRECISION WSEL(199)
C
     A(NCS)=0.0
     TW(NCS)=0.0
     P(NCS)=0.0
     R(NCS)=0.0
     I=0
C
 100 I=I+1
     IF(I-MYPTS(NCS))102,101,101
 101 R(NCS)=A(NCS)/(P(NCS)+TW(NCS))
     RETURN
 102 IF(WSEL(NCS)-H(NCS,I))104,104,103
 103 IF(WSEL(NCS)-H(NCS,I+1))200,200,300
 104 IF(WSEL(NCS)-H(NCS,I+1))105,105,200
 105 DA=0.0
     DT=0.0
     DP=0.0
     GO TO 400
C
 200 S=(B(NCS,I+1)-B(NCS,I))/(H(NCS,I+1)-H(NCS,I))
     X1=H(NCS,I+1)-WSEL(NCS)
     IF(X1)202,201,201
C
 201 X1=WSEL(NCS)-H(NCS,I)
 202 DT=S*X1
     X2=ABS(X1)
     DA=DT*X2*0.5
     DP=X2*SQRT(1.0+(S*S))
     GO TO 400
C
```

```
 300 DT=B(NCS,I+1)-B(NCS,I)
     X1=WSEL(NCS)-H(NCS,I)
     X2=H(NCS,I)-H(NCS,I+1)
     DA=DT*(X1+(X2*0.5))
     DP=SQRT((DT*DT)+(X2*X2))
C
 400 A(NCS)=A(NCS)+DA
     TW(NCS)=TW(NCS)+DT
     P(NCS)=P(NCS)+DP
     GO TO 100
     END
C
C*************************************************************
C
C  SECTION: COMPR
C
C*************************************************************
C  SUBROUTINE TO CALCULATE COMPOSITE ROUGHNESS OF CROSS-SECTION
C  USING SABANEEV EQUATION WITH EXPONENT EQUAL TO 0.25
C
     SUBROUTINE COMPR(NX,ROUGHI,ROUGHB)
     COMMON/ONE/SLOPE(199),ROUGHC(199),FSLOPE(199),RKR(199),WSLOPE(199)
     DIMENSION ROUGHI(NX),ROUGHB(NX)
     DO 50 J=1,NX
     RKR(J)=ROUGHI(J)/ROUGHB(J)
  50 ROUGHC(J)=ROUGHB(J)*(((1+(RKR(J)**0.25))/2)**4)
     RETURN
     END
C
C*************************************************************
C
C  SECTION: NORMD
C
C*************************************************************
C  SUBROUTINE TO CALCULATE UNIFORM FLOW DEPTH
C  USING KEULEGAN LOGARITHMIC FLOW EQUATION
C
     SUBROUTINE NORMD(NX,Q,WSEL,SERR,THALW)
     COMMON/ONE/SLOPE(199),ROUGHC(199),FSLOPE(199),RKR(199),WSLOPE(199)
     COMMON/THREE/A(199),P(199),R(199),TW(199)
     DIMENSION THALW(NX)
     DOUBLE PRECISION WSEL(NX)
C
     TOLER=0.001
C
C  UNIFORM FLOW DEPTH FOUND USING SECANT METHOD
C
     DO 50 K=1,NX
     KC=0
     WL1=WSEL(K)
     CALL XPROP(K)
     A1=A(K)
     R1=R(K)
     WL2=WSEL(K)*1.01
     CK=ROUGHC(K)
```

```
      SO=SLOPE(K)
      IF(SO.LE.0.) SO=0.001
C
      DEP1=FUNC(A1,R1,CK,SO,Q)
   10 WSEL(K)=WL2
      CALL XPROP(K)
      A2=A(K)
      R2=R(K)
      DEP2=FUNC(A2,R2,CK,SO,Q)
      IF(DEP2.EQ.DEP1) GO TO 21
      WLNEW=WL2-((WL1-WL2)*DEP2/DEP1)/(1.-DEP2/DEP1)
      ERROR=ABS(WLNEW-WL2)
C
      IF(ERROR-TOLER)30,30,20
   20 IF(WLNEW.LE.THALW(K)) WLNEW=THALW(K)+0.1
      WL1=WL2
      WL2=WLNEW
      DEP1=DEP2
      KC=KC+1
      IF(KC.LT.40)GO TO 10
   21 SERR=1.0
      RETURN
   30 WSEL(K)=WLNEW
      CALL XPROP(K)
   50 CONTINUE
      RETURN
      END
C
C
C*************************************************************
C
C  SECTION: FUNC
C
C*************************************************************
C  FUNCTION TO EVALUATE LOGARITHMIC FLOW EQUATION
C
C
      FUNCTION FUNC(A,R,C,S,Q)
      FUNC=(A*(SQRT(9.81*R*S))*((2.5*ALOG(R/C))+6.2))-Q
      RETURN
      END
C
C
C*************************************************************
C
C  SECTION: MINDEP
C
C*************************************************************
C
C  THIS SUBROUTINE CALCULATES THE MINIMUM DEPTH OF FLOW
C  SUCH THAT THE SPECIFIED MAXIMUM VELOCITY IS NO EXCEEDED
C
      SUBROUTINE MINDEP(NX,Q,KERR,THALW,VMAX,WMIN)
      COMMON/TWO/WSEL,MYPTS(199),B(199,25),H(199,25),XSERR(199)
      COMMON/THREE/A(199),P(199),R(199),TW(199)
```

```
      DIMENSION WMIN(NX),THALW(NX)
      DOUBLE PRECISION WSEL(199)
C
      DO 99 IX=1,NX
      WSAVE=WSEL(IX)
      WSEL(IX)=THALW(IX)+3.
C
C  DETERMINE DEPTH SUCH THAT VELOCITY IS JUST
C  EQUAL TO MAXIMUM USING SECANT METHOD.
C
      TOLER=0.0001
      KC=0
C
      CALL XPROP(IX)
      WL1=WSEL(IX)
      WL2=WL1-0.025
      A1=A(IX)
      DIF1=VFUN(A1,VMAX,Q)
      IF(DIF1.EQ.0.) DIF1=0.00001
C
  103 WSEL(IX)=WL2
      CALL XPROP(IX)
      A2=A(IX)
      DIF2=VFUN(A2,VMAX,Q)
      IF(DIF2.EQ.0.) DIF2=0.00001
      WLNEW=WL2-((WL1-WL2)*DIF2/DIF1)/(1.-DIF2/DIF1)
      ERROR=ABS(WLNEW-WL2)
      IF(ERROR-TOLER)105,105,104
C
  104 IF(WLNEW.LE.THALW(IX)) WLNEW=THALW(IX)+0.1
      WL1=WL2
      WL2=WLNEW
      DIF1=DIF2
      KC=KC+1
      IF(KC.LT.100) GO TO 103
      KERR=5
      RETURN
C
  105 WMIN(IX)=WLNEW
      WSEL(IX)=WSAVE
      CALL XPROP(IX)
   99 CONTINUE
      END
C
C
C*************************************************************
C
C  SECTION: THICK
C
C*************************************************************
C
C  SUBROUTINE TO CALCULATE THICKNESS PROFILE OF AN ICEJAM
C
      SUBROUTINE THICK(NX,Q,DFLAG,FLAG,KSTEP,KERR,TAT,TSAVE)
C
      COMMON/ONE/SLOPE(199),ROUGHC(199),FSLOPE(199),RKR(199),WSLOPE(199)
```

```
      COMMON/TWO/WSEL,MYPTS(199),B(199,25),H(199,25),XSERR(199)
      COMMON/THREE/A(199),P(199),R(199),TW(199)
      COMMON/FOUR/TINIT,TANPHI,RHO,E,XK,PK,CI
      COMMON/FIVE/TCK(199),X(199)
      DIMENSION DFLAG(NX),TSAVE(NX)
      DOUBLE PRECISION WSEL(199),TERM1,TERM2,DTDX
C
C  INITIALIZE THICKNESS FOR FIRST TRIAL (IE. IF KSTEP = 1)
C
      IF(KSTEP.GT.1) GO TO 9
      TCK(1)=TAT
      DO 8 JX=2,NX
    8 TCK(JX)=TINIT
C
C  CALCULATE WATER SURFACE SLOPE AT EACH NODE
C
    9 CALL WATSLO(NX,WSEL,RHO)
      DO 7 I=2,NX
    7 TSAVE(I)=TCK(I)
C
C  CALCULATE THICKNESS PROFILE USING FORWARD DIFFERENCE SCHEME
C
      LIM=NX-2
      GRAV=9.81
      DO 100 II=1,LIM
      IX=NX-II
      IM=IX+1
      T1=TCK(IM)
      T21=TCK(IX)
      ISTEP=0
C
      TOP=(TW(IX)+TW(IM))/2.
      AA=(-XK*TANPHI)/TOP
      DFLAG(IX)=0.
      GAMMA=GRAV*1000.
      GAMME=(GRAV*RHO*0.5)*(1.-E)*(1.-(RHO/1000.))
      R1=(A(IM)/P(IM))/(1.+RKR(IM)**(-0.25))
      R2=(A(IX)/P(IX))/(1.+RKR(IX)**(-0.25))
      RI=(R1+R2)/2.
      SF=(FSLOPE(IM)+FSLOPE(IX))/2.
      BB=(GAMMA*RI*SF)/(2.*PK*GAMME)
      SW=(WSLOPE(IM)+WSLOPE(IX))/2.
      CC=((GRAV*RHO*SW)/(2.*PK*GAMME))
     <-(CI/(TOP*PK*GAMME))
   10 TAV=(T21+T1)/2.
C
      TERM1=AA*TAV
      TERM2=(BB/TAV)+CC
      TERM3=BB/TAV
      DTDX=TERM1+TERM2
C
      T22=T1+(DTDX*(X(IM)-X(IX)))
      IF(T22.LT.0.) GO TO 99
      TDIF=ABS(T22-T21)
      TOL=0.0001
```

```
      IF(TDIF.LT.TOL)GO TO 99
      ISTEP=ISTEP+1
      T21=T21+(0.33*(T22-T21))
      IF(ISTEP.LT.50) GO TO 10
      DFLAG(IX)=1.
      GO TO 19
C
C  CHECK IF TCK(IX) IS LESS THAN TINIT.  IF SO, SET TCK(IX) EQUAL
C  TO EITHER TINIT OR TNS WHICH EVER IS GREATER
C     TNS = THICKNESS OF NARROW JAM BASED ON NO SPILL CONDITION
C
   99 TCK(IX)=T22

C
C  PRINT TERMS IN THICKNESS EQUATION BY REMOVING
C  'C' IN THE FOLLOWING LINES
C
C     IF(KSTEP.NE.25) GO TO 18
C     WRITE(6,66) IX,AA,BB,CC,RI,SF,SW,TAV,TERM1,TERM2,TERM3,DTDX
   66 FORMAT(I4,11(2X,G9.3))
   18 CONTINUE
C
      IF(TCK(IX).GT.TINIT) GO TO 100
      DFLAG(IX)=2.
   19 TNS=((Q/A(IX))**2)/(2*GRAV*(1.-(RHO/1000.)))
      IF(TNS-TINIT)20,20,21
   20 TCK(IX)=TINIT
      GO TO 100
   21 TCK(IX)=TNS
  100 CONTINUE
C
C  LIMIT CHANGE IN THICKNESS TO 33% OF CALCULATED
C  CHANGE FOR STABILITY
C
      DO 98 I=2,LIM
   98 TCK(I)=TSAVE(I)-(0.33*(TSAVE(I)-TCK(I)))
C
C
      RETURN
      END
C
C*************************************************************
C
C  SECTION: WATSLO
C
C*************************************************************
C  SUBROUTINE TO CALCULATE WATER SURFACE SLOPE AT EACH NODE
C
C
      SUBROUTINE WATSLO(NX,WSEL,RHO)
      COMMON/ONE/SLOPE(199),ROUGHC(199),FSLOPE(199),RKR(199),WSLOPE(199)
      COMMON/FIVE/TCK(199),X(199)
      DOUBLE PRECISION WSEL(199),WLB,WLC,WLF
C
      NL=NX-1
```

```
      DO 50 I=2,NL
C
      SI=RHO/1000
      IB=I-1
      IC=I
      IF=I+1
      WLB=WSEL(IB)+(SI*TCK(IB))
      WLC=WSEL(IC)+(SI*TCK(IC))
      WLF=WSEL(IF)+(SI*TCK(IF))
C
      WSLOPE(IC)=(((WLF-WLC)/(X(IF)-X(IC)))
     <+((WLC-WLB)/(X(IC)-X(IB))))/2
      IF(WSLOPE(IC).LT.0.0) WSLOPE(IC)=SLOPE(IC)
   50 CONTINUE
C
      WSLOPE(1)=((WSEL(2)+(SI*TCK(2)))-(WSEL(1)+(SI*TCK(1))))/
     <(X(2)-X(1))
      IF(WSLOPE(1).LT.0.0) WSLOPE(1)=SLOPE(1)
      WSLOPE(NX)=((WSEL(NX)+(SI*TCK(NX)))-(WSEL(NL)+(SI*TCK(NL))
     <))/(X(NX)-X(NL))
      IF(WSLOPE(NX).LT.0.0) WSLOPE(NX)=SLOPE(NX)
      RETURN
      END
C
C*************************************************************
C
C  SECTION: GVF
C
C*************************************************************
C  SUBROUTINE TO EVALUATE GRADUALLY VARIED FLOW PROFILE
C
C
      SUBROUTINE GVF(NX,Q,TOLERH,KSTEP,KERR,THALW,ROUGHB,RHO,
     <IERR,VMAX,WMIN)
      COMMON/ONE/SLOPE(199),ROUGHC(199),FSLOPE(199),RKR(199),WSLOPE(199)
      COMMON/TWO/WSEL,MYPTS(199),B(199,25),H(199,25),XSERR(199)
      COMMON/THREE/A(199),P(199),R(199),TW(199)
      COMMON/FIVE/TCK(199),X(199)
      DIMENSION THALW(NX),ROUGHB(NX),IERR(NX),WMIN(NX)
      DOUBLE PRECISION WSEL(199)
C
C  CALCULATE TOTAL HEAD AND FRICTION SLOPE AT
C  DOWNSTREAM NODE
C
      HTD=HEAD(1,Q)
      FSD=FRIC(1,Q)
C
C  CALCULATE DEPTH AT UPSTREAM NODES USING
C  STANDARD STEP METHOD
C
      IX=2
      II=0
      SI=RHO/1000.
C
  100 WSAVE=WSEL(IX)
```

```
      WLAST=WSAVE
C
C  CALCULATE DEPTH OF FLOW AT NEXT UPSTREAM NODE
C
C
C  ESTIMATE HEAD AT NEXT NODE
C
  102 HTU=HEAD(IX,Q)
      FSU=FRIC(IX,Q)
      SFAV=(FSU+FSD)/2
      HTT=HTD+(SFAV*(X(IX)-X(IX-1)))
      ERR=ABS(HTT-HTU)
C
C  IF ERROR IS TOO LARGE REFINE ESTIMATE
C
      IF(ERR.GT.0.001) GO TO 50
      HTD=HTU
      FSD=FSU
      TERR=ABS(HTU-((Q*Q*0.5/9.81)/(A(IX)*A(IX)))
     <-(0.92*TCK(IX))-WSAVE)
C
C  CHECK CHANGE IN WATER LEVEL FROM LAST STEP
C  SET KERR=4 IF THIS NODE DOES NOT MEET TOERANCE (TOLERH)
C
      IF(TERR.LE.TOLERH) GO TO 60
      KERR=4
      XSERR(IX)=TERR
      GO TO 61
C
C  GO ON TO NEXT NODE OR RETURN IF HEAD OF JAM
C  IS ENCOUNTERED
C
   60 XSERR(IX)=0.0
   61 II=0
      IX=IX+1
      IF(IX.GT.NX) RETURN
      GO TO 100
C
C  REFINE ESTIMATE OF HEAD AT NEXT NODE
C
   50 T1=0.25
      T2=0.15
      T3=0.1
      T4=0.05
      T5=0.01
      IF(ERR.LT.T1) GO TO20
      IF(HTT-HTU)31,31,30
   20 IF(ERR.LT.T2) GO TO 21
      IF(HTT-HTU)33,33,32
   21 IF(ERR.LT.T3) GO TO 22
      IF(HTT-HTU)35,35,34
   22 IF(ERR.LT.T4) GO TO 23
      IF(HTT-HTU)37,37,36
   23 IF(ERR.LT.T5) GO TO 40
      IF(HTT-HTU)39,39,38
```

```
 30 HTN=HTT-0.1
    GO TO 51
 31 HTN=HTT+0.1
    GO TO 51
 32 HTN=HTT-0.05
    GO TO 51
 33 HTN=HTT+0.05
    GO TO 51
 34 HTN=HTT-0.03
    GO TO 51
 35 HTN=HTT+0.03
    GO TO 51
 36 HTN=HTT-0.01
    GO TO 51
 37 HTN=HTT+0.01
    GO TO 51
 38 HTN=HTT-0.003
    GO TO 51
 39 HTN=HTT+0.003
    GO TO 51
 40 HTN=HTT
C
C  CHECK MAX. NUMBER OF ITERATIONS
C
 51 II=II+1
    IF(II.GT.75) GO TO 99
    WSEL(IX)=HTN-((Q*Q*0.5/9.81)/(A(IX)
   <*A(IX)))-(SI*TCK(IX))
C
C  LIMIT CHANGE IN WSEL TO 0.3 TIMES THE CALCULTED
C  CHANGE FOR STABILITY
C
    WSEL(IX)=WLAST+(.3*(WSEL(IX)-WLAST))
    WLAST=WSEL(IX)
C
C
C  CHECK THAT WATERWAY IS NOT TOO SMALL
C
    IF(WSEL(IX).LT.WMIN(IX)) GO TO 98
 90 CONTINUE
    CALL XPROP(IX)
    GO TO 102
C
C  IF WATERWAY IS TOO SMALL CHANGE THICKNESS TO
C  MAKE VELOCITY UNDER JAM EQUAL TO VMAX
C
 98 TCK(IX)=(HTN-((Q*Q*0.5/9.81)/(A(IX)*A(IX)))-WMIN(IX))/SI
    IERR(IX)=2
    GO TO 102
 99 WSEL(IX)=WMIN(IX)
    XSERR(IX)=0.
    CALL XPROP(IX)
    IERR(IX)=1
    HTD=HEAD(IX,Q)
    FSD=FRIC(IX,Q)
```

```
      GO TO 61
      END
C
C*************************************************************
C
C  SECTION: VFUN
C
C*************************************************************
      FUNCTION VFUN(A,VMAX,Q)
      VFUN=(Q/A)-VMAX
      RETURN
      END
C
C*************************************************************
C
C  SECTION: HEAD
C
C*************************************************************
C  FUNCTION TO CALCULATE TOTAL HEAD AT A CROSS-SECTION
C
      FUNCTION HEAD(N,Q)
      COMMON/TWO/WSEL,MYPTS(199),B(199,25),H(199,25),XSERR(199)
      COMMON/THREE/A(199),P(199),R(199),TW(199)
      COMMON/FOUR/TINIT,TANPHI,RHO,E,XK,PK,CI
      COMMON/FIVE/TCK(199),X(199)
      DOUBLE PRECISION WSEL(199)
C
      SI=RHO/1000
      HEAD=WSEL(N)+(SI*TCK(N))+((Q*Q*0.5/9.81)/
     <(A(N)*A(N)))
      RETURN
      END
C
C*************************************************************
C
C  SECTION: FRIC
C
C*************************************************************
C  FUNCTION TO CALCULATE FRICTION SLOPE AT A CROSS-SECTION
C
      FUNCTION FRIC(N,Q)
      COMMON/ONE/SLOPE(199),ROUGHC(199),FSLOPE(199),RKR(199),WSLOPE(199)
      COMMON/THREE/A(199),P(199),R(199),TW(199)
      FRIC=(Q*Q)/((((2.5*ALOG(R(N)/ROUGHC(N)))+6.2)
     <**2)*9.81*R(N)*A(N)*A(N))
      FSLOPE(N)=FRIC
      RETURN
      END
C
C*************************************************************
C
C  SECTION: OUTPUT
C
C*************************************************************
C  SUBROUTINE TO DISPLAY ERROR MESSAGES AND OUTPUT
```

```
C  RESULTS IN GRAPHICAL FORM
C
      SUBROUTINE OUTPUT(Q,NUMBER,KSTEP,KERR,NX,THALW,ROUGHI,R,
     <DFLAG,IERR)
      COMMON/TWO/WSEL,MYPTS(199),B(199,25),H(199,25),XSERR(199)
      COMMON/FOUR/TINIT,TANPHI,RHO,E,XK,PK,CI
      COMMON/FIVE/TCK(199),X(199)
      DIMENSION THALW(NX),TP(199),ROUGHI(199),R(199),DFLAG(NX),EWAT(199)
      DIMENSION IERR(NX),OPTN(12),ADUMMY(2,2),BDUM(8,199)
      DIMENSION IDUM(3,3),LABEL(6),WEL(199),TICE(199)
      DOUBLE PRECISION WSEL(199)
C
      IF(KERR.NE.4) GO TO 99
      WRITE(6,100)
  100 FORMAT(//'THESE CROSS-SECTIONS DID NOT MEET THE TOLERANCE')
      DO 50 I=2,NX
      IF(XSERR(I).LE.0.00001) GO TO 50
      WRITE(6,101) I,XSERR(I)
  101 FORMAT('SECTION ',I3,' ,ERROR = ',F8.5)
   50 CONTINUE
C
   99 IF(KERR.EQ.5) GO TO 41
      DO 97 I=1,NX
      IF(DFLAG(I).EQ.0.) GO TO 97
      GO TO 30
   97 CONTINUE
   30 DO 31 I=1,NX
      IF(DFLAG(I).EQ.1.) GO TO 35
   31 CONTINUE
   33 DO 32 I=1,NX
      IF(DFLAG(I).EQ.2.) GO TO 40
   32 CONTINUE
      GO TO 41
   35 WRITE(6,36)
   36 FORMAT(/'*** WARNING ***
     <'/'FIFTY ITERATIONS EXCEEDED IN SUBROUTINE:THICK
     <'/'AT SECTION:',I3,'
     <'/'THICKNESS WAS SET EQUAL TO TNS OR TINIT')
      DO 37 I=1,NX
      IF(DFLAG(I).EQ.1.)WRITE(6,38) I
   38 FORMAT(10X,I3)
   37 CONTINUE
      GO TO 33
   40 WRITE(6,75)
      DO 43 I=1,NX
      IF(DFLAG(I).EQ.2.) WRITE(6,42) I
   42 FORMAT(10X,I3)
   43 CONTINUE
   41 CONTINUE
C
      GO TO (81,62,83,62,85), KERR
C
   81 WRITE(6,61)
   61 FORMAT('ALL CROSS-SECTIONS MET TOLERANCE')
   62 WRITE(6,63)KSTEP
```

```
 63 FORMAT(/'AFTER ',I2,' STEPS, THE PROFILE
   <'/'IS AS FOLLOWS:')
C
C  OUTPUT IN TABULAR FORM
C
    SI=RHO/1000
    STG=0.
    DO 65 JI=1,NX
    TP(JI)=WSEL(JI)+TCK(JI)
    EWAT(JI)=WSEL(JI)+(SI*TCK(JI))
    STT=EWAT(JI)-THALW(JI)
    IF(STT-STG) 65,65,64
 64 STG=STT
 65 CONTINUE
    WRITE(6,803)
803 FORMAT(/' NO.  CHAINAGE  THALWEG   BOT. OF ICE  TOP OF ICE
   < WAT.SURF   STAGE'/)
    DO 66 I=1,NX
    STT=EWAT(I)-THALW(I)
 66 WRITE(6,802) I,X(I),THALW(I),WSEL(I),TP(I),EWAT(I),STT
802 FORMAT(I4,3X,F10.3,2X,F8.3,2X,F10.3,3X,F10.3,3X,F9.3,F9.3)
    WRITE(6,804)
804 FORMAT(/' NO.  CHAINAGE(M)  ICE ROUGH.(M)  HYD. RAD.(M)
   <  THICKNESS(M)'/)
    DO 67 I=1,NX
 67 WRITE(6,805) I,X(I),ROUGHI(I),R(I),TCK(I)
805 FORMAT(I4,3X,F10.3,3X,F12.3,3X,F11.3,3X,F10.3)
C***
C    GO TO 987
C
C  OUTPUT IN GRAPHICAL FORM USING **GRAPH**
C  SUBROUTINE PACKAGE
C
    DO 20 I=1,12
 20 OPTN(I)=-1.
    OPTN(1)=1.
    OPTN(2)=0.42
    OPTN(3)=302000.
    OPTN(4)=235.
    OPTN(5)=17.
    OPTN(6)=11.0
    OPTN(7)=1000.
    OPTN(8)=2.5
    OPTN(11)=1.
    LABEL(1)=10HICEJAM PRO
    LABEL(2)=10HFILE  NO.
    ENCODE(8,21,LABEL(3))NUMBER
 21 FORMAT(I8)
    LABEL(4)=10HCHAINAGE
    LABEL(5)=10HELEVATION
    LABEL(6)=10HTHALWEG
    NPP=NX+2
    CALL GRAPH(X,THALW,NPP,LABEL,1,3,CPTN,IDUM,BDUM)
C
    DO 22 I=1,NX
```

```
      WEL(I)=WSEL(I)*1.0
   22 TICE(I)=WEL(I)+TCK(I)
      LABEL(6)=10HBOT. ICE
C
      CALL GRAPH(X,WEL,NPP,LABEL,2,3,OPTN,IDUM,BDUM)
      LABEL(6)=10HTOP ICE
C
      CALL GRAPH(X,TICE,NPP,LABEL,-3,3,OPTN,IDUM,BDUM)
   72 CALL JAMVOL(NX,WEL,TICE,X,E,VOL)
      WRITE(6,73)VOL
   73 FORMAT(/'JAM VOLUME = ',E14.7)
  987 CONTINUE
      WRITE(6,74) STG
   74 FORMAT(/'MAXIMUM STAGE = ',F10.3)
      RETURN
C
C
   83 WRITE(6,75)
   75 FORMAT(/'*** WARNING *** AT SOME POINT ALONG THE CROSS-SECTION,
     <'/'THE JAM WAS FOUND TO BE NARROW.  THE THICKNESS AT THIS NODE(S)
     <'/'WAS SET AT EITHER THE NARROW JAM THICKNESS OR TINIT WHICH EVER
     <'/'WAS GREATER.  THE AFFECTED SECTIONS ARE:')
      DO 76 I=1,NX
      IF(DFLAG(I).EQ.2.) WRITE(6,86) I
   76 CONTINUE
   86 FORMAT(10X,I3)
      GO TO 62
C
   85 WRITE(6,77) KSTEP
   77 FORMAT(/'***DURING STEP NUMBER ',I2,' THE MAXIMUM
     <'/'NUMBER OF ITERATIONS WAS EXCEEDED IN SUBROUTINE: MINDEP
     <'/'WHILE CALCULATING NEW VALUE OF WSEL TO SATISFY
     <'/'MAXIMUM VELOCITY REQUIREMENTS
     <'/'***EXECUTION WAS TERMINATED***')
      GO TO 62
      END
C
C
C*********************************************************************
C
C  SECTION: JAMVOL
C
C*********************************************************************
C
C  THIS SUBROUTINE CALCULATES THE VOLUME OF SOLID ICE
C  IN THE SIMULATED JAM
C
      SUBROUTINE JAMVOL(NX,WEL,TICE,X,E,VOL)
      DIMENSION WEL(199),TICE(199),X(199)
      COMMON/TWO/WSEL,MYPTS(199),B(199,25),H(199,25),XSERR(199)
      COMMON/THREE/A(199),P(199),R(199),TW(199)
      DOUBLE PRECISION WSEL(199)
C
C  CALCULATE VOLUME UNDER TOP OF ICE
C
```

```
      DO 10 I=1,NX
      WSEL(I)=TICE(I)
   10 CALL XPROP(I)
C
      LIM=NX-1
      VOL1=0.
      DO 20 I=1,LIM
   20 VOL1=VOL1+(((A(I)+A(I+1))/2.)*(X(I+1)-X(I)))
C
C  CALCULATE VOLUME UNDER BOTTOM OF ICE
C
      DO 30 I=1,NX
      WSEL(I)=WEL(I)
   30 CALL XPROP(I)
C
      VOL2=0.
      DO 40 I=1,LIM
   40 VOL2=VOL2+(((A(I)+A(I+1))/2.)*(X(I+1)-X(I)))
C
C  JAM VOLUME EQUALS DIFFERENCE BETWEEN VOL1 AND VOL2
C  TIMES 1-E
C
      VOL=(VOL1-VOL2)*(1-E)
      RETURN
      END
C
C
C  GRAPH
C
C*****************************************************
C*                                                   *
C*                  " GRAPH "                        *
C*                                                   *
C*     VERSION: 1     LAST REVISION: JAN20/86        *
C*                                                   *
C*        WRITTEN BY: GREG FLATO                     *
C*                                                   *
C*     DEPARTMENT OF CIVIL ENGINEERING               *
C*     UNIVERSITY OF ALBERTA                         *
C*                                                   *
C*****************************************************
C
C
C
C  THIS IS A FORTRAN CALLABLE SUBROUTINE PACKAGE
C  WHICH ALLOWS OUTPUT FROM A PROGRAM TO BE PLOTTED
C  DIRECTLY ON THE CALCOMP PLOTTER
C
C  THIS PACKAGE WAS WRITTEN FOR USE ON THE CYBER
C  SYSTEM AT CANADA CENTRE FOR INLAND WATERS
C
C
      SUBROUTINE GRAPH(XARRAY,YARRAY,NDP2,LABEL,NC,MNC,OPTN,IDUMMY
     <,BDUMMY)
      DIMENSION XARRAY(NDP2),YARRAY(NDP2),OPTN(12)
```

```
      DIMENSION LABEL(6),ADUMMY(2,2),IDUMMY(MNC,3)
      DIMENSION BDUMMY(8,NDP2)
C
      NPTS=NDP2-2
      NP1=NPTS+1
      NP2=NPTS+2
C
C
C  SET DEFAULTS
C
      IF(NC.GT.1.OR.NC.LT.0)GO TO 98
      FACT=1.0
      XORIG=0.
      YORIG=0.
      XLEN=8.
      YLEN=6.
      XSCAL=-1.
      YSCAL=-1.
      ONLEG=-1.
      POSLEG=2.
C
C  SET SPECIFIED OPTIONS IF ANY
C  ---
      IF(OPTN(1).LE.0.) GO TO 99
      IF(OPTN(2).GT.0.) FACT=OPTN(2)
      IF(OPTN(3).GE.0.) XORIG=OPTN(3)
      IF(OPTN(4).GE.0.) YORIG=OPTN(4)
      IF(OPTN(5).GT.0.) XLEN=OPTN(5)
      IF(OPTN(6).GT.0.) YLEN=OPTN(6)
      IF(OPTN(7).GT.0.) XSCAL=OPTN(7)
      IF(OPTN(8).GT.0.) YSCAL=OPTN(8)
      IF(OPTN(9).GT.0.) ONLEG=OPTN(9)
      IF(OPTN(10).GT.0.) POSLEG=OPTN(10)
   98 DATREP=2.
      SYMSEL=-1.
      IF(OPTN(11).GT.0.) DATREP=OPTN(11)
      IF(OPTN(12).GE.0.) SYMSEL=OPTN(12)
   99 CONTINUE
C
      IF(NC.GT.1.OR.NC.LT.0) GO TO 7
      GO TO 8
    7 XORIG=ADUMMY(1,1)
      XSCAL=ADUMMY(1,2)
      YORIG=ADUMMY(2,1)
      YSCAL=ADUMMY(2,2)
C
C  IF AUTOMATIC SCALING IS TO BE USED, CALL SUBROUTINE
C  SCALE.  IF NOT, PLACE SPECIFIED SCALING PARAMETERS
C  IN ARRAYS
C
    8 CALL FACTOR(FACT)
      IF(XSCAL.LT.0.) GO TO 10
      XARRAY(NP1)=XORIG
      XARRAY(NP2)=XSCAL
C
```

```
 9 IF(YSCAL.LT.0.) GO TO 11
   YARRAY(NP1)=YORIG
   YARRAY(NP2)=YSCAL
   GO TO 12
C
 10 CALL SCALE(XARRAY,XLEN,NPTS,1)
   GO TO 9
C
 11 CALL SCALE(YARRAY,YLEN,NPTS,1)
 12 CONTINUE
   IF(NC.GT.1.OR.NC.LT.0) GO TO 32
C
C  USE SUBROUTINE AXIS TO DRAW AXES AND BORDER
C
C**  CALL TEKPLTS(-1.0,-1.0,13.67,10.0)
    CALL PLOT(0.,1.0,-3)
    CALL AXIS(0.,0.,LABEL(4),-10,XLEN,0.,XARRAY(NP1),XARRAY(NP2))
C
   IY=YLEN
    CALL PLOT(XLEN,0.,3)
C
   DO 30 I=1,IY
   YINC=1.*I
    CALL PLOT(XLEN,YINC,2)
    TICK=XLEN+0.1
    CALL PLOT(TICK,YINC,2)
    CALL PLOT(XLEN,YINC,2)
 30 CONTINUE
    CALL PLOT(0.,0.,3)
C
    CALL AXIS(0.,0.,LABEL(5),10,YLEN,90.,YARRAY(NP1),YARRAY(NP2))
C
   IX=XLEN
    CALL PLOT(0.,YLEN,3)
C
   DO 31 I=1,IX
   XINC=1.0*I
    CALL PLOT(XINC,YLEN,2)
    TICK=YLEN+0.1
    CALL PLOT(XINC,TICK,2)
 31 CALL PLOT(XINC,YLEN,2)
 32 CONTINUE
C
C
C  PLOT POINTS AND DRAW CURVES
C
C
    IDAT=DATREP
    IF(SYMSEL.GE.0.)GO TO 88
    NO=IABS(NC)
    SYMSEL=NO-1
 88 ISYM=SYMSEL
C

    GO TO (100,200,300,400,500) IDAT
```

```
C
 100 CALL LINE(XARRAY,YARRAY,NPTS,1,-1,ISYM)
     GO TO 600
C
 200 CALL LINE(XARRAY,YARRAY,NPTS,1,1,ISYM)
     GO TO 600
C
 300 CALL LINE(XARRAY,YARRAY,NPTS,1,0,ISYM)
     GO TO 600
C
 400 CALL CURVE(XARRAY,YARRAY,NP2,1,ISYM,BDUMMY)
     GO TO 600
C
 500 CALL CURVE(XARRAY,YARRAY,NP2,0,ISYM,BDUMMY)
C
 600 CONTINUE
C
C  IF CURVE NUMBER (NC) IS POSITIVE, RETURN, IF NOT, CONTINUE
C
     IF(NC.LT.0) GO TO 60
     ADUMMY(1,1)=XARRAY(NP1)
     ADUMMY(1,2)=XARRAY(NP2)
     ADUMMY(2,1)=YARRAY(NP1)
     ADUMMY(2,2)=YARRAY(NP2)
     IDUMMY(NC,1)=LABEL(6)
     IDUMMY(NC,2)=ISYM
     IDUMMY(NC,3)=DATREP
     RETURN
C
C  DRAW AND LABEL LEGEND
C
  60 IF(ONLEG.LT.0.) GO TO 66
     NC=IABS(NC)
     IDUMMY(NC,1)=LABEL(6)
     IDUMMY(NC,2)=ISYM
     IDUMMY(NC,3)=DATREP
     XLEG=XLEN-2.
     HLEG=(NC*0.1)+0.2
     IPOS=POSLEG
C
     GO TO (61,62,63) IPOS
C
  61 YLEG=(YLEN-HLEG)
     CALL PLOT(XLEG,YLEG,-3)
     GO TO 64
C
  62 YLEG=(YLEN-HLEG)/2
     CALL PLOT(XLEG,YLEG,-3)
     GO TO 64
C
  63 YLEG=0.
     CALL PLOT(XLEG,YLEG,-3)
C
  64 CALL PLOT(0.,0.,3)
     CALL PLOT(0.,HLEG,2)
```

```
      CALL PLOT(2.,HLEG,2)
      CALL PLOT(2.,0.,2)
      CALL PLOT(0.,0.,2)
      CALL PLOT(0.2,0.1,-3)
C
      DO 65 I=1,NC
      XARRAY(1)=0.
      XARRAY(2)=0.75
      XARRAY(3)=0.
      XARRAY(4)=1.
      YARRAY(1)=(I*0.1)-0.05
      YARRAY(2)=YARRAY(1)
      YARRAY(3)=0.
      YARRAY(4)=1.
      ISYM=IDUMMY(I,2)
C
      GO TO(50,51,52,51,52) IDUMMY(I,3)
   50 CALL LINE(XARRAY,YARRAY,2,1,-1,ISYM)
      GO TO 53
   51 CALL LINE(XARRAY,YARRAY,2,1,1,ISYM)
      GO TO 53
   52 CALL LINE(XARRAY,YARRAY,2,1,0,ISYM)
   53 YLAB=YARRAY(1)-0.05
      CALL SYMBOL(1.05,YLAB,0.08,IDUMMY(I,1),0.,10)
C
   65 CALL PLOT(XARRAY(1),YLAB,3)
C
C  DRAW TITLE
C
      CALL PLOT(0.,0.,3)
      CALL PLOT(-0.2,-0.1,-3)
      XN=-(XLEN/2)+XLEG+2.25
      YN=YLEG+0.8
   67 CALL PLOT(-XN,-YN,-3)
      CALL SYMBOL(0.,0.,0.15,LABEL,0.,30)
      CALL PLOT(0.,0.,999)
      RETURN
   66 CONTINUE
      XN=2.25-(XLEN/2)
      YN=0.8
      GO TO 67
      END
C
C*************************************************
C
      SUBROUTINE CURVE(X,Y,NDP2,LT,ISYM,BDUMMY)
C
C  SUBROUTINE TO FIT A CUBIC SPLINE APPROXIMATION
C  TO A SET OF DATA POINTS AND DRAW THE RESULTING CURVE
C
C  THE ALGORITHM FOR CUBIC SPLINE FITTING WAS TAKEN FROM
C  'NUMERICAL ANALYSIS , SECOND ED.' BY R. L. BURDEN,
C  J. D. FAIRES, AND A. C. REYNOLDS; PWS PUBLISHERS,
C  BOSTON, MASS., 1978.
C
```

```
C
      DIMENSION X(NDP2),Y(NDP2),BDUMMY(8,NDP2)
      NP=NDP2-2
      NP2=NP+2
      NP1=NP+1
      NM1=NP-1
      BDUMMY(6,1)=1.

      BDUMMY(7,1)=0.
      BDUMMY(8,1)=0.
      BDUMMY(6,NP)=1.
      BDUMMY(8,NP)=0.
      BDUMMY(4,NP)=0.
C
      DO 9 I=1,NM1
    9 BDUMMY(1,I)=X(I+1)-X(I)
C
C  PLOT POINTS IF LT=1
C
      IF(LT.EQ.0) GO TO 10
      CALL LINE(X,Y,NP,1,-1,ISYM)
C
C  CALCULATE COEFFICIENTS FOR CUBIC INTERPOLATING
C  POLYNOMIAL
C
   10 CONTINUE
      NM1=NP-1
      DO 95 I=1,NM1
   95 BDUMMY(1,I)=X(I+1)-X(I)
C
      DO 96 J=2,NM1
      BDUMMY(2,J)=3*((Y(J+1)*BDUMMY(1,J-1))-(Y(J)
     <*(X(J+1)-X(J-1)))+(Y(J-1)*BDUMMY(1,J)))
     </(BDUMMY(1,J-1)*BDUMMY(1,J))
   96 CONTINUE
C
      DO 97 I=2,NM1
      BDUMMY(6,I)=(2*(X(I+1)-X(I-1)))-(BDUMMY(1,I-1)*
     <BDUMMY(7,I-1))
      BDUMMY(7,I)=BDUMMY(1,I)/BDUMMY(6,I)
      BDUMMY(8,I)=(BDUMMY(2,I)-(BDUMMY(1,I-1)*BDUMMY(8,I-1)
     <))/BDUMMY(6,I)
   97 CONTINUE
C
      J=NP
   98 J=J-1
C
      BDUMMY(4,J)=BDUMMY(8,J)-(BDUMMY(7,J)
     <*BDUMMY(4,J+1))
C
      BDUMMY(3,J)=((Y(J+1)-Y(J))/BDUMMY(1,J))
     <-(BDUMMY(1,J)*(BDUMMY(4,J+1)+(2*BDUMMY(4,J)))/3)
C
      BDUMMY(5,J)=(BDUMMY(4,J+1)-BDUMMY(4,J))/(3*BDUMMY(1,J))
C
```

```
      IF(J.GT.1) GO TO 98
   99 CONTINUE
C
C  PLOT CURVE
C
      XO=(X(1)-X(NP1))/X(NP2)
      YO=(Y(1)-Y(NP1))/Y(NP2)
      CALL PLOT(XO,YO,3)
C
      DO 20 I=1,NM1
      DJ=(X(I+1)-X(I))/50
      X1=(X(I)-X(NP1))/X(NP2)
      Y1=(Y(I)-Y(NP1))/Y(NP2)
      CALL PLOT(X1,Y1,2)
        DO 20 J=1,49
        XK=(DJ*J)+X(I)
        XJ=(XK-X(NP1))/X(NP2)
        YJ=(SOFX(XK,I,BDUMMY,X(I),Y(I),NP)-Y(NP1))/Y(NP2)
        CALL PLOT(XJ,YJ,2)
   20 CONTINUE
C
      XN=(X(NP)-X(NP1))/X(NP2)
      YN=(Y(NP)-Y(NP1))/Y(NP2)
      CALL PLOT(XN,YN,2)
      RETURN
      END
C
C*****************************************************
C
      FUNCTION SOFX(X,I,BDUMMY,XJ,AJ,NP)
C
C  THIS FUCTION CALCULATES THE INTERPOLATED VALUE
C  OF Y AT THE GIVEN VALUE OF X
C
      DIMENSION BDUMMY(8,NP)
C
      T2=BDUMMY(3,I)*(X-XJ)
      T3=BDUMMY(4,I)*((X-XJ)*(X-XJ))
      T4=BDUMMY(5,I)*((X-XJ)**3)
C
      SOFX=AJ+T2+T3+T4
      RETURN
      END
```

SAMPLE DATA FILE

The following is a sample data file which represents the Athabasca River case study in Chapter 7. As in the program listing, the proportional spacing makes it appear as though the columns of data overlap. The actual format for the B and H coordinates (the only data which appears as pairs on a line) is 2F10.3. The remaining real variables (ie. those whose names do not begin with the letters I through N) all have an F10.3 format. The run ID number, NUMBER, has an I8 format and the other integer variables (whose names begin with I through N) have an I6 format.

```
33000096  ATHABASCA RIVER, DOYLE AND ANDRES, 1978
 35       MAXIMUM NUMBER OF ITERATIONS (MAXIT)
0.75      INITIAL THICKNESS (TINIT)
1.00      THICKNESS AT TOE OF JAM (TAT)
1200.     DISCHARGE,(Q)
1.190     TANPHI
920.0     ICE DENSITY (RHO)
0.40      POROSITY (E)
0.240     SHEAR COEFFICIENT (XK)
 7.55     PASSIVE PRESSURE COEFFICIENT (PK)
0.0       COHESION (CI)
0.01      TOLERH
1.250     MAXIMUM VELOCITY
22        NX
303000.
8,
 0.005
 0.15
241.178
      0.   300.
      0.   248.
    18.42  239.8
   197.4   239.2
   294.7   238.5
   381.6   240.2
   418.    248.
   418.    300.
303200.
8,
10.2
 0.15
241.25
      0.   300.
      0.   248.
    18.42  239.8
   197.4   239.2
   294.7   238.5
   381.6   240.2
   418.    248.
   418.    300.
```

```
303450.
8,
 10.2
 0.15
241.35
      0.    300.
      0.    248.5
     25.    240.2
    174.    239.6
    291.    238.5
    380.    240.2
    409.    248.5
    409.    300.
303700.
8,
 10.2
 0.15
241.45
      0.    300.
      0.    249.
     33.    240.6
  150.2     239.3
  288.1     238.4
  379.1     240.2
  401.2     249.
  401.2     300.
303900.
8,
 10.2
 0.15
241.55
      0.    300.
      0.    249.5
     40.    240.
    160.    239.6
    285.    238.3
    378.    240.2
    390.    249.5
    390.    300.
304200.
```

```
10,
 10.2
 0.15
241.65
      0.    300.
      0.    250.
     47.6   241.3
    103.    239.3
    166.4   240.
    225.9   239.7
    281.4   238.3
    376.5   240.2
    384.4   250.
    384.4   300.
304600.
10,
 10.2
 0.15
241.81
      0.    300.
      0.    250.
     47.6   240.6
    103.    238.6
    166.4   239.3
    225.9   239.
    281.4   237.6
    376.5   239.5
    384.4   250.
    384.4   300.
305000.
10,
 10.2
 0.15
241.97
      0.    300.
      0.    250.782
     47.6   241.382
    103.    239.382
    166.4   240.082
    225.9   239.782
```

```
    281.4   238.382
    376.5   240.282
    384.4   250.782
    384.4   300.
305400.
9,
 10.2
 0.15
242.13
      0.    300.
      0.    250.
   49.05   241.2
    112.    240.9
    168.5   240.3
    299.8   239.4
    421.9   241.1
    449.8   250.
    449.8   300.
306000.
9,
 10.2
 0.15
242.37
      0.    300.
      0.    251.17
   49.05   242.373
    112.    242.073
    168.5   241.473
    299.8   240.573
    421.9   242.273
    449.8   251.17
    449.8   300.
306600.
9,
 10.2
 0.15
242.61
      0.    300.
      0.    251.11
   50.5    242.25
```

```
    121.2   243.01
    171.7   241.61
    318.2   241.51
    467.2   243.01
    515.2   251.11
    515.2   300.
306800.
9,
 10.2
 0.15
242.69
      0.    300.
      0.    251.5
     50.5   242.64
    121.2   243.4
    171.7   242.
    318.2   241.9
    467.2   243.4
    515.2   251.5
    515.2   300.
307500.
8,
 10.2
 0.15
242.97
      0.    300.
      0.    255.392
     38.    243.392
    167.    242.292
    308.    242.592
    436.    243.092
    469.    255.392
    469.    300.
308400.
8,
 10.2
 0.15
243.33
      0.    300.
      0.    259.496
```

```
  25.5   244.396
 163.    242.796
 298.    243.496
 405.    242.996
 423.    259.496
 423.    300.
310000.
8,
 10.2
 0.15
243.97
   0.    300.
   0.    260.392
  25.5   245.292
 163.    243.692
 298.    244.392
 405.    243.892
 423.    260.392
 423.    300.
311800.
8,
 10.2
 0.15
247.5
   0.    300.
   0.    259.9
  35.6   246.6
 131.    244.7
 311.    245.1
 418.    246.1
 451.    254.9
 451.    300.
313600.
8,
 10.2
 0.15
252.74
   0.    300.
   0.    261.808
  35.6   248.508
```

```
   131.    246.608
   311.    247.008
   418.    248.008
   451.    256.808
   451.    300.
315500.
8,
 10.2
 0.15
254.75
     0.    300.
     0.    263.822
    35.6   250.522
   131.    248.622
   311.    249.022
   418.    250.022
   451.    258.822
   451.    300.
317500.
8,
 10.2
 0.15
256.87
     0.    300.
     0.    265.942
    35.6   252.642
   131.    250.742
   311.    251.142
   418.    252.142
   451.    260.942
   451.    300.
318000.
10,
 10.2
 0.15
257.4
     0.    300.
     0.    265.972
    45.6   254.372
    98.7   252.272
```

```
   324.    252.372
   349.    251.272
   430.    251.872
   440.    254.772
   479.    256.572
   479.    300.
318500.
10,
 10.2
 0.15
257.9
     0.    300.
     0.    266.502
    45.6   254.902
    98.7   252.802
   324.    252.902
   349.    251.802
   430.    252.402
   440.    255.302
   479.    257.102
   479.    300.
318800.
10,
 10.2
 0.15
258.3
     0.    300.
     0.    266.82
    45.6   255.22
    98.7   253.12
   324.    253.22
   349.    252.120
   430.    252.72
   440.    255.62
   479.    257.42
   479.    300.
```